



NTNU – Trondheim
Norwegian University of
Science and Technology

Leakage of CO₂ along Annular Well Cement

Gutlug Jafarzade

Petroleum Engineering

Submission date: August 2014

Supervisor: Sigbjørn Sangesland, IPT

Co-supervisor: Nils Opedal, SINTEF
Malin Torsæter, SINTEF

Norwegian University of Science and Technology
Department of Petroleum Engineering and Applied Geophysics

Dedicated to my beloved family

NTNU

Norges teknisk-naturvitenskapelige
universitet

Studieprogram i Geofag og petroleumsteknologi

Fakultet for ingeniørvitenskap og teknologi

Faculty of Engineering and Technology



Study Programme in Earth Sciences and Petroleum Engineering

Institutt for petroleumsteknologi og anvendt geofysikk
Department of Petroleum Engineering and Applied Geophysics

HOVEDOPPGAVE/DIPLOMA THESIS/MASTER OF SCIENCE THESIS

Kandidatens navn/The candidate's name:

Gutlug Jafarzade

Oppgavens tittel, norsk/Title of Thesis, Norwegian:

Lekkasje av CO₂ langs brønnsement

Oppgavens tittel, engelsk/Title of Thesis, English

Leakage of CO₂ along annular well cement

Utfyllende tekst/Extended text:

Background: Leakage along wells penetrating CO₂ storage sites has in numerous scientific publications been identified as the main threat towards cost-efficient and safe geological CO₂ storage. The huge efforts made to capture, transport and inject CO₂ into a subsurface reservoir will be in vain if large enough leakage rates along wells are allowed to develop. Reduced sealing ability of the annular well cement has proven to be one of the most common causes of well integrity problems and subsequent leakages in CO₂ wells. Poor cement bonding to rock and steel casing is a typical cause of such failure. The quality of cement bonding is dependent on several factors, such as the type of rock formation, type of cement, type of casing surface and type of drilling fluid used during drilling. This Master project is based on experimental work. The student will study the bonding of well cement to various types of surfaces and investigate how the bonding quality is affected by CO₂.

Task:

- 1) Prepare samples for experimental study of cement bonding
- 2) Expose samples to CO₂ and investigate effects on chemistry/porosity
- 3) Discuss the findings and the implication towards well integrity.

Supervisor

Sigbjørn Sangesland

Co-supervisor (Sintef)

Nils Opedal, Malin Torsæter.

Studieretning/Area of specialization:

Petroleum Engineering, Drilling Technology

Fagområde/Combination of subject:

Drilling

Tidsrom/Time interval:

*January **xx** – June **xx**, 2014*

.....
Sigbjørn Sangesland

Abstract

Carbon Capture and Storage (CCS) projects are aimed to store CO₂ underground and to prohibit/restrict any leakage to the well, formation and to the surface. Standards applied to control a well and to keep its integrity are aimed to stop this fluid entrance. Nevertheless, leakage can occur from the debonded formation cement interfaces.

The main goal in this experimental work was to study leakage of CO₂ along cement formation interface. In order to investigate debonding degree, samples were prepared as a small well model with a cement/formation interface. During sample preparations 4 rock, 2 cement and 3 fluid types were used to see appearance of weak bonds. 24 different samples were scanned with μ -CT and modeled with Avizo to see interface porosity and morphology. Scanned samples had been tested in CO₂ batch exposure to visualize chemical alterations on the samples. Setup had been made for CO₂ core flooding to measure the amount of fluid leaked through the cement-formation interface.

Result before experiments showed that porous and permeable rocks with good mud/cake fluid coverage give lower bonding degree while pristine samples (model of ideally cleaned well) give 100% bonding percentage. In addition from the μ -CT results it was found that the samples treated with filter cake had higher bonding degree than the samples treated with mud. After the flooding/batch exposure experiments degradation has been observed on the cement and rock surfaces. Meanwhile CO₂ and brine cleaned cement-rock interface from mud/cake on core flooding experiments. Moreover, the amount of fluid leaked through the debonding was measured and compared for three rock samples.

Acknowledgement

This thesis has been carried out as a collaboration between Norwegian University of Science and Technology and the SINTEF petroleum research center. The thesis is the continuation of specialization project “Leakage along annular cement” (Jafarzade, 2014) and is a final result for the course TPG4920- master thesis in Drilling Engineering.

The completion of this project would not have been possible without the help, guidance and support from some important people. I would like to give special thanks to my NTNU supervisor, Sigbjørn Sangesland, Professor at the Department of Petroleum Engineering and Applied Geophysics, whose motivation, advices enabled me to complete this project work.

I am very grateful to my co-supervisor at SINTEF petroleum research Dr. Malin Torsæter for advice in writing this project.

A very special thanks to my co-supervisor Nils Van Der Tuuk Opedal, PhD-research scientist at SINTEF petroleum research, for advices, suggestions on technical aspects.

I am also grateful to Jelena Todorovich for μ -CT training, help and instructions during sample scan, and with a work she has done with Avizo software. Moreover, I would like to thank Roger Overå for assisting me in a lab during μ -CT scan.

Finally, I would like to express gratitude and sincere thanks to my family and girlfriend Yasmine Bekkouche for their patience, understanding, encouragement, and love during my thesis writing in Trondheim.

Table of Contents

ABSTRACT	IV
ACKNOWLEDGEMENT	V
TABLE OF CONTENTS.....	VI
LIST OF FIGURES.....	X
LIST OF TABLES.....	XIII
1. INTRODUCTION.....	1
1.1. CARBON CAPTURE AND STORAGE (CCS)	3
1.2. WELL INTEGRITY.....	6
1.2.1. Well barriers	6
1.2.2. Number of wells with issues	7
1.2.3. Well integrity concerns for CO ₂ sequestration projects.....	8
1.2.4 Well integrity concerns for cement.....	9
1.3. PORTLAND CEMENT	11
1.3.1. Cement Chemistry	11
1.3.2. Additives.....	12
1.3.3. Objectives of primary cementing.....	12
1.3.4. Secondary cementing methods (Nelson and Guillot, 2006).....	15
2. PARAMETERS CAUSING WEAK CEMENT/INTERFACE.....	17
2.1. PRIOR TO SLURRY PHASE: MIXING OF THE CEMENT	17
2.2. SLURRY PHASE	18
3. CO₂ LEAKAGE ALONG ANNULAR WELL CEMENT	22
3.1. MICRO-ANNULI.....	22
3.1.1. Cement shrinkage.....	23
3.1.1. Pressure.....	24
3.1.2. Temperature	26
3.1.3. Mechanical loads.....	27
3.1.4. Permeability	28

3.2. CEMENT BONDING	28
3.2.1. Cement/formation bond	29
3.2.2. Cement-casing bond	31
3.3. CO ₂ EFFECT ON CEMENT AND FORMATION	31
3.4. RELEVANT PUBLISHED EXPERIMENTAL WORK	35
3.5. KNOWLEDGE GAPS	36
4. EXPERIMENTAL DETAILS	37
4.1. MATERIALS:.....	37
4.2. METHODS.....	44
4.3. EXPERIMENTAL MATRIX.....	49
4.4. FURTHER CHARACTERIZATION.....	49
4.4.1. X-ray μ -CT.....	49
5. RESULT.....	51
5.1. VISUALIZATION OF THE CEMENT-ROCK INTERFACE BEFORE AND AFTER EXPERIMENTS..	51
5.1.1. Cement-rock interface before experiments	51
5.1.2. Cement-rock interface after experiments	56
5.2. EXPERIMENTS WITH CO ₂	59
5.2.1. CO ₂ batch exposure	59
5.2.2. CO ₂ core flooding	59
6. DISCUSSION	63
6.1. DISCUSSION OF SAMPLE PREPARATION	63
6.2. DISCUSSION OF BONDING BEFORE EXPERIMENTS	64
6.3. DISCUSSION OF RESULTS AFTER EXPERIMENTS	67
6.3.1. CO ₂ batch exposure	67
6.3.2. CO ₂ core flooding	67
6.3.3. Rock-mud bonding	68
6.3.4. Cement-formation bonding changings	68
7. CONCLUSION	70
8. RECOMMENDATION FOR FUTURE WORK	71
9. LIMITATIONS	72

10.	REFERENCES	73
11.	NOMENCLATURE.....	83
12.	APPENDIX A	85
13.	APPENDIX B.....	95

List of Figures

Figure 1.1. CO ₂ underground storage conditions (CCS Browser, 2014)	4
Figure 1.2. CO ₂ reduction by year and CCS sector (CCS Browser, 2014).....	5
Figure 1.3. Poor zonal isolation. The figure outlines several possible leakage paths along wells. Based on (Celia et al., 2004).....	9
Figure 1.4. GOM wells with SCP (Nelson and Guillot, 2006).....	10
Figure 1.5. Fluid leakage on well cement. "Incorrect cement densities may create hydrostatic imbalance. Poor mud and filter cake removal leaves space for gas to flow upward through the annulus. Premature gelation leads to loss of hydrostatic pressure control. Excessive fluid loss contributes to available space in the cement slurry column for gas to enter. Highly permeable slurry has little resistance to gas flow and may leads to poor zonal isolation. High cement shrinkage leads to increased porosity and stresses in the cement sheath which may cause a microannulus to form. Cement failure under stress helps gas fracture cement sheaths. Poor bonding can cause failure at cement-casing and/or cement-formation interfaces". Based on (Bonett and Pafitis, 1996).....	13
Figure 1.6. Typical primary cementing involves different stages such as, circulation of mud, spacers, and displacement of the cement. (Chief Council's Report, 2011).....	15
Figure 2.1 Fluid flow patterns: a) laminar flow, b) turbulent flow. c) mud removal with increasing flow rate (Nelson and Guillot, 2006).....	19
Figure 2.2. Decentralized wellbore: a) Fluid channels, b) flow velocity (Gekengineering, 2014).....	20
Figure 3.1 Micro-annulus: Inner (left), b) Outer (right).....	22
Figure 3.2. A schematic of the small-wellbore simulator (Ladva et al., 2004)	25
Figure 3.3. Radial and tangential stresses creates micro-annulus and cracks (Bellabarba et al., 2008).....	28
Figure 3.4 Bonding properties of cement to dry limestone (Evans and Carter, 1961).....	29
Figure 3.5. Bonding properties of cement to formation with cement not squeezed and walls not cleaned (Evans and Carter, 1961).....	30

Figure 3.6. Illustration of the cement reactions zones in cement formation. A) Chemical reaction illustration: First zone (dissolution)- $\text{Ca}(\text{OH})_2$ dissolves and CaCO_3^{2-} forms. Second zone (carbonation)- CaCO_3 dissolves when $\text{Ca}(\text{OH})_2$ is spent. Third zone (redissolution of carbonate) - porous silica forms on a surface (Kutchko et al., 2007). B) Zone illustrations in 3D dimensions (Munz et al., 2009).33

Figure 3.7. SEM images: a) Unreacted sandstone, b) Sandston/cement interface with CO_2 brine, c) Unreacted shale, d) Shale/cement interface with CO_2 brine (Carrol et al., 2011)34

Figure 3.8. An illustration of the sample geometry of Opedal et al. (2013).35

Figure 4.1 Rock samples: a) Castlegate sandstone, b) Mons chalk, c) Marcellus shale, d) Eagle Ford shale.....38

Figure 4.2. Dimensions of samples to be prepared. a) rock cylinder. b) rock cylinder with cement sheath.....39

Figure 4.3. 3D model of steel chamber with dimensions.40

Figure 4.4. Pressure chamber (left) and 3D cross section view during curing time (right).42

Figure 4.5. Illustration of a Cell (left), sample preparation (right) and 3D drawing of the Cell in AutoCAD (below).43

Figure 4.6. Simplified sketch of CO_2 flooding setup.43

Figure 4.7. Treated rock samples before cementing procedure.44

Figure 4.8. OFITE Constant Speed Blender used for preparing cement paste (OFITE, 2014).45

Figure 4.9. Illustration of the sample preparation: a) placement of rock cylinder inside steel compartment, b) placement of cement paste, c) disassemble steel compartment after curing.46

Figure 4.10. Cured cemented rock samples.46

Figure 4.11. The realistic (above) and simplified (below) 3D view of CO_2 flooding setup (Drawn with AutoCAD). Red arrows for fluid flow and black arrows for confinement. HPPB, high pressure piston bottle.48

Figure 5.1. Two cross-section segmentation images of Eagle Ford shale with mud and salty cement in different heights. The meaning of colors: Grey-cement, yellow-rock, blue-mud/filter cake, and red- interface voids/pores.52

Figure 5.2. Eagle Ford shale prepared in pristine conditions showed total bond both for OPC and SPC. Yellow color- cement-rock interface, red- voids.54

Figure 5.3. Visualization of bonding morphology, cement-fluid-rock interface for different type of rock samples55

Figure 5.4. Visualization of bonding morphology, rock-fluid interface for differet Eagle Ford shale types. Color meaning in the pictures: Yellow-rock, blue-mud/filter cake, red-interface voids/pores. Some of samples are shifted. Samples with OPC are scanned after batch exposure and samples with SPC scanned after core flooding. Samples with SPC shows obvious reduction of mud and increase of voids in the interface.57

Figure 5.5. Visualization of the cement-rock interface for Eagle Ford shale. The yellow-grey surfaces indicate where rock and cement are in physical contact. The bonding percentage between cement and rock are given for each sample.58

Figure 5.6. .Samples after CO₂ batch exposure degradation and showed white, grey and orange colors.59

Figure 5.7. Weight change of brine vs differential pressure (pristine sample)..... 60

Figure 5.8. Weight change of brine and CO₂ vs differential pressure (Eagle Ford shale sample with mud) 61

Figure 5.9. Weight change of brine and CO₂ vs differential pressure (Eagle Ford shale sample with filter cake) 61

Figure 5.10. Eagle Ford shale with treated mud and SPC showed degradation on a contact area with brine and CO₂. 62

List of Tables

Table 1.1. Well integrity categories (Ptil, 2008, Ptil, 2009 and Skjerven et al., 2008).	8
Table 1.2. Generic check-list of failure modes and failure mechanisms for wells under exposure to carbon dioxide (CO ₂) – cement (DNV, 2012).	8
Table 1.3. Mineralogical composition of unhydrated cement. Based on Nelson and Guillot (2006).	11
Table 1.4. Additives and their functions on cement system (Nelson and Guillot, 2006):	12
Table 4.1 The compounds of each rock sample (Bruner KR and Smosna R, 2011, Alqahtani et al., 2013, Schultz, 1964).....	38
Table 4.2. Mineralogical composition of classic Portland cement clinker (Nelson and Guillot, 2006).....	39
Table 4.3. Chemical composition of the water based drilling fluid	40
Table 4.4 The composition of homemade formation water (brine).....	41
Table 4.5. Experimental matrix. Squares with orange represent batch exposure and yellow squares represent core flooding. Samples in white square were exposed to CO ₂ due time limitation.	49
Table 5.1. Rock-cement bonding percentage before experiments.....	52
Table 5.2. Rock-mud bonding percentage before experiments	53
Table 5.3. Cement-rock interface percentage after CO ₂ batch exposure and flooding experiments.	56
Table 5.4. Rock-mud interface percentage after CO ₂ batch exposure and flooding experiments.	56



Chapter 1

Introduction

Negative climate change with industry gases like CO₂ makes companies to think about long-term carbon capture and storage (CCS). The CCS requires high well integrity norms that can restrict gas leakage through centuries. Cement is the main well integrity element for CO₂ injection/storage wells which means this barrier has to withstand to time factor, operational modes and geological/physical conditions. Otherwise it may lead to loss of the well, cause environmental damage and lethal injuries. Experience shows that cement has failures both during both gelling and setting periods by resulting micro-annuli. Micro-annuli is a micro fluid flow path between cement/formation or cement/casing which caused by micro-cracks and de-bonding. In CCS projects this tiny de-bonds put whole project under danger by allowing CO₂ to flow easily upwards and reenter to the atmosphere.

Experiments of Kutchko et al. (2007) and Bachu and Bennion (2009) revealed that CO₂ with the reaction of cement/rock can heal micro-annulus/debondings. However, Krilov et al. (2000) showed negative reaction of CO₂ with cement which weakens cement and cement-formation interfaces by allowing carbon dioxide flow through micro-annulus. This reaction called degradation. With degraded cement it is easier for CO₂ contact casing and start corrosion. Corrosion of the casing means possible CO₂ leak and lose of well integrity. The objectives of this experimental work are:

- 1) Prepare samples for experimental study of cement bonding
- 2) Expose samples to CO₂ and investigate effects on chemistry/porosity
- 3) Discuss the findings and the implication towards well integrity.

Scope of the Thesis: During slurry phase cement and formation interaction get restricted by drilling mud which weakens bonding at interfaces. Thorough setting time this weak bonding get either cracked or separated by thermal and mechanical load. Through all its life cycle well



get exposed to different pressure loads which increase debonding in the cement formation interfaces.

This thesis includes three approaches that explain whole CO₂ leakage process. The first approach is to examine debonding at interfaces, its morphology and porosity. The second approach is to see cement degradation which also affect whole cement and formation by creating future leakage pathways. The third approach is to see the amount of leaked fluid through the cement/formation interface and the parameters affecting the leakage. After CO₂ flooding test samples were checked for cement/rock/mud/cake/void alterations.

Thesis outline: Chapter 1 introduces the thesis, and briefly describes need for CCS, the importance of well integrity, the compounds of cement and cementing procedure.

Chapter 2 analyses pre-causes of micro-annulus and debonding based on literature study.

Chapter 3 carry out a literature review on debonding which forms micro-annuli.

Chapter 4 precisely describes experimental procedure and materials which had been used.

Chapter 5 shows the result of this thesis work.

Discussion and conclusion are in chapter 6 and chapter 7 respectively.

Chapter 8 and 9 are focused on future recommendation and limitations before and during the experiments.

This thesis will assist on well integrity problems caused by CO₂ leaks from cement-formation interfaces.



1.1. Carbon Capture and Storage (CCS)

The IEA World Energy Outlook (WEO) Reference Scenario projects that, based on policies in place, by 2030 CO₂ emissions will have increased by 63% from today's level, which is almost 90% higher than 1990 level (IEA, 2014). CO₂ increases green gas housing effect and can reduce the thickness of ozone layer in atmosphere which prevents Earth from direct rays of sunlight. Without ozone layer the temperature of the Earth would be higher. To avoid substantial increases of CO₂, governments try to cut emissions significantly by putting strong environment policies regarding CO₂. Consequently, it triggered development of technology options to reduce CO₂ emission. One such option is Carbon Capture and Storage (CCS) that has potential to capture the CO₂ from the major emission points and prevent its reach to atmosphere by storing it underground (IEA, 2014).

How to capture CO₂? Three main technologies: post-combustion, pre-combustion and oxyfiring are used to capture CO₂ from large scale industrial processes, such as power generation, oil/gas production and cement manufacture. Capture schemes are shown on Appendix A, Fig A1 (IEA, 2014).

Transportation: Transportation is possible by pipelines for close/ medium distances and by ships for long distances (IEA, 2014).

Storage: Fluids such as water, oil, and gasses (CO₂, CH₄) have been accumulated and trapped in the Earth's layers for several millions years. This natural trap scheme has been studied and was a basis for CO₂ sequestration projects. Fig 1.1 illustrates two main conditions for carbon gas storage. First there should be enough place to store CO₂ which would allow gas to flow (permeability) through the storage space (porosity) which is called capacity. Second required condition is barriers to prevent such gasses to distribute over boundaries of storage space.

Additionally, storage in saline aquifers gives one more advantage. Hence, CO₂ reaction with brine leads to carbonation process of CO₂ which increases chance of storage.

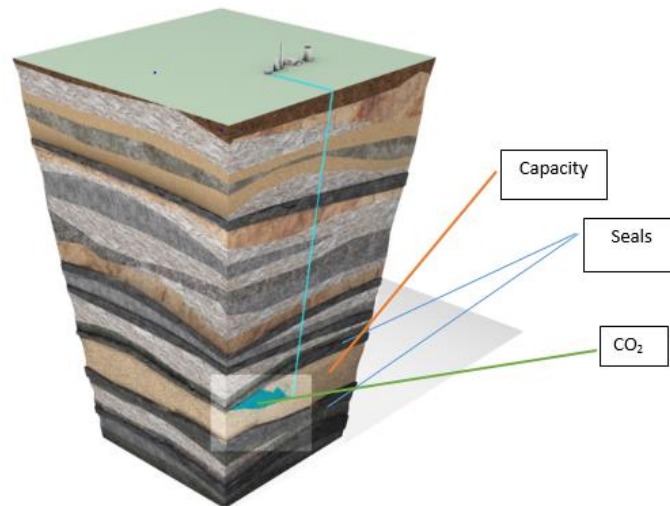


Figure 1.1. CO₂ underground storage conditions (CCS Browser, 2014)

Storage capacity in the world: IEA reported that 120 gigatonnes of CO₂ have to be stored in a year of 2050. However, viable storage for 2050 will be 1680 Gt which according to IEA is just 10% of the theoretical capacity (Fig A0, Appendix A). Every year Sleipner field (Norway) capture and store 1 million tonnes of CO₂ while Snøhvit safely inject and store 0.7 Million ton of CO₂ (Global CCS Institute, 2014). According to Statoil by early 2013, a total of nearly 2 million tonnes of CO₂ has been stored on Snøhvit (Statoil, 2014).

Overall costs: CCS involves capture of CO₂, transport of it by pipelines and tankers, and storing in depleted oil/gas reservoirs, saline aquifers and unmineable coal seams. Capture, transportation and storage costs are shown on table A1 Appendix.

Environmental benefits: The IEA has produced a roadmap (Fig 1.2) for reducing greenhouse gas emissions by 50% by 2050 to keep temperature rises to no more than 2°C. In the end of 2050 14% (approximately 5.74 Gt) of CO₂ will be reduced by CCS (CCS Browser, 2014).

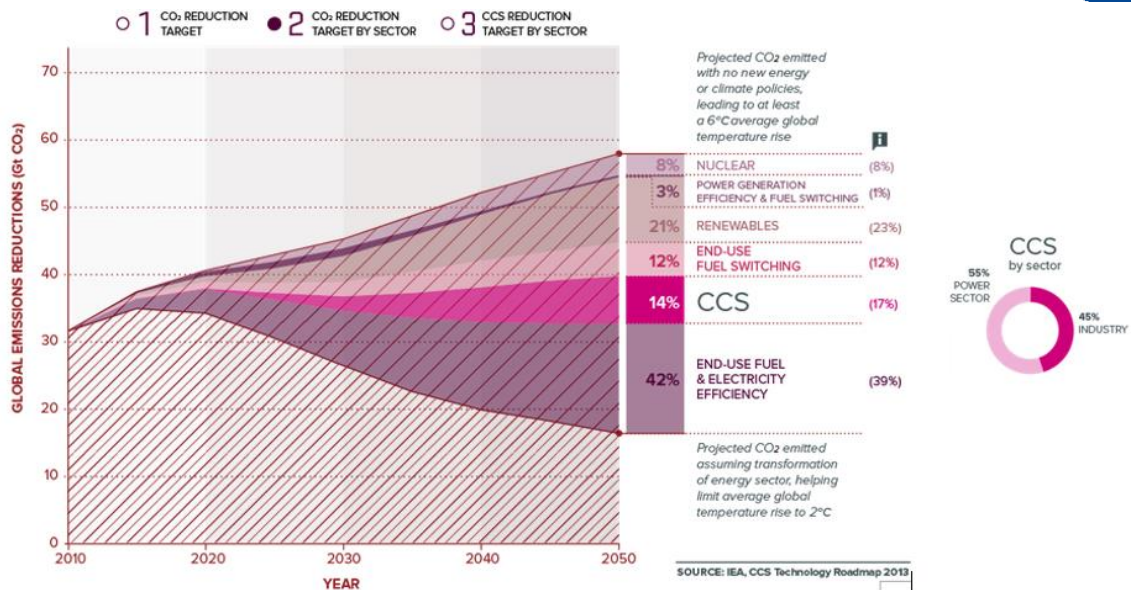


Figure 1.2. CO₂ reduction by year and CCS sector (CCS Browser, 2014)

CO₂ as an Enhanced Oil Recovery (EOR) Method: When the reservoir depletion happens water/gas injection is required to maintain the production. CO₂ is the cheapest solution among the gasses, and with the development of CO₂ capture companies are more interested in injection of carbon gas to increase EOR. This technique may extend a field’s productive life from 20 to 40 % of the original oil in place (OIP) (IEA, 2014).

What if CO₂ leaks and how to prevent it? CO₂ sequestration technology should be considered proven technology. However, concerns are whether CO₂ will leak from underground and reenter atmosphere or not. Two essential discussions have to be made in the case of leakage. Firstly, the leakage from well, formation can reduce effectiveness of CCS. Secondly, public concerns about the danger of CO₂ leakage.

Small leakages may happen for a long period of time that reduces effectiveness of CO₂. Large scale aquifer storage project at Sleipner has monitored no leakage since it started from 1996. Also storage in depleted reservoirs didn’t show any leakage. Field experience shows that most of leaks occur on the well casing/cement interface, cement itself and cement/formation interfaces.

CO₂ in high concentrations may cause suffocation (lack of oxygen). Significant amount of leakage from underground scares local residents; however, this scenario is highly unlikely and companies try hard to avoid this. In order to monitor a leakage field tests, model studies



have been applied to the CCS projects. To prevent CO₂ leakage, well integrity has to be insured.

1.2. Well integrity

General duty of well-operators is to ensure that a well is so designed, constructed, modified, commissioned, equipped, operated, maintained, suspended and abandoned in a way that there can be no unplanned escape of fluids from the well. Moreover, risks to the health and safety of persons from it or anything in it, or in the strata to which it is connected, has to be minimized (Richardson, 2012).

NORSOK D-010¹ (2013) defines well integrity as: *“Application of technical, operational and organizational solutions to reduce risk of uncontrolled release of formation fluids throughout the life cycle of a well”*.

The definition emphasizes the importance of technical and technological solutions to avoid flow of formation fluids from one formation zone to another, or to the surface throughout the life cycle of a well. According to Sangesland et al. (2012) well integrity is not only influenced by equipment robustness, but on the total process, resources and competence of the organization and individual.

The consequences of well integrity loss are blowout and leaks that damage materials, injure the personal, halt the production and destroy neighboring environment. Results are costly and risky repairs. Often loss of production in NCS exceeds the cost of the repair of the well.

1.2.1. Well barriers

The ability of a well to control well fluids and pressures (well integrity) throughout the all life cycle of the well is possible by providing it with operative well barriers. NORSOK D-0101 (2013) specifies that: *“There shall be two well barriers available during all well activities and operations, including suspended or abandoned wells, where a pressure differential exists that may cause uncontrolled outflow from the borehole/well to the external environment”*.

¹ Norsok D-010 is a functional standard and sets the minimum requirements for the equipment/solutions to be used in a well, but leaves it up to the operating companies to choose the solutions that meet the requirements.



“Well barriers (WB) are envelopes of one or more dependent well barrier elements preventing fluids or gases from flowing unintentionally from the formation, into another formation or surface.” (Vignes, 2011)

There are two main types of WB: Primary and secondary. The types of barriers depend on whether the well is for exploration or production purposes, which normally include cement, casing, valves and seals (NORSOK STANDARD, 2013).

1.2.2. Number of wells with issues

In 2009 OTM consulting reported 760,000 wells which are globally affected by integrity issues. Approximately 68400 (9 %) of them are permanently shut-in and 76000 (10%) are temporarily shut-in. Over 45% active wells had sustained annular pressure in deepwater and shelf GOM. 19% of the wells are shut-in that costs approximately \$1.09 billion per day (US Minerals Management Service survey, 2004). 34% of active wells (1600 out of 4700) in UKCS meet at least one anomaly (SPE forum North Sea well integrity challenges, 2009).

The Petroleum Safety Authority (PSA) in Norway made a “pilot well integrity survey” in 2006 based on supervisory audits and demanded input from 7 operators, 12 facilities and 406 wells. The survey showed that 73 wells-18% of 406 wells- have well integrity failures, issues, or uncertainty , and 28 wells (7% of 406 wells) of these are shut in because of well integrity issues.

In 2008 and 2009 24% of wells had integrity problems. After PSA’s well integrity analyses in Norway, risk level on the NCS well integrity was categorized and made in different colors (Norsk olje&gass, 2014). Table 1.1 shows the well integrity categorization and results from 2008 and 2009 (Vignes, 2011). Vignes (2011) reported 26% (452 of 1741) well integrity failures in 2011. The report has shown more serious well barrier element failures. Hence, 20% (142) of 711 wells were reported to have well barrier failures. In addition, 17% (89) of 526 production wells and 29% (53) of 185 injection wells are suffering with well barrier element failure.



Table 1.1. Well integrity categories (Ptil, 2008, Ptil, 2009 and Skjerven et al., 2008).

Well integrity category	Description:	2008	2009
Red	One barrier failure and the other is degraded/not verified, or leak to surface	1%	1%
Orange	One barrier failure and the other is intact, or a single failure may lead to leak to surface	10%	7%
Yellow	One barrier degraded, the other is intact	13%	16%
Green	Healthy well-no or minor issue	76%	76%

1.2.3. Well integrity concerns for CO₂ sequestration projects

Well integrity plays essential role on preventing of CO₂ leakages through wells. It has to be ensured before/during production and during well abandonment. Moreover, well integrity has to be guaranteed even after abandonment if carbon capture and storage (CCS) is applied. The (CCS) projects requires that CO₂ should be safely stored in reservoirs and prevented from rising to the surface or to formations higher up in the geological succession in the foreseeable future.

Table 1.2 demonstrates failure modes and mechanisms of WBE (cement), which also implement importance of every well barrier in CCS projects (DNV, 2012). Well barriers has to be designed to withstand for 1000 years on CCS

Table 1.2. Generic check-list of failure modes and failure mechanisms for wells under exposure to carbon dioxide (CO₂) – cement (DNV, 2012).

Well Component	Failure mode	Failure mechanism
Cement	Leak behind casing	- CO ₂ degradation of cement - H ₂ S degradation of cement - magnesium chloride degradation - thermal cracking and/or de-bonding (micro-annulus between cement and casing) due to Joule-Thomson effect during injection into, e.g., depleted gas reservoir - pre-existing channels in cement - pre-existing micro-annulus between casing and cement.
	Cracked cement and casing and/or de-bonding	- different relative movement along wellbore due to subsidence of reservoir and/or expansion due to injection (e.g. “shear, kink, collapse”).
	Poor cement job	- centralisers did not function properly, mud wiper trip before cementing did not remove mud residue effectively.
	Damaged cement across reservoir interval	- pressure tests (higher pressures) - temperature and pressure cycling - acids, chelators, stimulation.



1.2.4 Well integrity concerns for cement

Zonal isolation (ZI): ZI is an isolation of drilled hydrocarbon formations with cement or non-cement materials in wells to prevent any fluid communication. Hydrocarbon flows may originate from pay zones, or from non-commercial hydrocarbon-bearing formations. Pathways of fluid leakage in a well that results with poor ZI has shown in Figure 1.3 (Celia et al., 2004).

More dangerous gas leaks can be sustained behind the conductor, surface or intermediate casing that are filled with cement. Thus, zonal isolation which is part of well integrity depends on cement sheath integrity.

ZI has to be achieved during all life of the well, especially for CCS projects. Good ZI keeps the casing from deterioration, prevents blowouts by establishing a seal, guards the casing from shock loads and seals the thief zones (Nelson and Guillot, 2006).

Poor ZI leads to problems in controlling of the well and contamination of underwater sources, which can be tragic for the ecology and the local population.

“Improving primary cementing in new wells and repairing leaking wells are logical steps toward successful ZI and protecting environment” (Raafat et al., 2002).

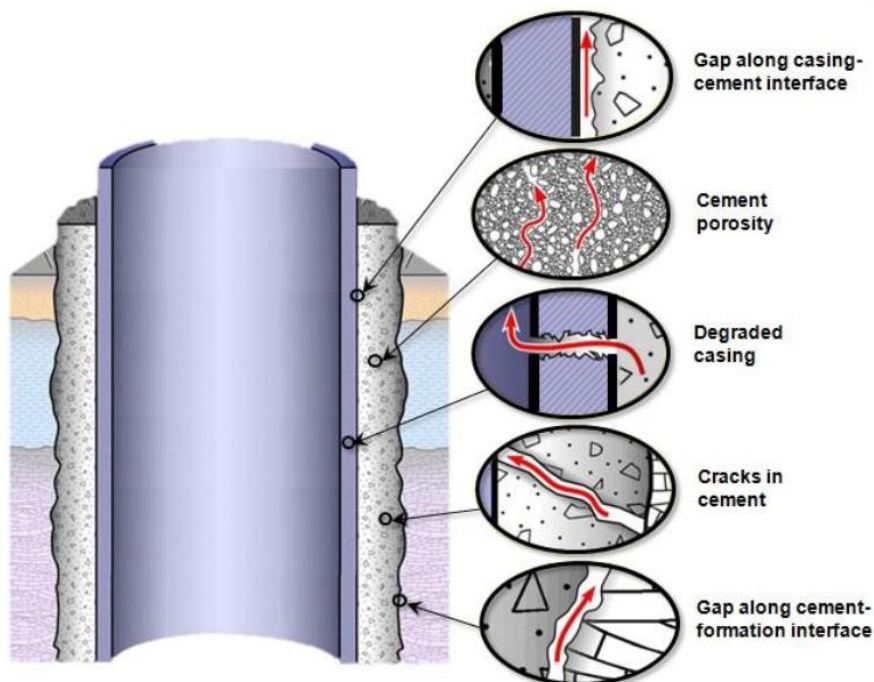


Figure 1.3. Poor zonal isolation. The figure outlines several possible leakage paths along wells. Based on (Celia et al., 2004).



Sustained Casing Pressure: Sustained casing pressure (SCP) is an excessive casing pressure in wells that persistently rebuilds after bleed-down. It can be measured at the wellhead with needle valve. If after closing needle valve there is still increase on casing pressure, then the casing is said to exhibit SCP (Bourgoyne et al., 1999). Problem of SCP on leaking wells is massive in oil industry. For instance, Figure 1.4 shows the percentage of wells experiencing sustained casing pressure (SCP) versus age for the 22,000 wells in the U.S. Gulf of Mexico in 2003 (Nelson and Guillot, 2006), and in 2011 in the GOM 11498 casing strings in 8122 wells exhibited SCP (Wojtanowicz et al., 2001). Origins of sustained casing pressure are shown in Appendix A, Fig. A3)

Consequences of SCP are irreducible casing pressure at wellhead, loss of containment with environmental and material damages and/or production losses, human losses (Bourgoyne et al., 1999). Remediation work is necessary if SCP is found (Nelson and Guillot, 2006).

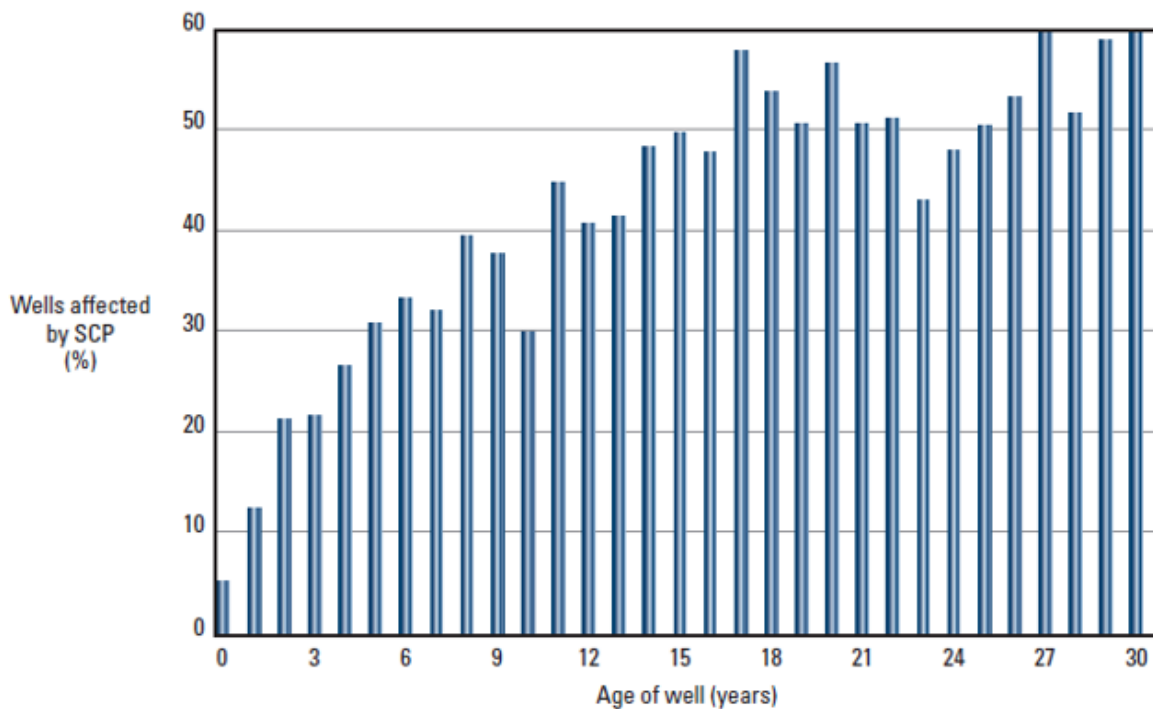


Figure 1.4. GOM wells with SCP (Nelson and Guillot, 2006).



1.3. Portland cement²

Portland cement is a common type of cement used around the world. It was developed from natural cements in Britain in 1824 and the name was patented from its similarity to Portland stone (Aspdin J, 1824). ASTM C150 defines Portland cement as: "*hydraulic cement (cement that not only hardens by reacting with water but also forms a water-resistant product) produced by pulverizing clinkers consisting essentially of hydraulic calcium silicates, usually containing one or more of the forms of calcium sulfate as an inter-ground addition*" (ASTM C150/C150M – 12 STANDARD, 2014).

1.3.1. Cement Chemistry

Calcium sulfate is later added to the clinker in order to produce the cement. Portland cement is comprised of 4 major compounds as shown in table 1.3. The compounds with the reaction of water form hydration products such as $3\text{CaO}\cdot 2\text{SiO}_2\cdot 3\text{H}_2\text{O}$ (CSH) and $\text{Ca}(\text{OH})_2$ (CH) (Nelson and Guillot, 2006).

Table 1.3. Mineralogical composition of unhydrated cement. Based on Nelson and Guillot (2006).

Oxide Composition	Cement Notation	Common Name	Concentration (wt%)
$3\text{CaO}\cdot\text{SiO}_2$	C_3S	Alite	55-65
$2\text{CaO}\cdot\text{SiO}_2$	C_2S	Belite	15-25
$3\text{CaO}\cdot\text{Al}_2\text{O}_3$	C_3A	Aluminate	8-14
$4\text{CaO}\cdot\text{Al}_2\text{O}_3\cdot\text{Fe}_2\text{O}_3$	C_4AF	Ferrite phase	8-12

Based on amount of compounds in cement ISO 10426:2000/API10A20 developed eight well cement classification system (A, B, C, D, E, F, G, and H) widely used in petroleum industry which are arranged according to the depth, temperature and pressure that they are exposed to (Appendix, Fig. A2, *ISO 10426-1, 2005*). Special cement systems were designed due to other well conditions such as weak formations, corrosive environments, Arctic conditions, SAGD wells, deepwater wells, HPHT, etc.

² Cement is a hydraulic binder, a substance that sets and hardens independently, and can bind other materials together. In the oil and gas industry it is mostly used to seal the space between formation and the casing, frequently applied for Plug and Abandonment operations.



1.3.2. Additives

Additives extend the usage range of cement, and change the properties such as, density, filtration rate, viscosity and Yield Point, thickening rate while the cement is in slurry phase.

Furthermore, properties like permeability, tensile and compressive strength, soundness and fineness can be changed by additives during settling phase. Commonly used additives are classified in Table 1.4.

Table 1.4. Additives and their functions on cement system (Nelson and Guillot, 2006):

Name	Function
Accelerators	Accelerate setting time of a cement system
Retarders	Slow down setting time of a cement system
Extenders	Materials that lower the density of a cement system, reduce the quantity of cement per unit volume of set product, or both
Weighting agents	Materials that increase the density of a cement system
Dispersants	Chemicals that used to reduce the viscosity of a cement system
Fluid-loss control agents	Materials that control fluid loss of a cement system to the formation
Lost-circulation control agents	Materials that control loss of the cement slurry to the formation
Specialty additives	Other additives such as, antifoam and defoam agents, fibers, etc.

1.3.3. Objectives of primary cementing

Primary cementing is the operation to place cement in the annulus between the casing and the formation. The objective of primary cementing is

- To create hydraulic seal between casing and cementing.
- To create hydraulic seal between cement and the formation.
- To avoid fluid or gas channels in the cement sheath (Nelson and Guillot, 2006, Bellabarba et al., 2008, Ladva et al., 2004).

Primary cementing operation eliminates drilling fluid from both wide and narrow annulus and tries to fill the entire annulus with competent cement or sealant (Tahmourpour and Griffith, 2004).



Poor cake removal, decentralized wellbore, fluid channels, corrosion, slurry design problems have been investigated to restrict gas flow into the system. Nevertheless, cyclic temperature/pressure loads/unloads, cement shrinkage, high cement permeability, hydraulic pressure variations affects cement during its setting time by creation of radial cracks, mud channels, micro-cracks and micro-annulus (Fig. 1.5). These lead to poor zonal isolation and requires remedial cementing job (Jackson and Murphey, 1993). Today, companies focus more on the primary cementing because the costs of repairing the cement job can far exceed savings in drilling costs. Remediation costs could be as high as US \$1 million per well that also includes the costs of work-over rigs and finding/ fixing leaks (Raafat et al., 2002).

However, even with successful primary cementing the companies have to fill requirements such as: Economics, liability, safety and governmental regulations.

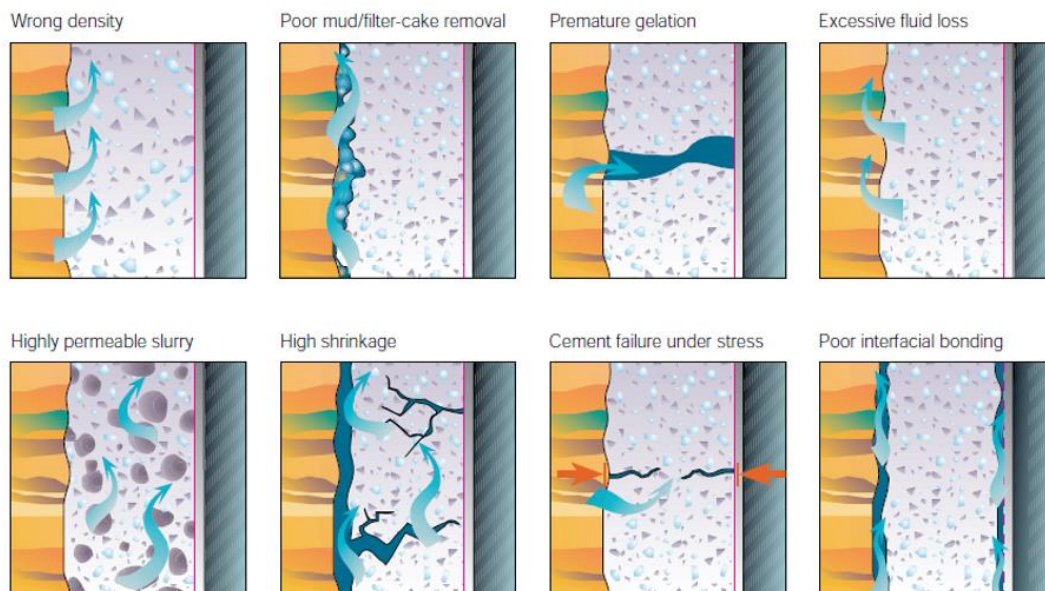


Figure 1.5. Fluid leakage on well cement. "Incorrect cement densities may create hydrostatic imbalance. Poor mud and filter cake removal leaves space for gas to flow upward through the annulus. Premature gelation leads to loss of hydrostatic pressure control. Excessive fluid loss contributes to available space in the cement slurry column for gas to enter. Highly permeable slurry has little resistance to gas flow and may leads to poor zonal isolation. High cement shrinkage leads to increased porosity and stresses in the cement sheath which may cause a microannulus to form. Cement failure under stress helps gas fracture cement sheaths. Poor bonding can cause failure at cement-casing and/or cement-formation interfaces". Based on (Bonett and Pafitis, 1996).

1.3.3.1. Mechanism of Primary Cementing

Primary cementing operation is performed after setting of the casing. During operation the cement slurry is pumped down the casing and up the annulus. Once the cement is set, it will



harden and gain mechanical properties with low permeability, by ensuring ZI and avoiding fluid flow behind the casing (Nelson and Guillot, 2006).

Before cementing job, cement powder is mixed with water and additives at surface facilities (batch and continuous mixing) to get desired slurry properties. Fig. 1.6, demonstrates normal primary cement placement with two plugs technique. Initially, casing is centralized so that cement could cover all area. To clean borehole from drilling fluids, remove mud cake, and to separate cement slurry from mud spacers (that creates mud channels) and chemical washers (dispersants, sweeps, and solvents) get pumped to the well.

Afterwards, cement slurry is displaced in the borehole followed by the bottom plug. After pumping desired volume into the string, a top plug is released from the plug container and is pressed down by displacement fluid. Bottom plug has a thin rupture rubber that make it dissimilar to top plug which has a solid rubber disk. Afterwards the diaphragm of the bottom plug can be ruptured by applied pressure. By sequence, the slurry is placed into the annulus among the well-casing and formation. Cementing job finishes when top plug reaches the bottom plug.

After cementing job the well is kept shut for 1-3 days to permit the setting of cement slurry. During that period, shut in casing pressure (SICP) should be monitored carefully. Because rapid pressure reduction can originate leak and fracture in settled cement. The advancement in the technology has introduced many new methods but primary cementing technique is still predominant and preferred (Bourgoyne et al., 1986).

Fluid flow pattern, density and viscosity effect, pipe movement, centralization have immense effect on primary cementing operation.

Several factors such as formation parameters, washouts, thief zones, wellbore geometry, and dissolved gas have also great impact on primary cementing (Saucer, 1987). General recommendations on primary cementing are shown in Appendix A, Table A2.

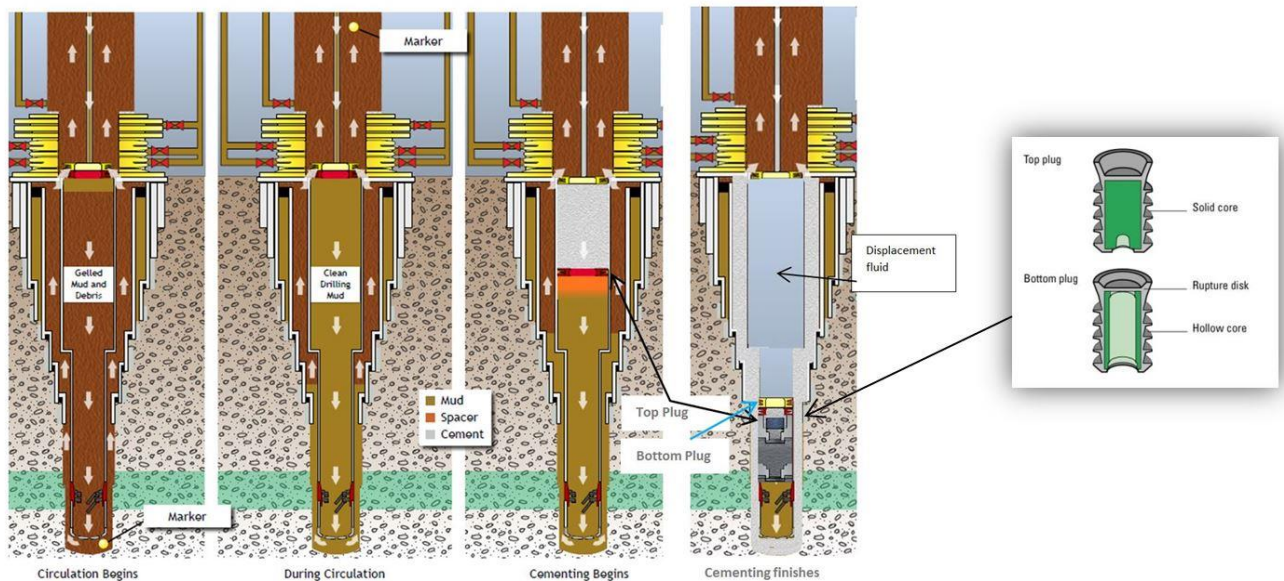


Figure 1.6. Typical primary cementing involves different stages such as, circulation of mud, spacers, and displacement of the cement. (Chief Counsel's Report, 2011).

1.3.4. Secondary cementing methods (Nelson and Guillot, 2006).

Secondary cementing is performed to repair primary cementing problems or to treat conditions arising after the wellbore has been constructed. Secondary cementing techniques are also named as remedial cementing. Before remediation the depth of leakage has to be determined. It is achievable by noise logs and carbon-isotope method.

The two most common types of secondary cementing method will be discussed:

Plug cementing: Cement plug is a common and cost effective method to isolate zones. The purpose of the operation is to shut off water, recomple higher or lower zones, or to protect a low pressure zone before performing a squeeze job or hydraulic fracturing operation. Plug cementing is also widely used in testing for exploration wells. Plug cementing is also used when drilling fluid circulation is lost during drilling. Cement is pumped through lost circulation zone. After cement set drilling can be continued.

Squeeze cementing: Squeeze cementing is defined as: “the processes of forcing cement slurry, under pressure, through holes or splits in the casing/wellbore annular space” (Fig10). Applications of squeeze cementing are: (1) *Repair of a primary cement job failures due to mud channels within cement*, (2) *Cement height is not sufficient*, (3) *Removing water invasion from above*, (4) *both hydrocarbon producing zone and its neighboring*, (5) *Repair of casing leakages due to corroded or split pipe*. Abandon a nonproductive or depleted zone, (6)



Seal off lost-circulation zones, (7) Avoidance of fluid migration into a producing zone
(Nelson and Guillot, 2006)



Chapter 2 Parameters causing weak cement/formation interface

Cement failures in the interfaces such as inner/outer micro-cracks, de-bonding can be caused by poor zonal isolation and due to that loss of well integrity. It is important to analyze cement from its mix time till after setting.

Several parameters and conditions that is origin of failures will be described and discussed in this chapter. Methods, scientific approaches, models and experiments will be discussed in order to understand and analyze the root of problems creating debonding (Nelson and Guillot, 2006).

2.1. Prior to slurry phase: Mixing of the cement

The quality of mixing and selection of mixing methods are important if the desired cement slurry wants to be obtained. *“The cement mixing procedure can be split into (1) a mechanical process that includes the wetting of the powder and the deflocculation³ and homogenization⁴ of the resulting suspension and (2) a physicochemical process that includes the dissolution of some cement phases, the formation of supersaturated solutions, and the precipitation of cement hydrates” (Vidick B, 1990).* (1) gives mixing energy and (2) gives mixing time which both determine good mixing. Mixing energy can be defined by Orban’s (1986) equation:

$$\frac{E}{m} = \frac{k\omega^2 t}{V} \quad (1)$$

³ Deflocculation is the absence of association which occurs when repulsive forces between particles predominate. Particles repel each other and remain as discrete, single particles (Wasan K, 2014)

⁴ Homogenization is any of several processes used to make a mixture of two mutually non-soluble liquids the same throughout (Wikipedia, 2014)



Where E is mixing energy (KJ), m is mass of slurry (kg), k is empirical constant ($6.1 \times 10^{-11} \text{ m}^2/\text{s}^3$), ω is the rotational speed (rad/s), t is residence time of a slurry in the blender (seconds), and V is slurry volume (m^3).

Low mixing time reduces the yield of the slurry and high mix time increases yield point (YP) of a cement slurry. The API determines mix time for cement slurry as 15 seconds at 400 rpm to mix water while adding cement powder, and 35 seconds at 1200 rpm (API specification 10A, 2002)

In the industry batch mixing and process controlled mixing methods are better than other methods (Bonett and Pafitis, 1996, Nelson and Guillot, 2006).

2.2. Slurry Phase

Improper wellbore clean-up (based on Nelson and Guillot, 2006).

The success of mud removal dictates the cement bond quality. Drilling mud sticks to the formation and creates filter cake. The filter cake alters the properties of rock that cement will interface. Consequently, the success of the cementing operation is being questioned.

The solution for mud removal comes with the use of preflushes⁵. Density of preflushes is slightly higher than drilling fluids. To meet requirements of a primary cementing, the drilling fluid and the preflushes must be fully removed from the annulus, and the annular space must be entirely filled with cement slurry. Fluid jets, scrapers, scratchers, casing reciprocation, and pumping acid are also helpful for mud removal. Some factors that influence cement in slurry phase are as follows:

Turbulence: Fluids flow patterns (laminar or turbulent) influence the fluid displacement in the borehole. Chaotic/swirled motion and the velocity of the fluid in borehole is almost same for turbulent flow. Contrarily, laminar flow has approximately zero velocity at the walls due to high friction and the maximum velocity in the center (Fig 2.1). Flat laminar flow doesn't have ability to displace mud, plus, clean formation and casing from filter cake. Meanwhile chaotic swirling motion of turbulent flow can displace mud, and remove filter cake. Improved turbulent flow with relatively high Reynolds number is desired for effective mud/mudcake removal (Kelessidis et al., 1996, Guillot et al., 2007).

⁵ Fluid containing no insoluble weighting agents used to separate drilling fluids and cementing slurries (API RP 10B-2).



Clark and Carter's (1973) experimental study on the effect of high eccentricities of gelled mud removal by cement slurries showed that laminar flow makes poor displacement. They got much better results by pumping cement slurry in turbulent flow.

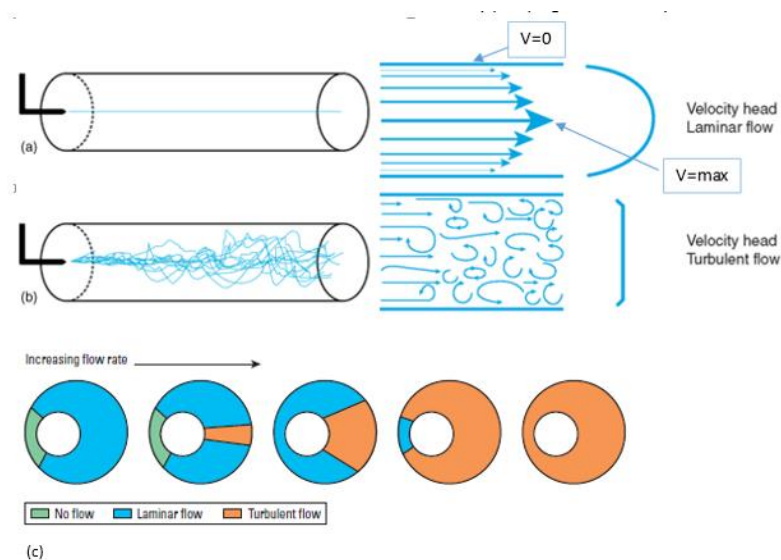


Figure 2.1 Fluid flow patterns: a) laminar flow, b) turbulent flow. c) mud removal with increasing flow rate (Nelson and Guillot, 2006).

Viscosity: Viscosity of fluids has to be considered properly because it can create unstable interface between fluids. In practice it is recommended that friction of displacing fluid (cement) must be greater than the displaced fluid (drilling fluid, spacer or washer), otherwise it can create fingering phenomenon (Schlumberger/NEXT, 2010).

Density: Density is playing great role when several fluids are in one system. If densities of fluids are close to each other they can mix or can be unstable in the interfaces. In order to avoid mixture, the displacing fluid density has always to be slightly higher than displaced fluid. If the displacing cement/preflushes has less density than the density of displaced mud it will lead to surface instabilities which cause remaining of mud in the wellbore.

Centrallizers: Casing centralizers are mechanical devices that avoid casing contact with wellbore wall, Fig 2.2. It improves the ability of the cement to cover all area on the pipe, assist on mud displacement and creates channel-free seal (McClean et al., 1967, Heathman and Rogers, 2005). Cement-mud mixture effect on rheology can be non-predictable. So if mixture is less viscous than the drilling fluid it may be squeezed to the wide side of the annulus, but mud in narrow side will remain due to less pressure on that side (Guillot et al., 2007). Fig



2.2b describes well flow profile with decentralized pipe. Most of the flow along the top of the pipe, and lower section of the wellbore can remain buried with cuttings and never have contact with any of the circulated fluids.

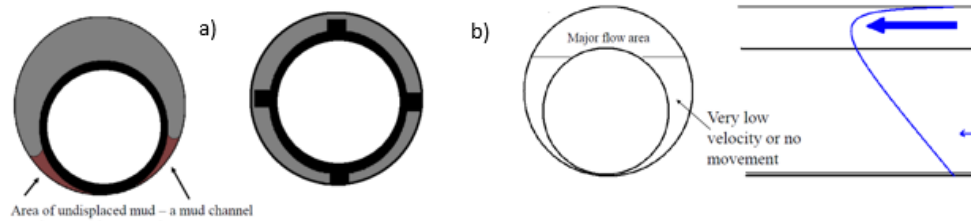


Figure 2.2. Decentralized wellbore: a) Fluid channels, b) flow velocity (Gekengineering, 2014)

Casing movement: In order to remove cuttings and reduce filter cake along their axes pipe movement applies during drilling. Pipe movement is possible by reciprocation and rotation motions (see Appendix A, Fig A4). McLean et al. (1967) observed that casing rotation is more efficient technique to remove mud/mudcake. Sanchez et al. (1999) mention that it is the orbital motion and not the rotation which improves wellhole cleaning.

Physical removal: In addition to mud cake removal with chemicals (dispersants, sweeps, and solvents), in oil industry it is wide to use physical removals such as, scrapers, scratchers and cable wipers. These mechanical removals are mechanical equipment that attached to the pipe. With the motion (rotation, reciprocation) of the pipe attached scrapers, scratchers physically remove mud from the wellbore (Raafat et al., 2002).

Wetting of the casing and formation: Cement de-bonding is influenced by surface wetting. During drilling operations casing and formation get wetted whether oil wetted (hydrophobic) or water (hydrophilic) wetted (Appendix A, Fig. A5). Thin layer of oil based mud remains between casing and formation, and restricts direct contact of interfaces by reducing the chance of good bonding (Halliburton-cementing, 2014).

Capillary action is the well-known physical process by which water moves through host materials (concrete) and eventually to the adhesive⁶-cohesive⁷/concrete interface and is believed to be the main cause for debonding. Capillary action depends on porosity, permeability and media discontinuities such as micro-fractures, fractures and imperfectly

⁶ Cohesion-ability of a similar material, solid or liquid to bind itself because of electrical attraction.

⁷ Adhesion- the tendency of dissimilar particles or surfaces to cling to one another.



sealed joints. For different types of rock this phenomena's effect will be different. Debonding will occur if the adhesive forces of the water to the concrete are greater than the adhesive forces between the adhesive and the concrete. To prevent debonding we need to change from hydrophobic to hydrophilic (Concure Products, 2010). The solution comes with hydrophilic-lipophilic (HLB) surfactants that water-wet the casing and formation Table A3, Appendix A (Nelson and Guillot, 2006).

Filter cake: During drilling, the wellbore and permeable formation the mud components concentrate at the wellbore due to pressure difference. It creates a low-permeable thin (2-5 mm) mud filter cake. The strength of cement/casing/formation bonding depends on the formed filter cake on wellbore walls. A good filter cake is desired during drilling process, although it becomes a problem on achieving a good seal between the cement and formation (Carter and Evans, 1961).

Randhol and Cerasi (2009) reported that shrinkage can occur with cement drawing water from the filter cake. Strength of the cake in contact with cement increases due to dehydration, and presence of filter cake reduces shear bond strength of cement with formation. Heathman and Vargo (2006) in their holistic review of salty and non-salty cement slurries reported the effect of salty cement to shrinkage. For their opinion medium or high amount of salty cement can reduce the effects of hydration bulk shrinkage.

The shear-bond strength between a cement and a Clashach sandstone in the presence of water-based mud (WBM) and oil-based mud (OBM) cake was measured by Ladva (2004) (Also by Carter and Evans, 1961, see Table A4). The mud compositions are given in Table A5 and Table A6, respectively (See Appendix A). From Ladva's (2004) experiments it can be concluded that OBM has the lowest shear bond strength (10^{-5} MPa versus 10^{-3} Mpa for WBM). This is because OBM cake does not interact with cement opposed to WBM. The washed WBM has share bond strength 3 times higher than unwashed WBM which is due to the removal of soft filter cake. Cement-Sandstone bond was very strong with existence of mudcake.



Chapter 3 CO₂ leakage along annular well cement

This chapter will discuss leakage of cement along well annulus which is caused by micro-annulus⁸ or de-bonding⁹. The chapter starts with the introduction of microannuli and the causes of debonding and micro-annulus creation. It will be followed by formation-cement-casing bond literature review and CO₂ effect on that bonds. Chapter will present relevant published works and knowledge gaps before to start chapters with experiments.

3.1. Micro-annuli

Micro-annuli is a micro fluid flow path between cement/formation or cement/casing which is caused by micro-annulus and de-bonding. Cement inability to form a good bond with the casing OD is called inner micro-annulus, while cement inability to form a good bond with the formation named as outer micro-annulus or micro-crack (Fig 3.1) (Talabani et al., 1993).

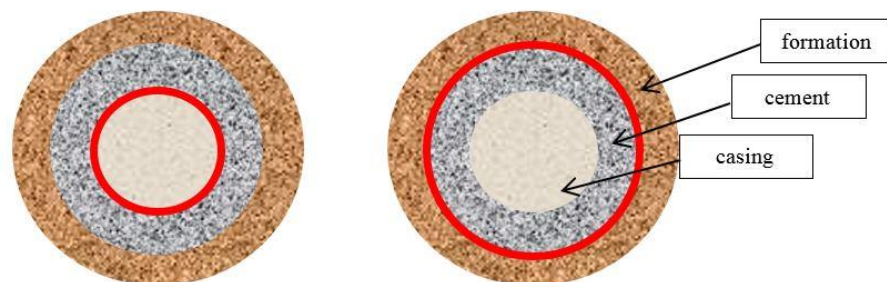


Figure 3.1 Micro-annulus: Inner (left), b) Outer (right)

Even though micro-cracks carries excessive importance for HSE, the companies have started to consider this problem few years ago. Companies know that micro-annuli formation means

⁸ Tiny cracks in microscopic level which forms in the cement/formation or casing interfaces.

⁹ The cement inability to bond the material after curing time.



loss of ZI, undesirable flow behind the casing (SCP), cross-flows between the reservoirs, and environmental damage by CO₂ which triggers loss of well integrity and costly remedial work or P&A operations (Bois et al., 2011).

Micro-annuli can be created by the contraction of the casing due to a decrease in mud density/low temperature/low pressure, hydration of the cement, and cement matrix deterioration by time factor (solutions for long term ZI). Talabani et al. (1993), Bois et al. (2011) and Nelson and Guillot (2006) report that factors such as poor mud cake removal, early cement set, casing decentralization, formation strains and stress, free water channel from the cement paste that form annuli at the top of the wellbore (horizontal well) are also the cause of micro-annuli formation.

Micro-annuli formation analysis showed that micro-annulus are originated from the operational phases such as well construction phase (drilling, cementing, completion) and lateral operational phases (depletion, operational regime, HPHT operation, injection, fracturing, perforation, hot oiling, killing of steam injection wells, etc) (Bosma et al., 1999, Bois et al., 2011).

3.1.1. Cement shrinkage

Micro-annuli formation mechanism can be enlightened by hydration process which leads to shrinkage of the cement. The hydration of cement without additives is an exothermic process (Ladva, 2004). Cement contact with water activates initial hydration process which afterwards slows down by the gelatinous hydrated material (calcium silicate hydrate -CSH-gel) (Nelson and Guillot, 2006). The main components of OPC (C₃S, C₂S, C₃A and C₄AF) have different hydration products:



The CSH gel depends on calcium concentration, temperature, additives and aging. Therefore, the formula of CSH is different in equation (2), (3) and (4).

By attraction of different compounds the gel structure becomes solid structure (silicate and aluminate phases) (Fig A6, Appendix A) (Bois et al., 2011). During that period reduction of the absolute volume happens. This is due to the volume occupied by the end of product.



Volume occupied by the end of product (cement hydration + water) is lesser than the volume occupied by the cement powder + water (Bois et al., 2011). The process named as chemical shrinkage which can be split up into two categories: Outer (bulk) and inner (matrix) shrinkage (Backe et al., 1998).

Bulk Shrinkage happens in the early phase of cement hydration and can be cause of micro-annulus formation (Rocha et al, 2013). According to Parcevaux and Sault (1984) bulk shrinkage is reported to be less than 1%. However, Reddy et al. (2009) found bulk shrinkage volume between 0.5% and 4.61 % without pressure and 1% -3.5% under high pressure which according to Jennings's (2005) realistic studies (3700 psi, 190 °F) (Reddy et al., 2009).

Different rock mineralogy influences shrinkage. Sandstone and basalt have greater shrinkage than limestone, dolomite and feldspar. Shrinkage also varies directly with water-cement ratio (Naus, 2005).

3.1.1. Pressure

Jackson and Murphey (1993), Goodwin and Crook's (1992) investigations showed excessive pressure influence on casing expansion with formation of a large inner micro-annulus while the cement is in gelation phase. They added the fact of mechanical/thermal loads which damage the cement sheath even after it had set. Investigations of Boukhelifa (2005) showed how formation strength can affect inner micro-annulus.

All the mentioned researchers measured flow-path of gas (micro-annuli) inside of cement which gave them permeability of cement interfaces. Big micro-annulus explained by high permeability numbers. During the test, pressure was manipulated in order to create micro-annulus.

Ladva's (2004) experiment is more interesting for a view point of this thesis. Ladva et al. (2004) made a small-wellbore simulator to understand gas tightness (Fig 3.2). The rock sample with diameter of 150 mm and length of 200 mm was used and placed inside of steel pressure vessel ($P_{\max}=31.5$ MPa). The outer cylindrical surface of the rock sample is surrounded by rubber sleeve through which a radial confining stresses can be applied. Capillaries placed between bottom platen and cement/rock interface are used to measure pore pressure during cement set and to supply gas for gas tightness testing. The capillaries are fully operational while the cement filled rock is under pressure and temperature. The experiment was held with marble-cement. 25 MPa overburden and confining pressures were selected to observe micro-annulus formation while the external pressure was decreased.



Cement was cured (80°C, 5 MPa, 5 days) while overburden and confining pressures were kept constant. Later on a gas tightness test was implemented with nitrogen at 5MPa pressure. Gas delivered at two points close to the bottom of the wellbore and at the interface between the cement and rock. The confining pressure was decreased from 25 MPa to 10 MPa while overburden stood constant at 25 MPa. The confining pressure decrease indicated creation of micro-annuli.

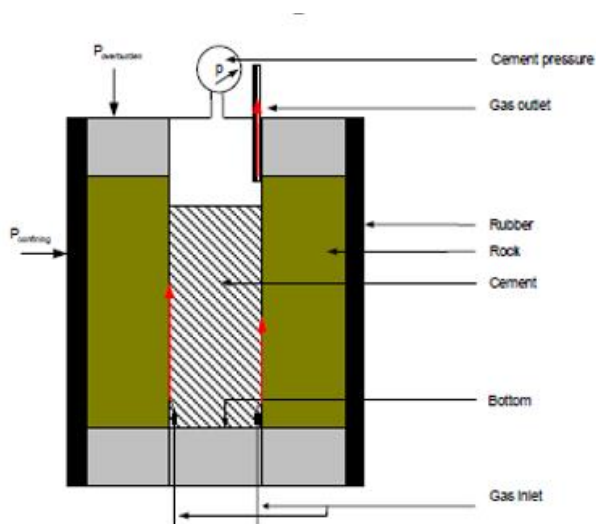


Figure 3.2. A schematic of the small-wellbore simulator (Ladva et al., 2004)

Theoretical Models: Based on experimental data, models were developed to find stress-strain relationship between casing, cement and rock. Many models were simulated and compared with laboratory tests and field examples. The first simulated model of long-term behavior of the cement sheath was created by Thiercelin et al. (1998). The model considered rock, cement and steel as a homogenous, isotropic system plus linearly elastic media where failure occurs. Bosma et al. (1999) introduced finite-element-analysis (FEA) to simulate the elastoplastic behavior of cement sheaths. Micro-annuli occurrence at the interfaces was analyzed due to de-bonding. The disadvantage of the model was the inability to show porous nature of cement and rock. After Saint-Marc et al. (2008) SealWell model which was based on the system response curve (SRC) method (Fourmaintraux et al, 2005) it was feasible to replace complex thermo-chemo-poro-mechanical model by simple wellbore-component simulations. It is the only model that included cement pro-mechanics behavior of cement until now (Bois et al., 2011). At the same time Garnier (2010) modeled tensile criteria which helped to see the



damages on the cement sheath (Fig A7, Appendix A). Bois et al. (2011) mentioned that increased pore pressure may close the micro-annulus.

3.1.2. Temperature

Temperature variations in the wellbore during injection or production lead to casing expansion and contraction. Moreover temperature affects volume of cement by hydration process. In both cases generation of micro-annuli is unescapable.

Goodwin's (1992) experiments verified the first mentioned temperature effect. He mentioned that in a flowing well temperature differences results with casing-diameter increase. The axial stresses created by the inner casing OD generate cracks in the cement sheath such as inner casing pressure does.

Temperature impact on hydration with a consequence of inner/outer micro-annuli was written by Nelson and Guillot (2006) and Ladva et al. (2004). Besides exothermic process, cement hydration is thermo-activated reaction. It means reaction is directly proportional with temperature. Elevated temperatures accelerate the cement hydration. Consequently setting time shortens and pressure drops rapidly which means high chances of micro-annulus formation.

Although thermal cycling¹⁰ at relatively low temperatures have some deleterious effects on the mechanical properties of concrete (i.e., cyclic heating generally gives lower strengths than a single heating), at higher temperatures, the first thermal cycle causes main percentage of damage. The extent of damage markedly dependent on aggregate type and is a loss of bond between the aggregate and cement paste matrix. Compressive strength reduces dramatically at elevated temperatures by reducing cement bonding (Naus, 2005).

Debonding or microannulus can form in a special temperature conditions when sudden temperatures are applied:

Steam Assisted Gravity Drainage (SAGD) environment: SAGD application performed by two parallel injector and production wells to exploit unconventional oil resources such as heavy oil, bitumen, and oil sand. SAGD applies hot steam injection to the formations and reduces the viscosity of heavy oil (Appendix A, Figure A8, Deutsch and McLennan, 2005).

¹⁰ Thermal cycling is a process of cycling between two (or more) temperature extremes. The test is used to evaluate material reliability and measure thermal failures.



Debonding, micro-annulus and other radial cracks form when temperature changes with an application of cold water killing technique on hot wells Bois et al. (2011)

Arctic environment: Operations in the Arctic environment with extreme temperature differences can fasten hydration, and affect in the same manner as killing of SAGD injector wells. This is because sometimes due to lower temperature on permafrost formations, upper layers of formation there are hole cleaning, stuck pipe, fishing problems which can be solved by hot mud during drilling and hot hydrocarbon steam produced up the tubing. These solutions increase casing/cement/formation temperature during operational phase; however, after end of the operation the temperature drops drastically. Arctic and SAGD operations are similar in that they experience temperature variations. But they also differ in that SAGD is a production method and the arctic challenge comes from the surrounding temperature (Kutasov and Caruthers, 1988, Pilisi et al., 2011).

3.1.3. Mechanical loads

Low Young's modulus, low friction angle and high cohesion are the most desirable cement mechanical properties (Randhol and Cerasi, 2009). These parameters can be altered by radial and tangential stresses. Radial and tangential stresses are generated due to pressure and/or temperature loads most commonly at the casing-formation or cement-formation boundaries. A failure of the casing/cement sheath interfaces occurs when radial stress is compressive and tangential stress is tensile. Since the radial stress is compressive in all materials, no debonding may form. However, magnitude and direction of radial stress is significant to be known since the development of micro-annuli in cement-casing and cement-formation interfaces is mostly as a result of occurrence of tensile radial stresses in the cement inner and outer surfaces. When the tensile radial stress is higher than the cement-casing or cement-formation bond strength, de-bonding occurs (Napibour and Joodi, 2010). Increase of Young's modulus can increase de-bonding occurrence in a cement (Randhol and Cerasi, 2009).

The mechanical properties of formation also have a big importance. For instance, expanding cements in a soft formation may create de-bonding (Randhol and Cerasi, 2009). Optimizing the relationship between the mechanical properties of the formation and the mechanical properties of cement sheath will increase the long-term cement integrity under different loads (Raafat et al, 2002).

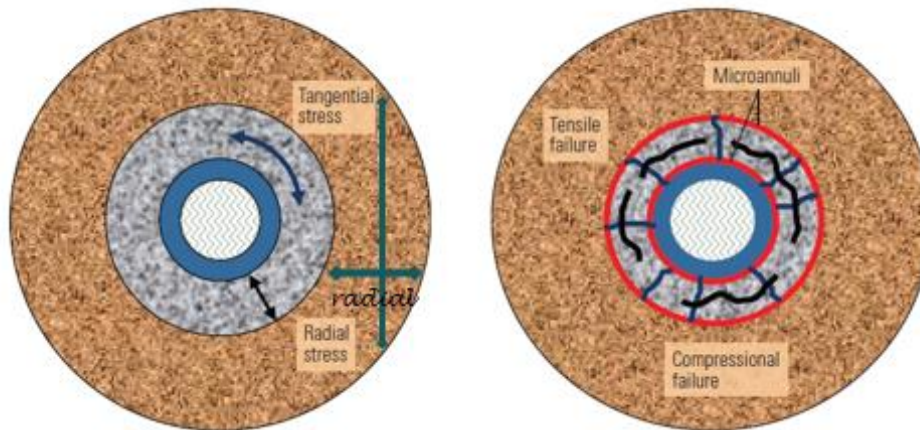


Figure 3.3. Radial and tangential stresses creates micro-annulus and cracks (Bellabarba et al., 2008).

3.1.4. Permeability

Several authors test results demonstrated that permeability measured at the time of micro-annulus/debonding formation varies significantly from one pressure loads/unloads to the next (Goodwin and Crook, 1992, Jackson and Murphey, 1993, Boukhelifa et al., 2005). From the experiments it is obvious that permeability depends on applied loads, cement system type, cement system mechanical stress failures, and hydration. The equation (5) for permeability was given by Darcy (Dake, 1977):

$$K = \frac{Q\mu}{A} \frac{dz}{dP} \quad (5)$$

Where: K is permeability of a material (Darcy or m²), μ is viscosity of the fluid (Pa•s), dP is pressure difference (Pa), A is cross-sectional area of material (m²), dz is a length over which the pressure drop is taking place (m) and Q is flow rate of the fluid (m³/sec).

3.2. Cement bonding

Cement provides a zonal isolation by following properties:

- Bonding between cement and casing
- Bonding between cement and formation

Two types of cement bond: shear and hydraulic bonds are criteria often considered for effective zonal isolation along the cement/casing and cement/formation interfaces. Shear



bonding mechanically supports the casing, and it is measured by the force is needed to initiate pipe movement.

Hydraulic bonding blocks the fluid flow in a cemented annulus and it is measured by the pressure needed to occur leakage on the casing/cement and cement/formation interfaces.

3.2.1. Cement/formation bond

Cement-sandstone/limestone bonding: High rock surface roughness gives better bonding between cement and formation (Tasong et al., 1998). Cement formation bonding depends also on the squeezed pressure and mud removal efficiency. Evans and Carter (1961) made experiments on Indiana limestone and Berea sandstone to measure the pressure required to break the shear and hydraulic bonds between the cement/formation interfaces. Six cement systems were placed against dry limestone cores in order to measure shear/hydraulic bond strength and compressive strength as shown in Fig 3.4. Prior to experiments sandstone core have been cracked therefore it wasn't used for experiments.

Figure 3.5 demonstrates results for a case when mud film remains on the formation surface and cement wasn't squeezed. The low numbers of bond strength shows the necessity of wellbore cleaning before cementing and careful selection of squeeze pressure.

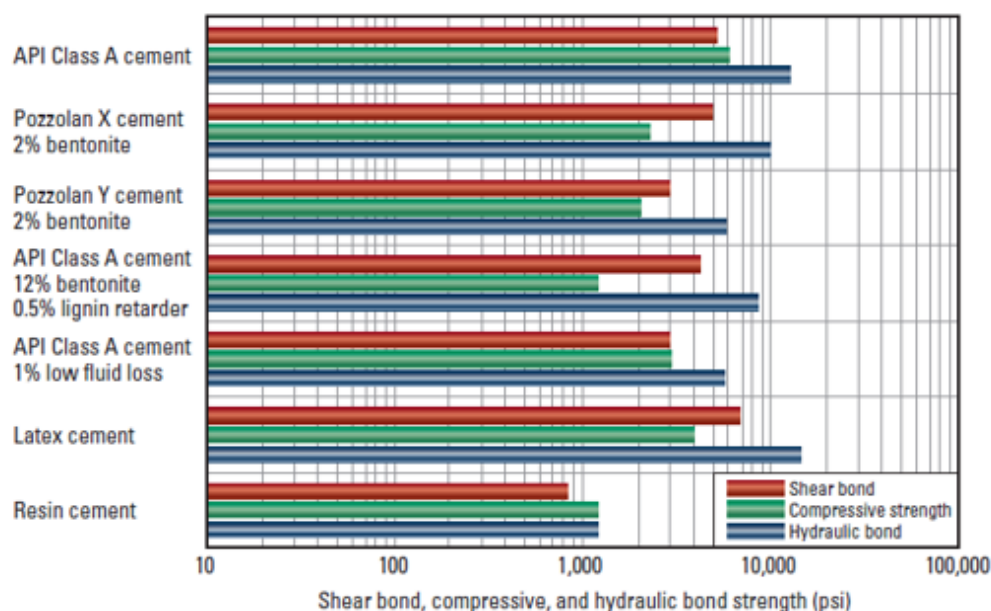


Figure 3.4 Bonding properties of cement to dry limestone (Evans and Carter, 1961).

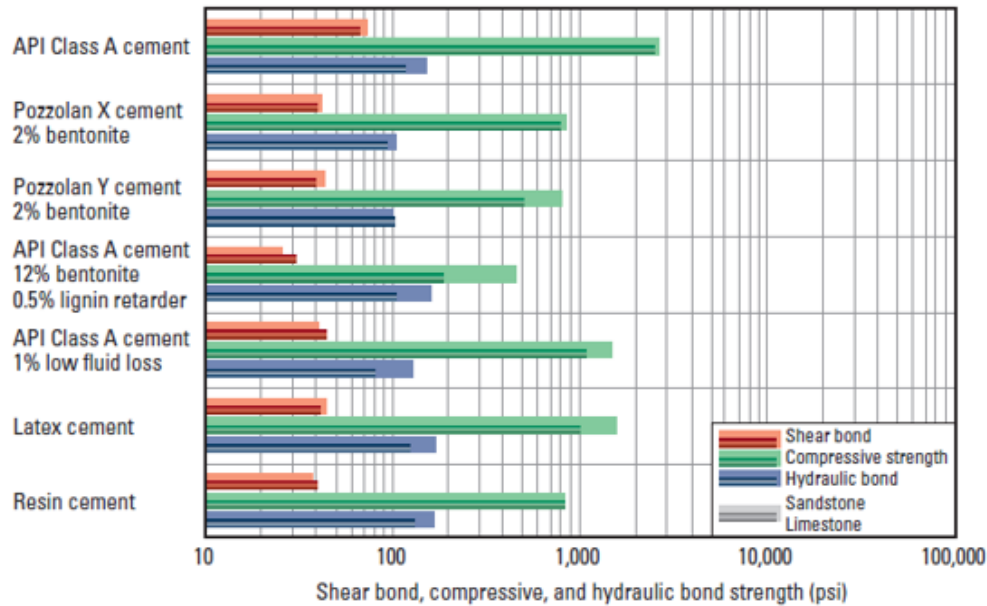


Figure 3.5. Bonding properties of cement to formation with cement not squeezed and walls not cleaned (Evans and Carter, 1961).

Cement-shale bonding: Shale formation interactions are complex; therefore, it is important to understand them for further analysis. Montmorillonite is one of the most common type of smectite which is most sensitive clay with high cation exchange capacity. The components of montmorillonite was given in Fig A6 (Appendix A). During drilling, water molecules of shale meet water inside of mud; consequently, water activity changes in shale formation. However, water activity of shale again changes when it meets cement. Depending on water activity of cement and shale, water can flow into the cement, by creating an exothermic reaction while setting. During this reaction reduction in pore pressure happens and cement will shrink. This creates debonding between shale/cement interfaces (Nelson and Guillot, 2006).

Ladva et al. (2004) made shear-bond or push-out tests to find shear-bond strength between the shale core or filter cake and set cement. He used swelling Oxford shale (17 wt% smectite) and non-swelling Catoosa shale (6 wt% smectite). The results demonstrated that Partially Hydrolyzed Polyacrylamide (PHPA) and glycol (or KCL) drilling fluids increase the swelling of the shale. However, OBM and silicate drilling fluids assist on shrinkage of the shale. Ladva's result showed that water activity affects shrinkage and hydration, and thus affects cement/shale bond strength.



Cement-formation bond with existence of filter cake: Peterson (1963) evaluated the effect of mud and filter cake contamination of cement on the cement-formation bond. In his experiments he used sandstone as a formation, TZ1 class cement and 3 types of mud (water bentonite mud, salt water bentonite mud and red mud). The interface between formation and cement had been tested in four modes: with mud cake presence, with mud cake scraped off, with mud cake scraped off and the surface washed with water, with mud cake scraped off and the surface washed with surfactant. After measuring bond strengths of the samples he reported that the lowest bond strengths was with a presence of mud cake and highest bond strength was obtained when the mud cake is scraped off and washed with surfactant.

3.2.2. Cement-casing bond

Successful bond between cement and casing interfaces depends on different parameters. Some of them were discussed earlier in “Improper wellbore clean up” subchapter. From experimental studies of Evans and Carter (1961) it was concluded that high roughness of pipe helps to establish strong shear and hydraulic bonds. Compare to new pipe rough casing surfaces as rusty, brushed and sandblasted increased the bonding strength (Table A7, Appendix A).

3.3. CO₂ effect on cement and formation

Over time cement degrades by surrounding environment and loses its beneficial properties such as mechanical integrity and hydraulic conductivity. It is under interest area to create durable cement and provide solutions on preventing cement degradation with time (Nelson and Guillot, 2006).

Portland cement: The contact of CO₂ with ordinary Portland cement (OPC) gives complex reactions by resulting chemical instability of the cement. During the reactions cement degrades and goes through carbonation. These unstable, reversible chemical reaction can be explained in three steps.

a) CO₂ reaction with water. CO₂ gases usually meet water which changes carbon dioxide from gas to aqueous state



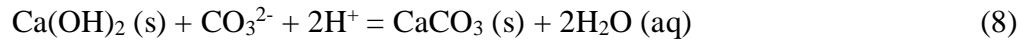
Kutchko et al. (2007) in his experimental work showed that after the reaction of Ca(OH)₂ during carbonation pH reduces significantly (Zone 1 on Figure 23).



b) Carbonation. After low pH more of the CO₂ reacts with water which forms HCO₃⁻ (Zone 2 on Figure 3.6).



The HCO₃⁻ reacts with calcium carbonate that forms calcium (II) carbonate.

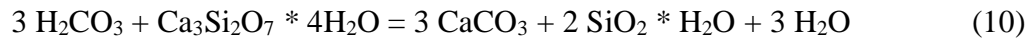


Last equation is named cement *carbonation*. Cement carbonation alter the cement chemical structure, and leads to lower the cement porosity. It happens because CaCO₃ molar volume is higher (36.9 cm³) than Ca(OH)₂ (33.6 cm³). Carbonation activates self-healing mechanism in the carbonate. It improves the properties of the cement, and assists on cement sheath integrity (Shen and Pye, 1989). Calcium (II) carbonate is soluble in water and can move out of the cement matrix through diffusion (Kutchko et al., 2007).

c) Cement degradation. The final reaction (Zone 3, close to the cement surface) is calcium silicate hydrate (CSH) reaction with H₂CO₃ that creates final product- calcium carbonate (CaCO₃):



or



“The stability of the C-S-H gel is compromised when the pH drops below 10, and once the C-S-H is degraded, the result is a highly porous amorphous silica gel” (Connell et al., 2012). The reaction increases the porosity and permeability of the cement in Zone 3 due to high volume of calcium silicate hydrate. Due increased porosity and permeability the influx of aggressive agents become and the corrosion process accelerates.

Duguid et al. (2005) reported that cement degradation appears first with white then grey, orange and finally with brown color. The orange color is due to iron-containing cement phases.

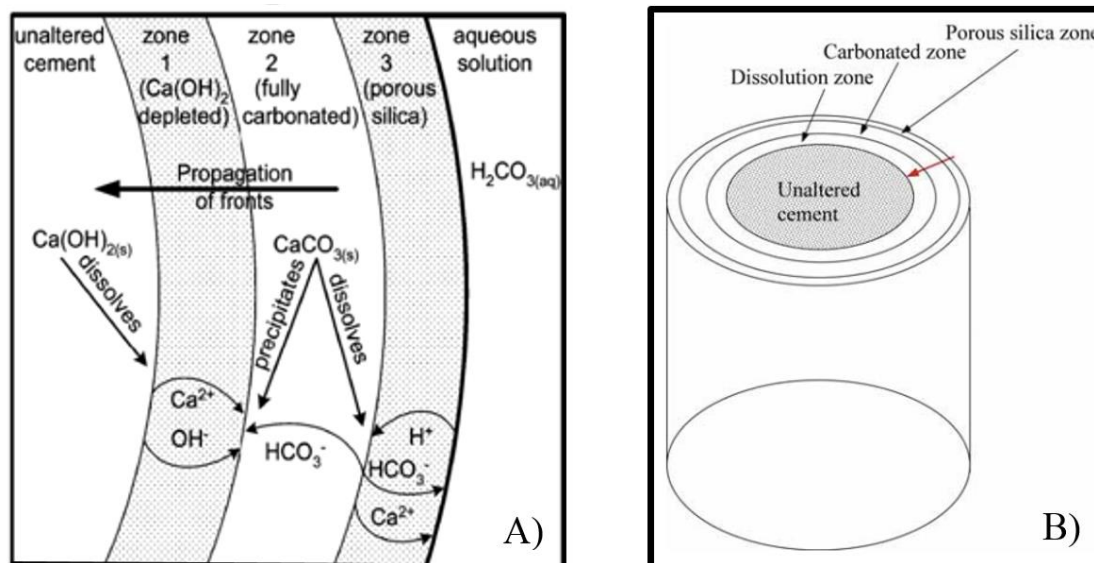


Figure 3.6. Illustration of the cement reactions zones in cement formation. A) Chemical reaction illustration: First zone (dissolution)- $\text{Ca}(\text{OH})_2$ dissolves and CaCO_3^{2-} forms. Second zone (carbonation)- CaCO_3 dissolves when $\text{Ca}(\text{OH})_2$ is spent. Third zone (redissolution of carbonate) - porous silica forms on a surface (Kutchko et al., 2007). B) Zone illustrations in 3D dimensions (Munz et al., 2009).

Experiments: The experiments of Barlet-Gouedarad et al. (2006)) and Kutchko et al. (2008) clearly documented reduction of carbonation rate with high salinity, and its increase by any fracture or weakness in the cement. Bachu and Bennion's (2009) experiments with CO₂ flow experiments (90 days, 60°) on a Class G cemented annulus monitored that the permeability of CO₂ flushed sample reduced during carbonation. Barlet-Gouedard et al. (2008) summarized CO₂ durability experiments for different cement mixtures (see Appendix A, Figure A9). Shen and Pye's (1989) monitoring on geothermal wells found out carbonation process dependency on temperature and CO₂ concentration. Krilov et al. (2000) studied these parameters' influence on carbonation. The study was based on wells exposed to high temperature (180°C) and high CO₂ concentrates (22%) for 15 years. These wells lost their performance through the years. They performed tests at simulated downhole conditions. Krilov et al. (2000) concluded that the loss of compressive strength and cement integrity was caused by high temperature and CO₂ concentration. This conclusion contradicted to previously mentioned authors work. However, Duguid et al. (2011) experiments on CO₂ exposed cement during one year time period showed that all authors are right. The cement exposed to CO₂ in his experiment started to degrade for 3 months, but degradation rate slow down by carbonation between 3 and 6 months. Thorough all experiment degradation has never stopped.



Portland cement-formation-CO₂-brine: Carrol et al. (2011) made experimental studies on cement-sandstone/shale-brine-CO₂ interaction. The core samples were taken from Salah field in Krechba, Algeria and were exposed to supercritical CO₂ in reservoir conditions. From the observations they made a simple geochemical model for the reaction of sandstone, shale and cement with CO₂ and brine in which chlorite, illite, albite, quartz and carbonate minerals are partially dissolved and boehmite, smectite, Fe(OH)₃ and amorphous silica precipitate. During experiments carbonation of cement was dominant (Fig 3.7, Carrol et al., 2011).

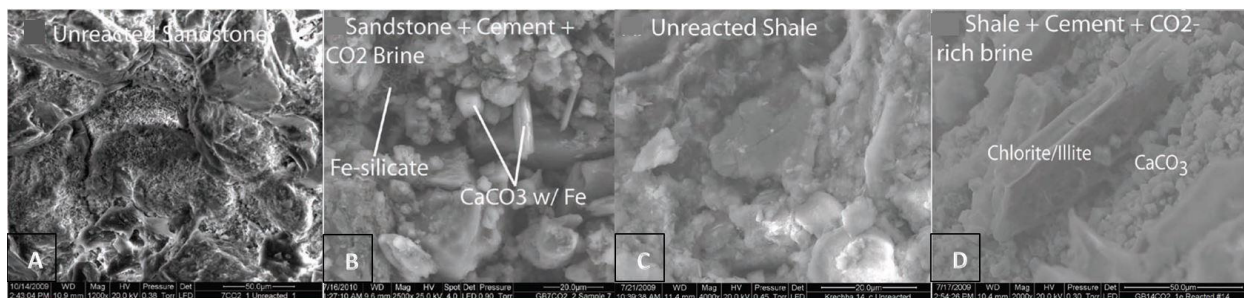


Figure 3.7. SEM images: a) Unreacted sandstone, b) Sandston/cement interface with CO₂ brine, c) Unreacted shale, d) Shale/cement interface with CO₂ brine (Carrol et al., 2011)

Meanwhile Duguid et al. (2011) had experimental studies on cement samples embedded in sandstone and limestone. The CO₂ saturated brine has been injected to see effect on cement/formation interfaces. Experiments were conducted at atmospheric condition, and pH adjusted for reservoir pressure and temperature by adding HCL. Brine was continuously replaced, and thus the reactant and reaction products diffused from the surrounding fluid into the cement-formation plug. It was found that the cement-formation interface may be subject to attack depending upon the mineralogy of the rock that makes up the host formation. Indeed, cement embedded in sandstone was shown to exhibit more damage than cement embedded in limestone, which showed no visible signs of attack and no increase in permeability after one year of exposure. In the limestone-cement experiments the water had been saturated with dissolved CaCO₃ prior to exposure to the cement to replicate the likely pore water chemistry within a limestone reservoir; this meant that some of the carbonation reactions would be constrained. The same study also observed that samples exposed to lower pH brine showed the most and fastest damage compared to those exposed to the highest pH which is a logical relationship with the understood role of acids in cement carbonation.

Formations within the seal lithology could play the key role in formation-cement interactions since the well integrity would need to be compromised over the seal in order for leakage to



occur via this route. In addition the ionic content of water has to be taken into consideration because it can affect reactions (Connell et al., 2012).

3.4. Relevant published experimental work

CO₂ leaks along annular cement has been studied by SINTEF Petroleum Research. In their experiment Opedal et al. (2013) studied the degree of debonding of the well cement as a function of varying surface properties of the rock. Experiment held where sandstone and shale were wetted by OBM and WBM, and OPC was squeezed into steel chamber which surrounded mud wetted rocks (Fig 3.8).

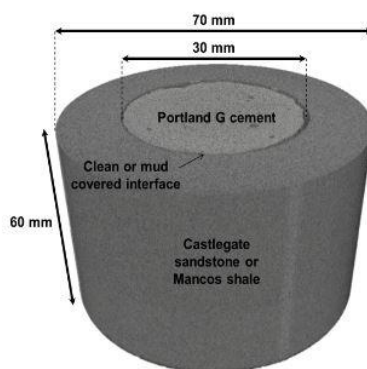


Figure 3.8. An illustration of the sample geometry of Opedal et al. (2013).

Opedal et al. (2013) investigated the debonding in cement/formation interfaces by μ -CT. It gave them an advantage to see the interface porosities that reflects the degree of bonding/debonding. However, they didn't cure samples under pressure which make it different from real cement curing process. Opedal et al. (2014) also studied sandstone, limestone, chalk and shale where they showed more debonding degree for sandstone and chalk. From the debonded areas they calculated how much CO₂ can flow through cement-formation interface.

Agbasimalo (2012) made experiment on cement-formation interfaces. The rock formation type was selected as Berea sandstone. The cement-rock composite cores had 0-10% mud contaminations. Samples (cement-rock interface area) had been characterized in micro scales before and after flow-through experiments with brine. He reported that the porosity increased at cement-rock interfaces for both 0% and 10% mud contaminated samples. Larger vugs¹¹

¹¹ Vug- Secondary porosity. Here it can be defined as pore.



were created on the cement-rock interface with the increased mud contamination which reduced the stability of the interface. Moreover, it was concluded that the vuggy porosity formed a larger area of contact between the cement and the flowing brine, leading to greater leaching of Portland cement. Leaching may lead to interconnectivity of the large pores in a long term that resulted in loss of zonal isolation. Although the experiments of Agbasimalo (2012) is close to explain real well CO₂ leakage mechanism on CCS projects, he just considered brine effect to the interfaces by skipping substantial effect of CO₂.

As discussed above Carroll et al. (2011) investigated cement formation CO₂ interaction geochemistry, Duguid et al. (2011) studied CO₂ flooding between cement/formation and finally Opedal et al. (2013) experimented de-bonding effect, and finally Agbasimalo (2012) mud contamination effect on the cement-formation interface. However, none of authors until now investigated de-bonding formation under more realistic conditions and CO₂ effect in a full scale.

3.5. Knowledge gaps

From literature study we can see that the microannuli created by debonding in the cement/formation interface is the main well integrity concern for CCS projects. These flow paths allows CO₂ to migrate upwards. CO₂ reaction with formation, cement, brine and the casing gives different reaction products. Different question arises concerning well integrity:

- What is the impact of pressure and temperature on debonding?
- What is the impact of different formation types on debonding?
- What is the impact of different cement types on debonding?
- What is the impact of different fluids (water/ mud / mudcake covered the rock) on debonding?
- What is porosity of interface and geometry of microannuli?
- What is the impact of CO₂ on a cement, formation and cement/formation interface?
- How much CO₂ flow we can expect along cement/formation interfaces and which factors affect it?



Chapter 4 Experimental details

The objective of this thesis work is to analyze the bonding at the cement-formation interface and see CO₂ effect on the interface. This preliminary study will assist on well integrity problem on CCS projects by focusing on CO₂ leakage along annular cement. Before to establish setup all the previous literature and experimental works were considered in order to eliminate problems in the lab. Different materials, equipment and software were used to achieve aimed goal.

4.1. Materials:

Rock Formations

Four different rock formations are to be prepared for the experiments: three shale types (Marcellus, Pierre and Eagle Ford), one chalk (Mons), and one sandstone (Castlegate) (Fig 4.1). Sandstone has high porosity and permeability while chalk permeability is medium and shale permeability is close to zero. Eagle Ford and Pierre shale samples were kept in oil for long term storage. Before sample preparation shale were wiped in order to make rock sample dry. The other rock samples were initially dry. Dimensions of cylindrical rock samples are shown in Fig 4.2a. Length, diameter and volume of each sample are shown in Table A8, Appendix B. The permeability and mineralogical compound distribution of rock samples are given in Table 4.1.

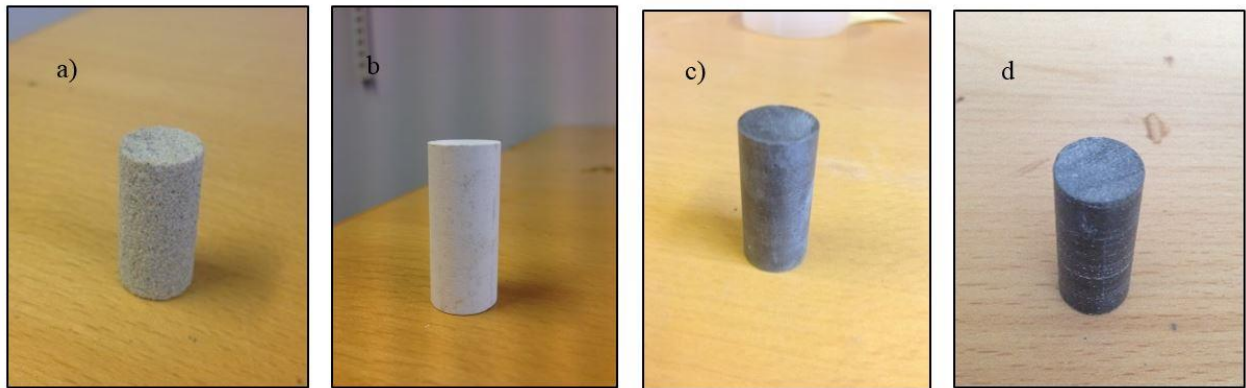


Figure 4.1 Rock samples: a) Castlegate sandstone, b) Mons chalk, c) Marcellus shale, d) Eagle Ford shale

Table 4.1 The compounds of each rock sample (Bruner KR and Smosna R, 2011, Alqahtani et al., 2013, Schultz, 1964)

Formation type	Name	Permeability	Calcite/Dolomite content	Quartz/Feldspar content	Clay content
Sandstone	Castlegate	800 mD			
Chalk	Mons	Average to high			
Shale	Marcellus	μD-nD range	3-48%	~30%	10-45%
Shale	Eagle Ford	nD range	~50%	~10-20%	~20%
Shale	Pierre	nD range	38%	7%	55%

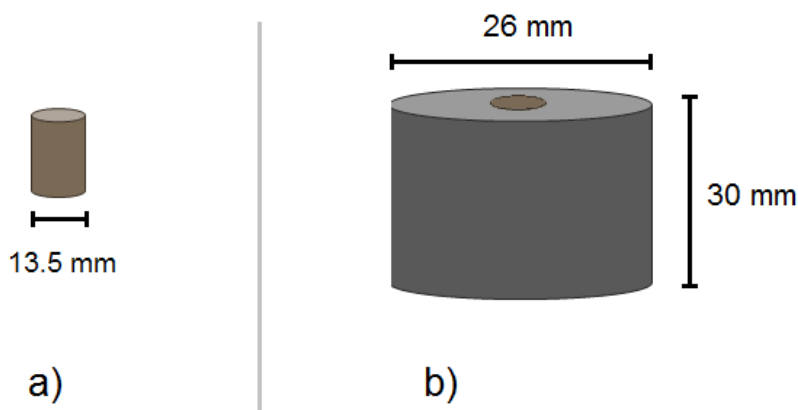


Figure 4.2. Dimensions of samples to be prepared. a) rock cylinder. b) rock cylinder with cement sheath.

Cement

Two cement types are to be used in the experiments: Ordinary Portland Cement (OPC) (Class G, NORCEM) and specialized cement type (SPC). OPC and SPC were used to cement around the rock samples. The specialized cement system is OPC with 2 % by weight of cement (BWOC) CaCl_2 (EMSURE). This cement can also be called as “Salty cement”. The mineralogical composition of OPC cement clinker are given in Table 4.2.

Table 4.2. Mineralogical composition of classic Portland cement clinker (Nelson and Guilloit, 2006)

Oxide Composition	Cement Notation	Common name	Concentration (wt%)
$3\text{CaO} \cdot \text{SiO}_2$	C_3S	Alite	55-65
$2\text{CaO} \cdot \text{SiO}_2$	C_2S	Belite	15-25
$3\text{CaO} \cdot \text{Al}_2\text{O}_3$	C_3A	Aluminate	8-14
$4\text{CaO} \cdot \text{Al}_2\text{O}_3 \cdot \text{Fe}_2\text{O}_3$	C_4AF	Ferrite phase	8-12

Drilling fluids

One in-house made drilling fluid is to be used in the experiments. The chemical composition of water based mud (WBM) is given in table 4.3.



The water used in the cement paste and in the mud was of Trondheim municipality tap water quality.

Table 4.3. Chemical composition of the water based drilling fluid

Compound	Mass (gr)	Function
Water	439	Continuous phase
Na ₂ CO ₃	6.0	pH control
Barite	230	Weighting material
Bentonite	12.6	Gel agent
Xanthan gum	0.9	Viscosifier

Steel Chamber

Steel chamber molds manufactured in workshop were used in the cementing procedure of rock samples. Steel chamber consists of two parts with half cylindrical shaped segments. The segments can be joined together by screws. The shape and dimensions of a steel chamber are shown in Figure 4.3. In order to get smooth surfaced samples inside, walls of cylinder were sprayed by friction free materials. Places where cement can flow were smeared by fat.

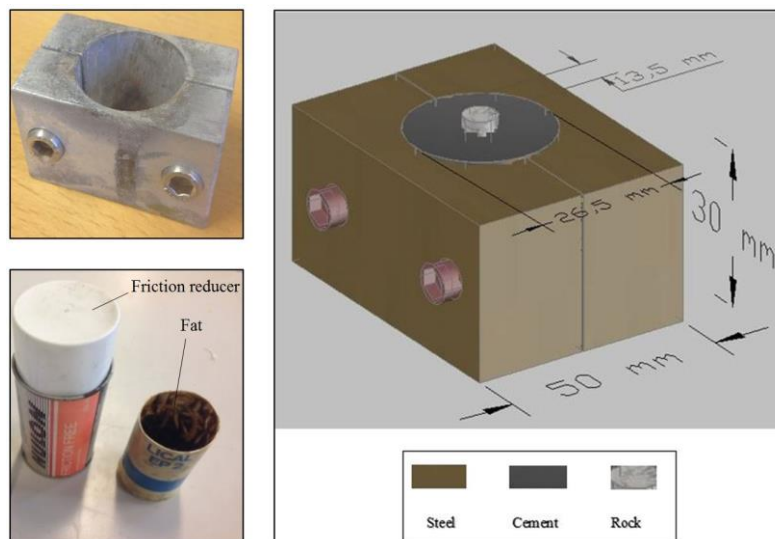


Figure 4.3. 3D model of steel chamber with dimensions.



Vacuum chamber

Vacuum chamber was used to create filter cake around the rock. Samples were treated with filter cake for 1 hour.

Brine

Brine was used in CO₂ exposure and flooding experiments. The composition of brine is shown in table 4.4.

Table 4.4 The composition of homemade formation water (brine)

Volume distilled water	1000 mL
Mass NaCl	30.158 gr
Mass CaCl₂ x 2 H₂O	3.194 gr
Mass MgCl₂ x 6 H₂O	3.057 gr

Pressure Chamber & Heating Oven

Cement rock sample curing process has been held in a pressure chamber and heating oven. After placing samples into the pressure chamber (Petek) pressure was kept constant (15 bar) (see Fig 4.4). Thus shrinkage factor was minimized. During curing period Nitrogen was injected into the pressure chamber. The location of pressure chamber is inside of heating oven with a constant temperature (66°C).

Pressure chamber and heating oven have also been used for batch exposure experiment. This time temperature and pressure was same as at curing time but CO₂ has been used instead of nitrogen.

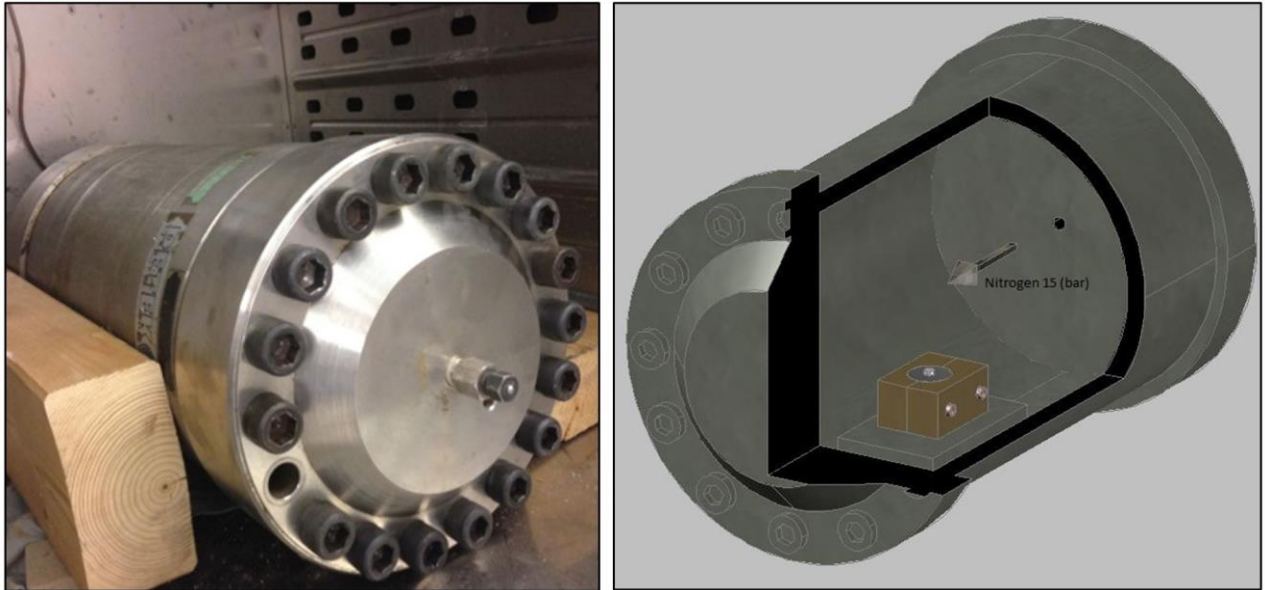


Figure 4.4. Pressure chamber (left) and 3D cross section view during curing time (right).

CO₂ flooding setup

Three Eagle Ford shale samples with special (salty) cement had been flooded up with brine and CO₂ in order to see detailed changings on a cement-rock interface. CO₂ flooding experiment wasn't conducted for every sample due to time limitation. Samples were cut to make better confinement. The dimensions of samples are given in Appendix B, Table A9. Shale samples had been covered with white plastic lent and nickel foil to create better confinement inside of a cell (Fig 4.5).

The Cell was located inside of heating cabinet. CO₂ and brine had been injected from High Pressure Piston Bottle (HPPB). The pressure inside of the High Pressure Piston Bottle was initiated by Beckman pump. Back pressure valve secured the setup if some unexpected increment on pressure is seen. The excluded fluid from the system had been weighted on a scale. The flooding setup had been simplified in figure 4.6.

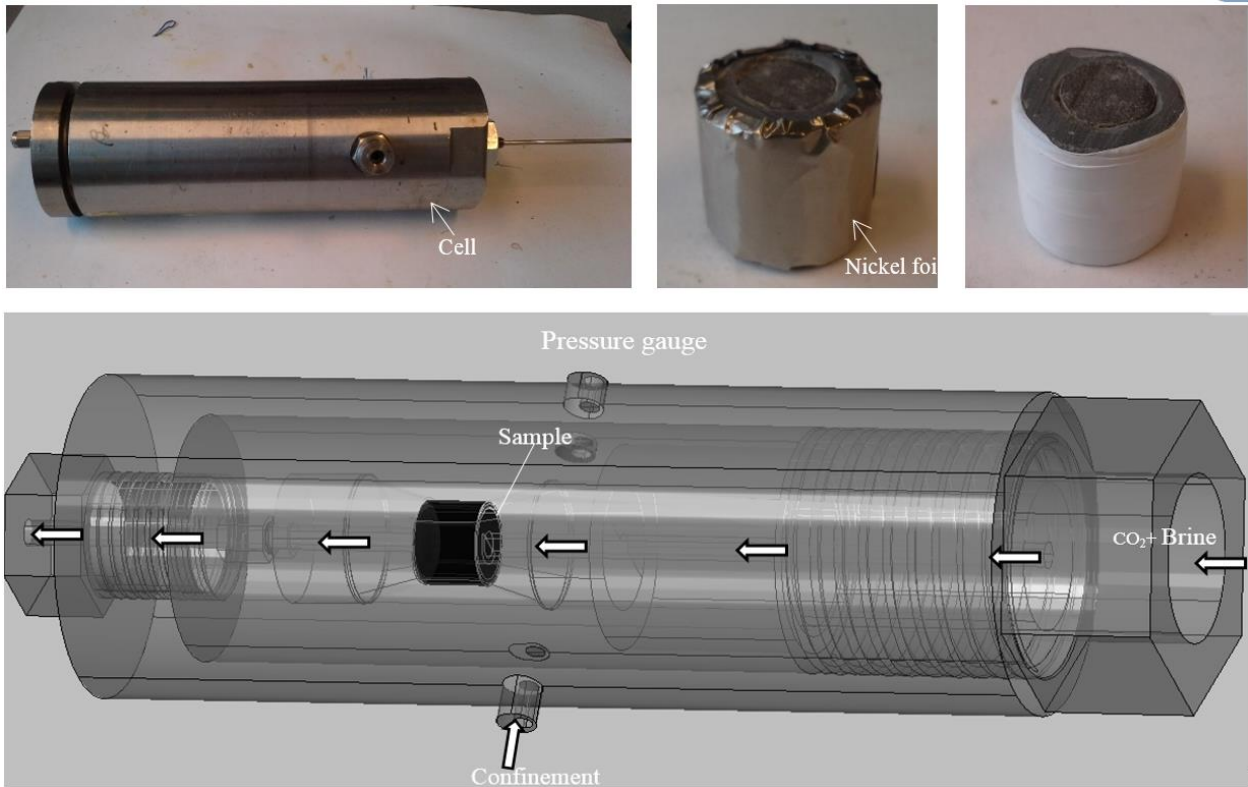


Figure 4.5. Illustration of a Cell (left), sample preparation (right) and 3D drawing of the Cell in AutoCAD (below).

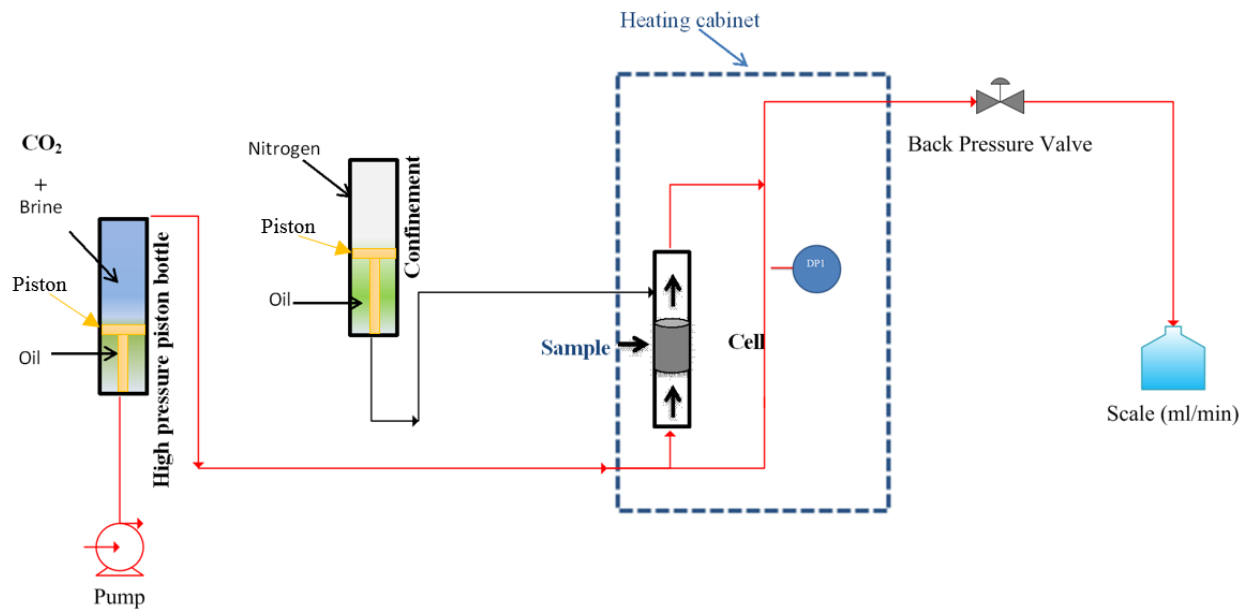


Figure 4.6. Simplified sketch of CO₂ flooding setup.



4.2. Methods

Application of drilling fluid

The rock cylinders are to be treated with fluids prior to cementing. The aim of the fluid treatment is to give different properties to the interfaces. This study include three different interfaces prior to cementing that reflects realistic conditions in a wellbore:

- a) A water wet rock formation
- b) Drilling fluid film
- c) Filter cake

Two fluid types will be used in this context, tap water and water based drilling fluid. The treatment of the rock cylinders is to be performed using two different methods, immersion at ambient pressure and temperature and immersion of drilling fluid at vacuum to facilitate filter cake formation. The treatment procedure starts with putting the rock cylinder(s) in a beaker fully covered by the intended fluid. Treatment time is 60 minutes both at ambient pressure and vacuum. Afterwards treated rock cylinder(s) removed gently from beaker to not damage fluid cover. Treated rock cylinders were kept for 10 minutes in normal temperature and pressure to run off excess fluid (Fig 4.7). During fluid treatment procedure, all Pierre shale rocks get destructed.

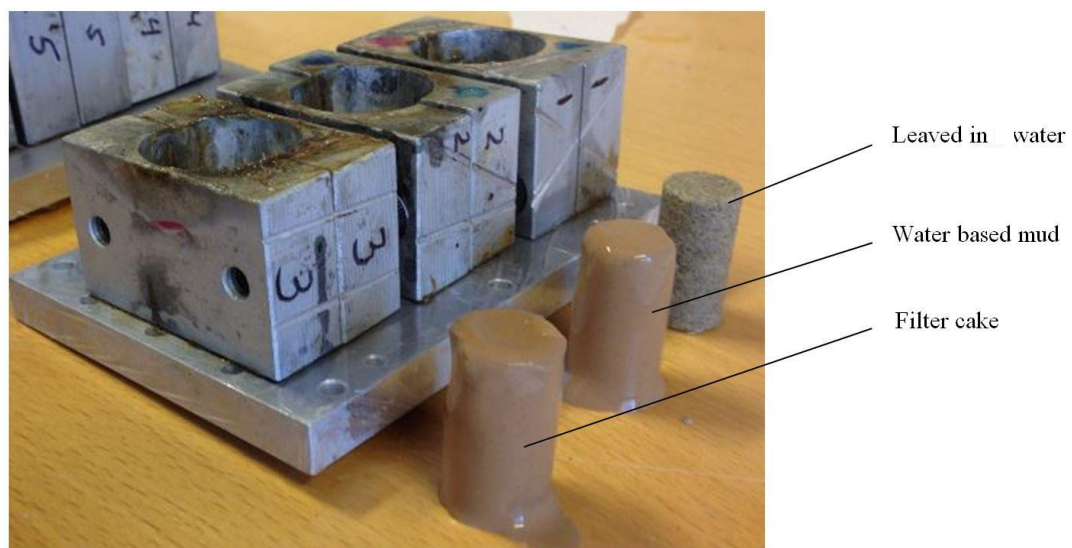


Figure 4.7. Treated rock samples before cementing procedure.



Preparation of cement paste

The cement is to be mixed according to API specification 10A using a Constant Speed Blender (Figure 4.8) manufactured by OFITE. The equipment automatically apply mixing energy and if desired set mixing time. The following cement paste composition should be used.

$$\text{Mass water / mass cement} = 0.44 \quad (10)$$

The mixing procedure begins with adding tap water to the blender and starting the motor at 400 rpm for 15 seconds. During that period cement powder has to be added to the blender. After 15 seconds of mixing at 400 rpm the motor is increased to 1200 rpm for duration of 35 seconds. All cement slurry were mixed very well.

Preparation of drilling fluid is also in the same way as preparation of cement paste.



Figure 4.8. OFITE Constant Speed Blender used for preparing cement paste (OFITE, 2014).

Application of cement and curing

The cement paste is to be placed using pipettes between two steel compartments jointed together. Before placement of cement, the rock cylinder is placed in the center of the



compartment, as illustrated in figure 4.9. After the cement is placed, the compartment is placed in an autoclave and let to cure for 7 days at 66°C and 15 MPa.

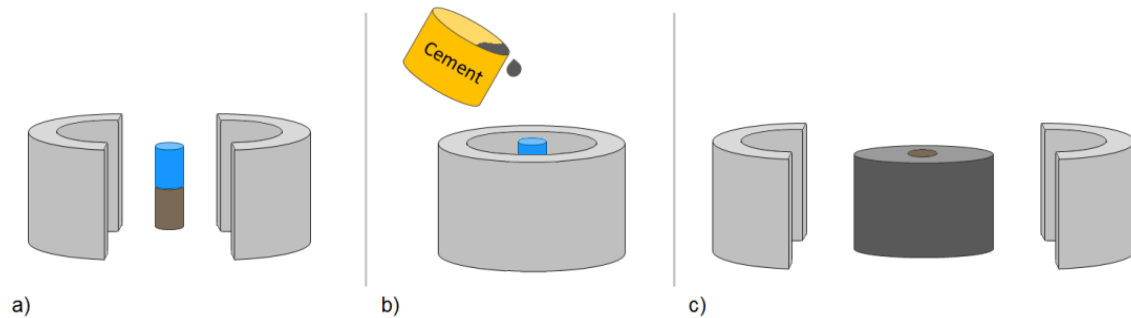


Figure 4.9. Illustration of the sample preparation: a) placement of rock cylinder inside steel compartment, b) placement of cement paste, c) disassemble steel compartment after curing.

After 7 days (168 hours) of curing, the samples (see fig 4.10) are taken out, and the steel compartment is gently disassembled while all the materials are warm. The dimensions of samples are given in Fig 4.2b.

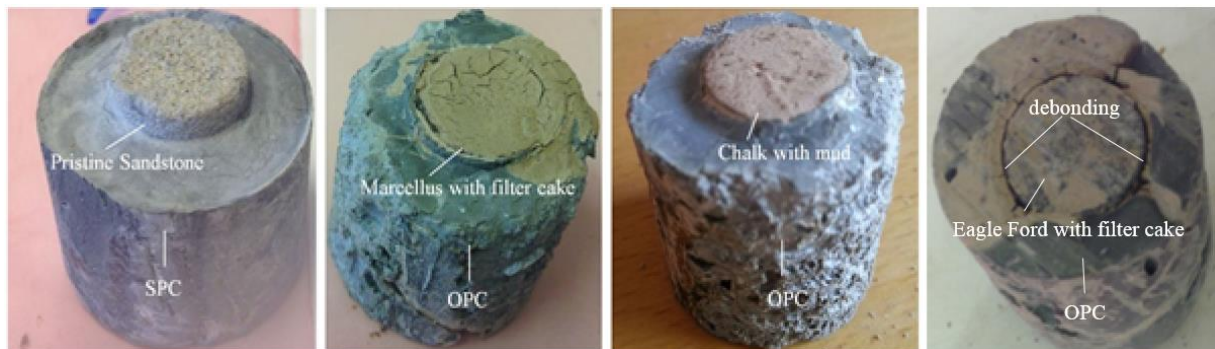


Figure 4.10. Cured cemented rock samples.

Preparation of CO₂/Brine fluid mixture

In most field cases CO₂ meets formation water; therefore, in this preliminary experimental study carbon dioxide and brine mixture was preferred as a flooding material. CO₂ tank connected to process side of bottle. Both valves were opened. In the High Pressure Piston Bottle, 100 mL of hydraulic oil was removed from hydraulic side while CO₂ was injected in the process side. The valve to the hydraulic side was closed and the process side with CO₂ and H₂O was pressured to 30 bar. The percentage of CO₂ in bottle had been calculated as



follows:

1) By calculating moles of CO₂ from Ideal gas law

$$PV = nRT \quad (10)$$

Where R is universal gas constant and equal to 8.314 J/(Kmol), T is temperature in standard condition (298 Kelvin), P is pressure inside of High Pressure Piston Bottle (30 bar or 29.607 atm), V is volume (100 mL= 0.0001 m³), n is molar mass (1.2x10⁻⁶ mol) and was calculated from equation (10).

2) By calculating moles of water:

$$n = \frac{m}{2+16} \quad (11)$$

Where V is the original volume of brine in tank (600 mL or 0.0006 m³, m is mass of H₂O (0.5982 kg) and was calculated by multiplying volume to density of brine (997 kg/m³), n is molar mass of brine (0.033233 mol) and was calculated from this equation (11).

4) Bottle was left to shake until CO₂ and H₂O had mixed. Molar ratio H₂O/CO₂ in bottle was 27810.31, percent of CO₂ in bottle was 3.6x10⁻⁵ mol%.

CO₂ Exposure

After curing samples were put in a glass or plastic cup filled with homemade formation water (brine). The glass/cups were placed into pressure chamber and heating oven. Pressure generated by CO₂ kept constant at 15 bar. Similar procedure has been shown in fig 4.5.

CO₂ + Brine Flooding

After assembling the cell it has been tested for negative pressure (leakage) first with nitrogen and then with oil. The cell with sample was located into heating cabinet and was tested again with nitrogen in bypass mode where fluid doesn't interact with sample. Afterwards flooding with nitrogen has been established in order to create steady-state flow. The flow rate was controlled with Beckman pump. The weight change of a sample was measured with flooded brine. Subsequently, CO₂ and brine had been injected in different flow rates and temperature of heating cabinet increased to 64⁰ C. Fluid flowed through the sample gathered in a scale where weight change had been recorded. During experiment injection, sleeve and differential pressure were also recorded. The realistic and simplified three dimensional view of setup is shown in figure 4.11.

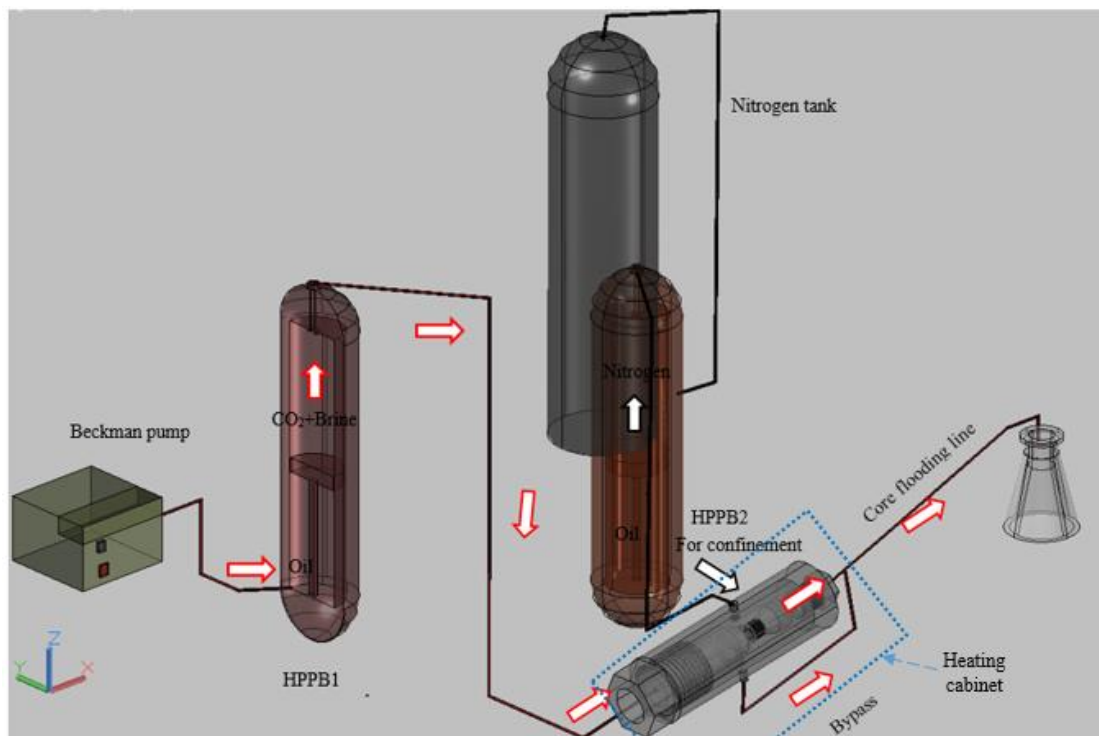


Figure 4.11. The realistic (above) and simplified (below) 3D view of CO₂ flooding setup (Drawn with AutoCAD). Red arrows for fluid flow and black arrows for confinement. HPPB, high pressure piston bottle.



4.3. Experimental matrix

Four different rock types are to be included in the experimental study. Additionally, two cement types and three rock interfaces are to be prepared, leaving the total number of samples to be prepared to $4 \times 3 \times 2 = 24$. Unfortunately, it wasn't possible to continue with Pierre shale due to its destruction during fluid treatment procedure. Experimental matrix of samples are given in table 4.5.

Table 4.5. Experimental matrix. Squares with orange represent batch exposure and yellow squares represent core flooding. Samples in white square were exposed to CO₂ due time limitation.

		Ordinary Portland Cement G			Specialized cement type		
Rock type	Name	Water	Drilling fluid film	Filter cake	Water	Drilling fluid film	Filter cake
Sandstone	Castlegate	S1	S2	S3	S4	S5	S6
Chalk	Mons	C1	C2	C3	C4	C5	C6
Shale	Mancos	M1	M2	M3	M4	M5	M6
Shale	Eagle Ford	E1	E2	E3	E4	E5	E6

4.4. Further characterization

4.4.1. X-ray μ -CT

Micro computed tomography (μ -CT) is a non-destructive tomographic method which uses X-rays to create cross-sections of a sample that afterwards can be used to create virtual 3D models. In this study a Bruker Skyscan 1172 μ -CT is used to visually analyze the samples. The cross-sections had been reconstructed by its own software called NRecon which employs a modified Feldkamp's back-projection algorithm. The samples were exposed to 75 kV X-rays and 134 μ A beam current. The rotation range for specimens was 360° with 0.30° steps. Camera's resolution was adjusted to 25.89 μ m pixels. During scanning an Al filter used for beam hardening. During reconstruction alignment, ring affect and smoothing had been done



for sample in order to get better images. μ -CT has been used twice before and after CO₂ exposure test. Overall scanning and reconstruction time took 40 hours (24x 50 min x 2).



Chapter Result 5

In this chapter, results are shown for Castlegate sandstone, Mons chalk, Eagle Ford shale and Marcellus shale treated with mud/cake and cemented with OPC and SPC. Results are not presented for Pierre shale because of its destruction during fluid treatment.

Due to analysis and experiments the result can be divided into two parts:

- Bonding (debonding) analysis of a cement from formation with μ -CT and Avizo software before and after batch exposure/flooding experiments.
- Chemical/mechanical alteration of a cement/rock/fluid with CO₂ on exposure/flooding test. a) Chemical alteration has been seen visually and compared with literature study while mechanical changes on interface were analyzed with μ -CT and Avizo software.
b) Measurement the amount of leakage, the parameters affecting it.

5.1. Visualization of the cement-rock interface before and after experiments

5.1.1. Cement-rock interface before experiments

The samples were scanned with Bruker Skyscan 1172 μ -CT to characterize the cement-rock-mud interface and to visualize the degree of debonding prior to CO₂ batch exposure/flooding experiments. The scanning images created by μ -CT after were reconstructed and imported to external software called Avizo. In this study Avizo was used to create 3D images of cement/rock/interface, to visualize degree of debonding, morphology and connectivity of debonded area. Distinguishing of different fluid and rock/cement types with different intensities is possible by Avizo in segmentation process. During segmentation Avizo was able to distinguish high intensity mud/cake and low intensity voids (Fig 5.1). The percentage



of bonding between cement and formation was given by Avizo by analyzing cement/formation interface porosity.

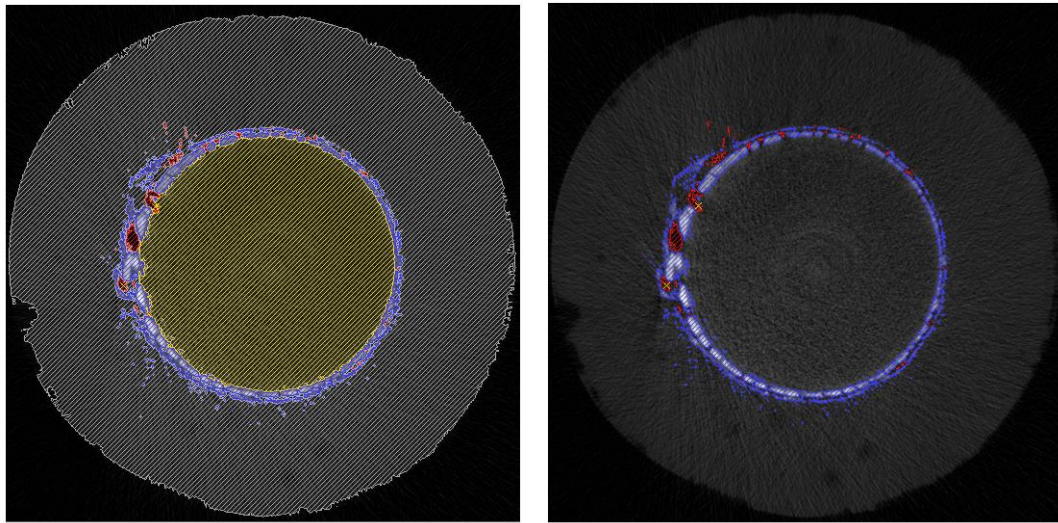


Figure 5.1. Two cross-section segmentation images of Eagle Ford shale with mud and salty cement in different heights. The meaning of colors: Grey-cement, yellow-rock, blue-mud/filter cake, and red- interface voids/pores.

Micro-CT results for rock-cement and rock-mud bonding before experiments are given in Table 5.1 and 5.2 respectively. Cement rock interface and bonding morphology for Eagle Ford shale (pristine) and Castlegate sandstone (filter cake) are shown in Fig 5.3.

Table 5.1. Rock-cement bonding percentage before experiments

Bonding Rock-Cem %		Ordinary Portland Cement G			Specialized cement type		
Rock type	Name	Water	Drilling fluid	Filter cake	Water	Drilling fluid	Filter cake
Sandstone	Castlegate	99	9	9	100	2	7
Chalk	Mons	100	3	21	99	17	34
Shale	Eagle Ford	100	20	36	100	20	28
Shale	Marcellus	99	63	69	99	81	69



Table 5.2. Rock-mud bonding percentage before experiments

Bonding Rock-Mud %		Ordinary Portland Cement G			Specialized cement type		
Rock type	Name	Water	Drilling fluid	Filter cake	Water	Drilling fluid	Filter cake
Sandstone	Castlegate	-	90	89	-	97	91
Chalk	Mons	-	92	76	-	83	61
Shale	Eagle Ford	-	76	63	-	79	70
Shale	Marcellus	-	36	30	-	14	28

5.1.1.1 Sandstone

Castlegate Sandstone showed 99% and 100% bonding with OPC and SPC respectively. As it is mentioned earlier drilling fluid has strong effect on interface bonding. Thus, mud covered interface showed 91% (OPC) and 98% (SPC) -maximum debonding (or 9% and 2% bonding) for this type of the rock. Filter cake also showed negative effect on a cement/formation bond. In filter cake case Castlegate sandstone with OPC made 9% bonding, but with SPC it has decreased to 7% (See Table 5.1). Bonding between sandstone and mud is also more than 90%.

5.1.1.2. Chalk

Mons chalk also showed 100% and 99% bonding with OPC and SPC respectively. Drilling fluid resulted 3% (OPC) and 17% (SPC) bond in the interface. With filter cake bonding were 3% (OPC) and 21% (SPC).

5.1.1.3. Marcellus shale

Marcellus shale also demonstrated high bonding percentage (99%) when samples are pristine. However, results for mud/cake covered samples are totally different from other rock and shale types. Drilling fluid presence in the interfaces resulted 37% (OPC) and 19% (SPC) debonding. Debonding of samples with existence of filter cake was 68-69%.

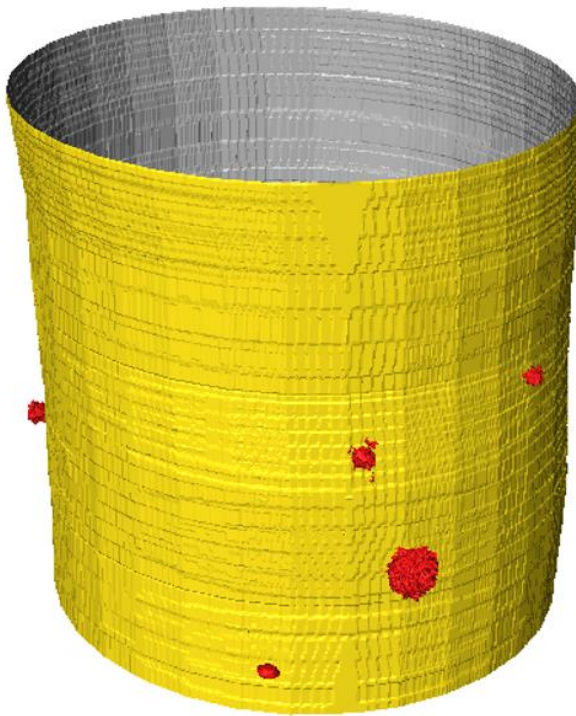
5.1.1.4. Eagle Ford shale

EagleFord shale showed complete (100%) bonding in a pristine state both with OPC and SPC (Figure 5.2). Mud covered interface had 80% - debonding (or 20% bonding) for this type of the shale.

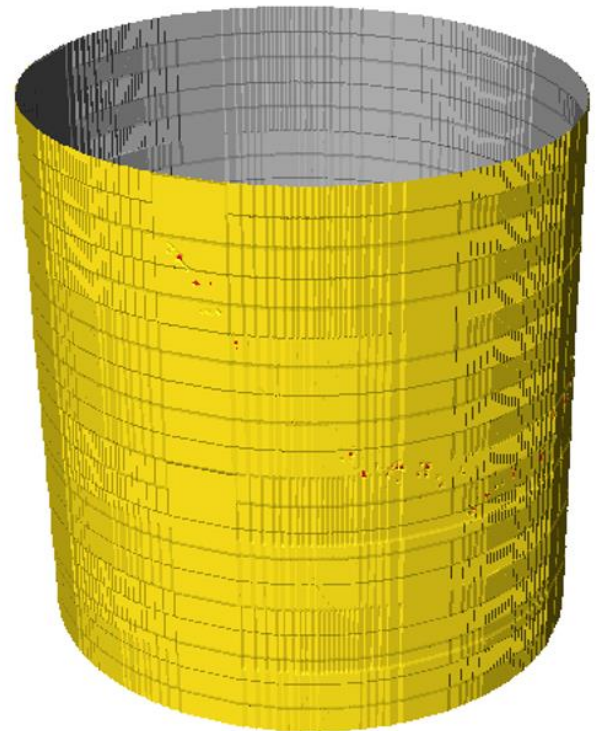


Eagle Ford shale pristine (OPC)

Eagle Ford shale pristine (SPC)



100% bonding



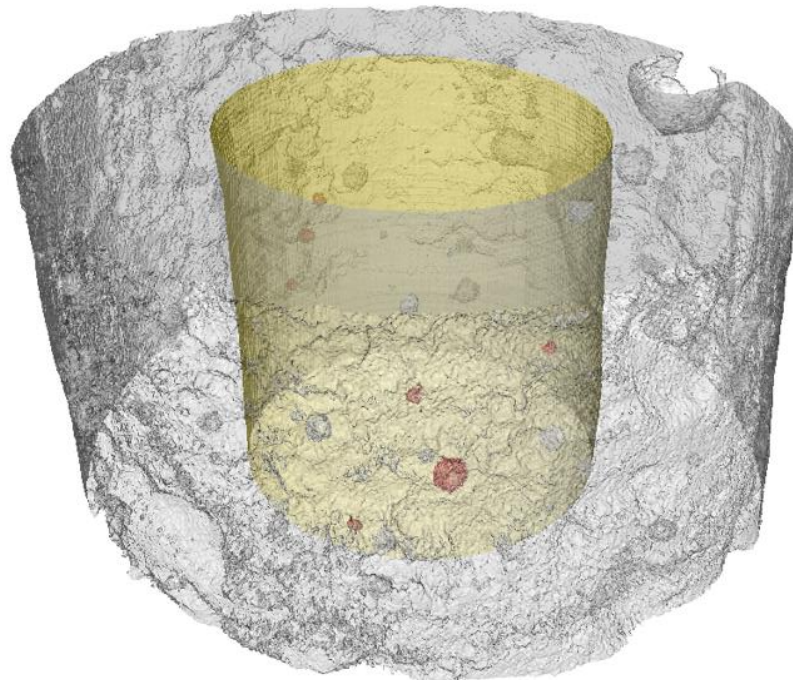
100% bonding

Figure 5.2. Eagle Ford shale prepared in pristine conditions showed total bond both for OPC and SPC. Yellow color- cement-rock interface, red- voids.

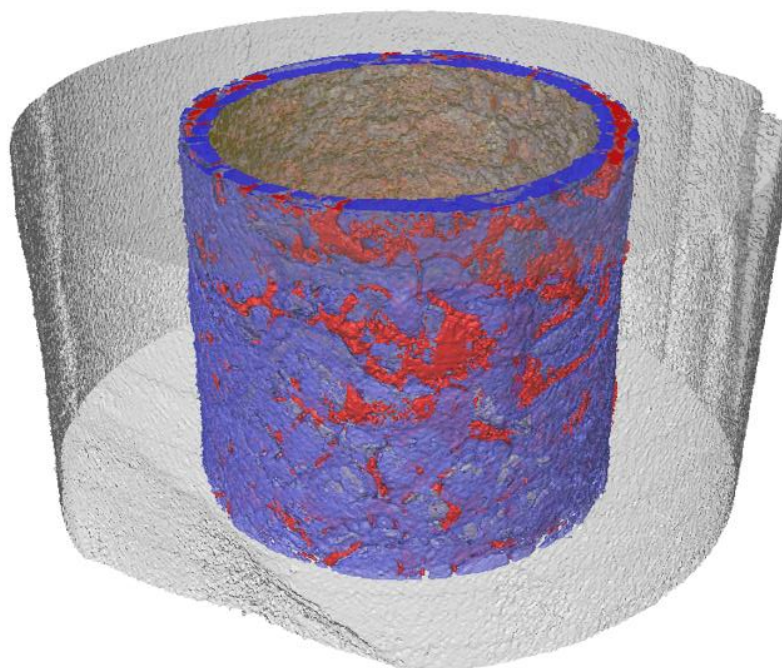
Filter cake also showed negative effect on a cement/formation bond. Eagle Ford shale with a presence of filter cake had slightly higher bonding; 36% (OPC) and 28% (SPC) (see Table 5.1). Avizo didn't detect any crack on cement for these samples; however, it detected crack on the rock (pristine shale with SPC) which can be neglected for these study.



Eagle Ford shale pristine (OPC)



Castlegate sandstone with filter cake (SPC)



■ Cement ■ Rock ■ Mud/filter cake ■ Interface voids

Figure 5.3. Visualization of bonding morphology, cement-fluid-rock interface for different type of rock samples



5.1.2. Cement-rock interface after experiments

After CO₂ batch and flooding experiments samples were scanned again in order to see the changings on the cement-rock interface. Due to time limitation it wasn't possible measure all samples. Only Eagle Ford and Castlegate sandstone were selected to see interface change. Cement-rock and rock-mud bonding percentages are shown in tables 5.3 and 5.4 respectively. The comparative study on visualization of bonding morphology, rock-fluid interface and cement-rock bonding for differet Eagle Ford shale types before and after experiments is shown in figures 5.4 and 5.5 correspondingly.

Table 5.3. Cement-rock interface percentage after CO₂ batch exposure and flooding experiments.

After Rock-Cem %		Ordinary Portland Cement G			Specialized cement type		
Rock type	Name	Water	Drilling fluid	Filter cake	Water	Drilling fluid	Filter cake
Sandstone	Castlegate	99	9	9	100	2	7
Shale	Eagle Ford	100	40	30	100	19	31

Table 5.4. Rock-mud interface percentage after CO₂ batch exposure and flooding experiments.

After Rock-Mud %		Ordinary Portland Cement G			Specialized cement type		
Rock type	Name	Water	Drilling fluid	Filter cake	Water	Drilling fluid	Filter cake
Sandstone	Castlegate	-	90	89	-	97	91
Shale	Eagle Ford	-	52	68	-	72	56

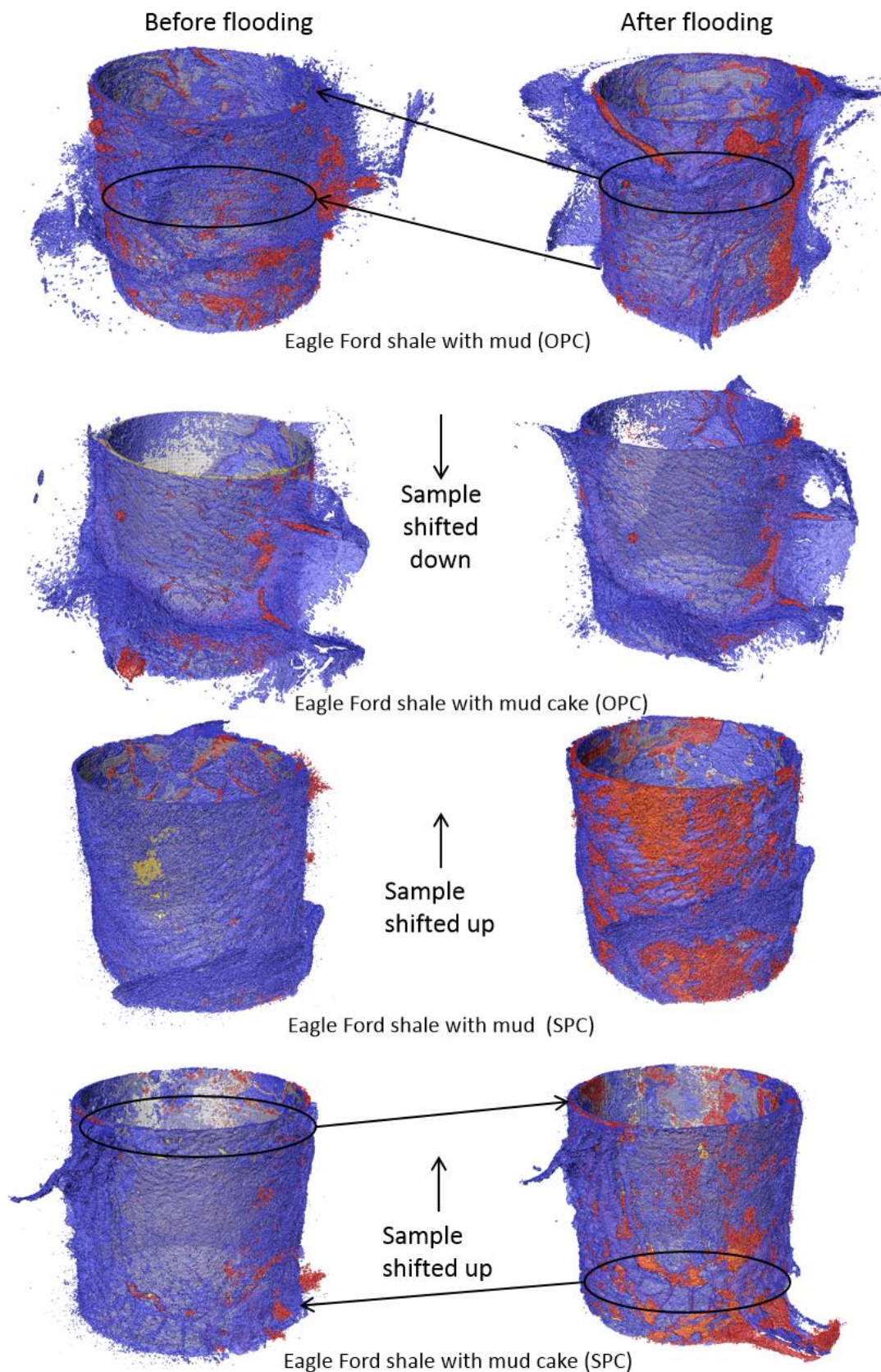


Figure 5.4. Visualization of bonding morphology, rock-fluid interface for differet Eagle Ford shale types. Color meaning in the pictures: Yellow-rock, blue-mud/filter cake, red-interface voids/pores. Some of samples are shifted. Samples with OPC are scanned after batch exposure and samples with SPC scanned after core flooding. Samples with SPC shows obvious reduction of mud and increase of voids in the interface.

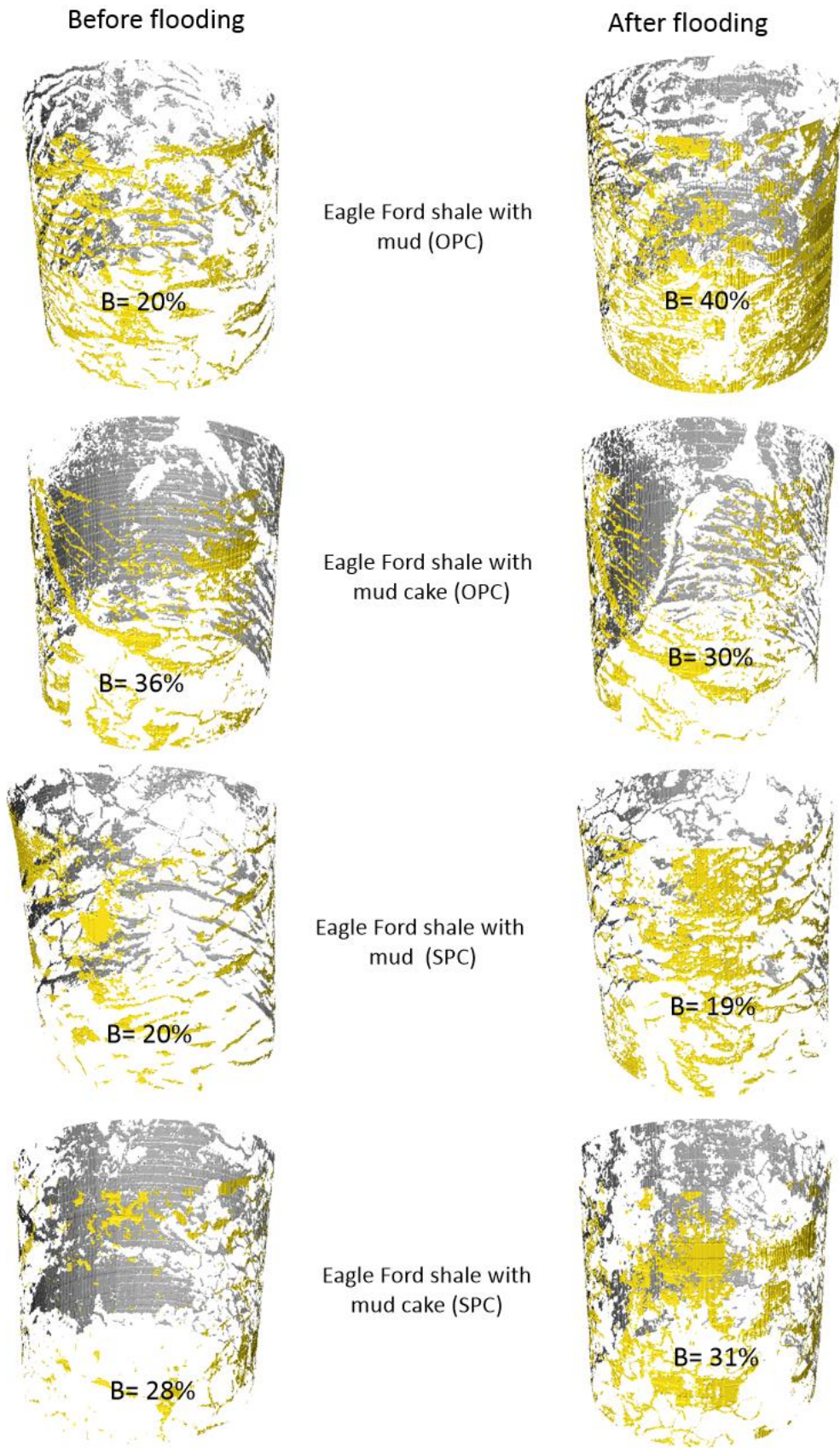


Figure 5.5. Visualization of the cement-rock interface for Eagle Ford shale. The yellow-grey surfaces indicate where rock and cement are in physical contact. The bonding percentage between cement and rock are given for each sample.



5.2. Experiments with CO₂

5.2.1. CO₂ batch exposure

The aim of CO₂ batch exposure experiment was the visualization of chemical or mechanical effect of brine and CO₂ on a cement and a rock. Some of the samples after 7 days CO₂ exposure got white, grey and orange colors on the cement surfaces which represents degradation process (Fig 5.6). Most of the samples with OPC get reacted and showed color changings, but only few samples with SPC got white color.

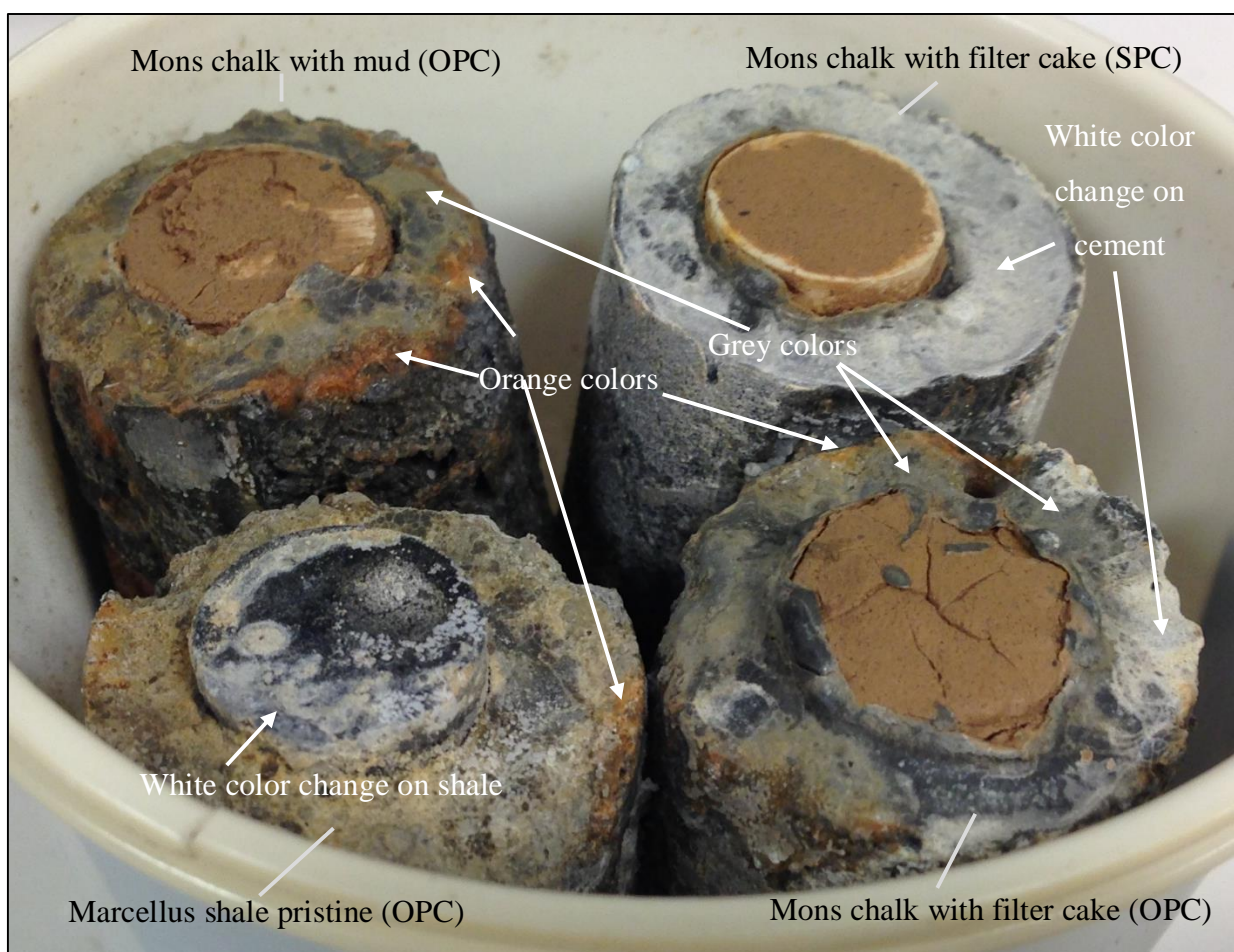


Figure 5.6. Samples after CO₂ batch exposure degradation and showed white, grey and orange colors.

5.2.2. CO₂ core flooding

Three Eagle Ford shale samples with salty cement had been tested in CO₂ core flooding experiment. Samples initially were tested with brine and then with a mixture of brine and CO₂. The purpose of the experiment was to measure the amount of brine and CO₂ flooded



through the cement-formation bond. Shale samples were chosen because of their impermeability. Thus during the all experiment amount of fluid flood only through the cement-formation interface. Appendix B, Table A10 shows data of core flooding experiment.

Figures 5.7-5.9 show the weight change dependency on differential pressure. Weight change is the flow rate in gr/min and it indirectly represents permeability of a sample. More weight change indicates high permeable media. Since shale is impermeable it causes a weight change of the fluid due to a weak bonding between the rock and cement. From the Darcy's law it is obvious that flow rate (weight change) is directly proportional to the differential pressure, permeability and cross-section area of material, and reversely proportional with viscosity of the fluid (see equation 5). Figure 5.7 shows weight change dependency on differential pressure for pristine sample.

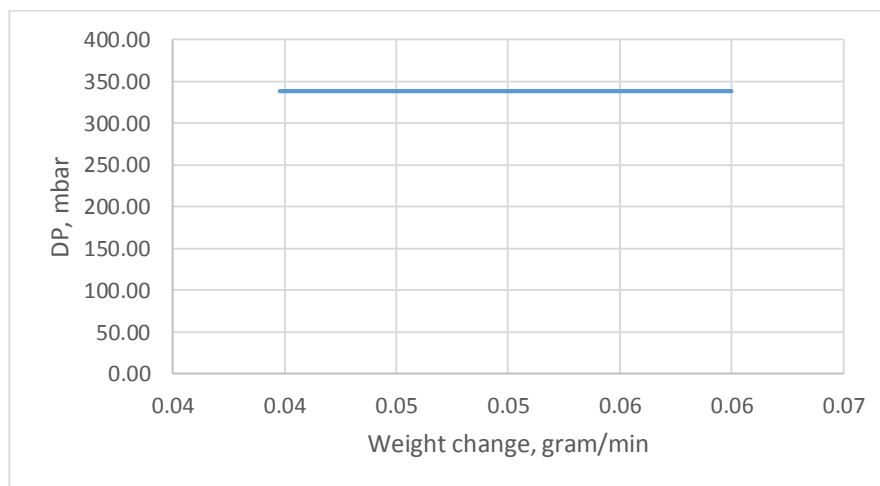


Figure 5.7. Weight change of brine vs differential pressure (pristine sample)

Because of pressure limitation on Beckman pump, system allowed low flow rates for pristine sample. Brine was used as core flooding fluid, but it has shown few weight change (in high injection and differential pressure). For this reason, the experiment hasn't been continued with CO₂. Other two shale samples had core flooding with brine and CO₂ mixture.

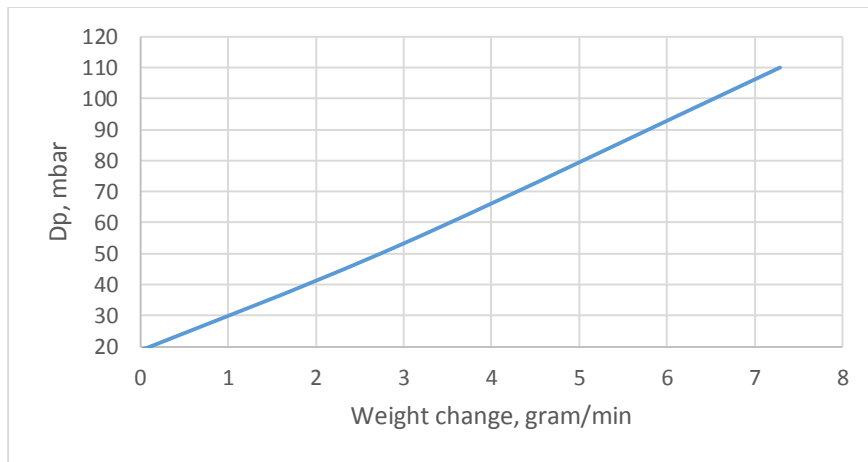


Figure 5.8. Weight change of brine and CO₂ vs differential pressure (Eagle Ford shale sample with mud)

Figures 5.8 and 5.9 and show weight change versus differential pressure for Eagle Ford shales treated with drilling fluid and filter cake respectively.

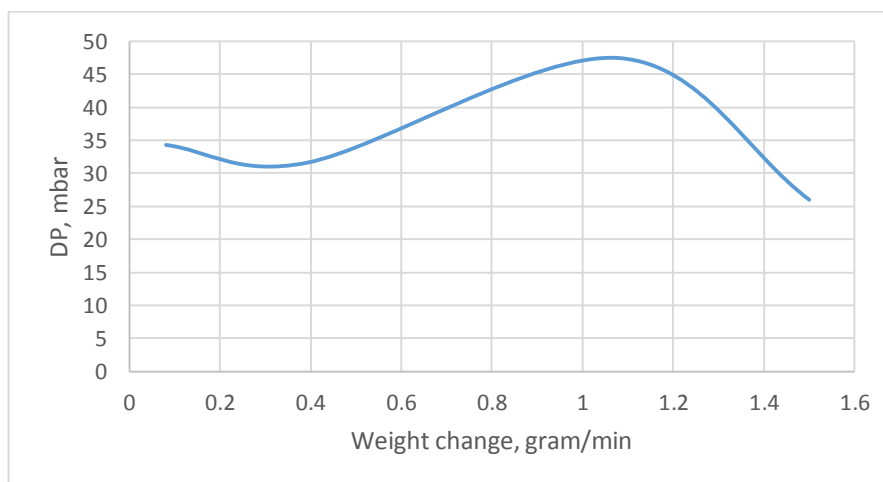


Figure 5.9. Weight change of brine and CO₂ vs differential pressure (Eagle Ford shale sample with filter cake)

After disassembling the Cell the slight degradation (white color) has been seen on a fluid contact area of a sample. Moreover, the mud in the interfaces has been partially washed by continuously flowing fluid (Fig. 5.10).

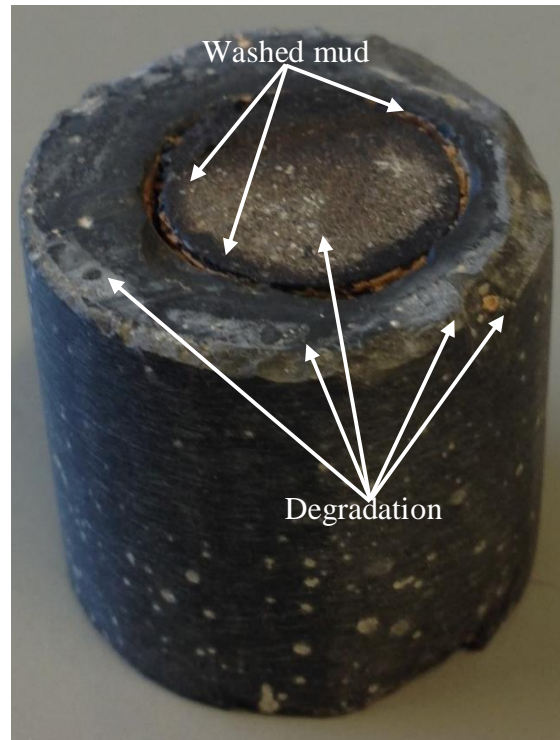


Figure 5.10. Eagle Ford shale with treated mud and SPC showed degradation on a contact area with brine and CO₂.



Chapter Discussion **6**

In this section sample preparation, bonding degree before/after experiments and CO₂ effect on cement-rock bond will be discussed. Discussion is based on Micro-CT, CO₂ batch and core flooding results, and previously done works.

6.1. Discussion of sample preparation

Prepared cement-rock samples represent small model of well without casing. Due to that, it was aimed to prepare samples according to well cementing experience. Cement and drilling fluid were prepared with API standards which are used in oil and gas industry. Cemented samples were cured in laboratory conditions for 7 days at 15 bar and 66° C which are equivalent to realistic well conditions. The pressure and temperature impacts created more severe cracks and debondings on a cement.

During curing time shrinkage of a cement would behavior differently because of reversed placement of cement and rock. It needs some additional research.

In this study pristine samples represent ideal cleaned wellbore. The sample preparation procedure for the pristine conditions is out of relevance to what wellbore is exposed to. Pristine samples were only prepared for comparative aims. Samples with drilling fluid and filter cake represent improper cleaned wellbore which has been discussed in Chapter 2.

Failure of Pierre shale

During sample preparation period it had been planned also to use Pierre shale, but shale samples cracked during fluid treatment time without reaching cementation process. Heathman and Voger (2006) reported that shale from younger geological regions is less compacted, and more hydrated. Pierre shale is also from younger-Upper Cretaceous formation (Sohl, 1967). This type of shale is highly reactive and doesn't respond well to fresh



water exposure. Freshwater exposures result in immediate swelling and associates stress cracking of the shale which also had been visualized in a sample preparation time of this preliminary study. Heathman and Voger (2006) suggest salty water treatment in order to reduce swelling of a shale.

Pressure and temperature

Wellbore and also cement get exposed to pressure/temperature loads thorough the all life cycle of a well. Therefore, real pressure/thermal loads must be considered and have to be applied both during sample preparation and experiment period. Results of this preliminary study are different from Opedal et al. (2013) results, and the main reason behind of it is the absence of pressure and temperature on their experiments. Because of realistic well loads samples of this experiment got more debonding degree. Pressure and temperature effect to the cement and formation have been previously discussed in Chapter 3.

6.2. Discussion of bonding before experiments

Bonding between cement and formation is the only one parameter which can determine whether fluid leakage will occur through interfaces or not. Result showed that for different rock and cement types there are different bonding degrees. Debonding degree for pristine samples were same as result of Opedal. et al. (2014); however, debonding for mud covered samples are slightly higher. This can be explained by difference on immersion time which allowed rock to adsorb more drilling fluid, lower Micro-CT voltage and intensity, and by use of different WBM.

Porosity and permeability

The different bonding degrees on sandstone, chalk and two shale types indicate that the rock formation is more significant when we analyze bonding area. This differences are because of porosity and permeability characteristics of the rocks. The high permeable/porous samples are more prone to obtain 1) a film of a certain thickness and 2) more coverage of mud at the cement/rock boundaries. More coverage of mud reduces the number of sites at the rock surface where cement can bond. Highly porous Catlegate sandstone and Mons chalk treated with drilling fluid had the highest debonding degrees (91% and 97% with OPC respectively). On the other hand less permeable/porous EagleFord and Marcellus shale samples showed less



debonding percentage (80% and 37% respectively). Table 5.2 shows how well the mud bonded to the rock. It can be assumed that mud/cake can be adsorbed by rock more when it meets higher porous media. Adsorption happens with a help of adhesive and cohesive forces. The debonding occurrence with that forces had been previously discussed in subchapter 2.2. In figure 5.3 filter cake was bonded good to the Castlegate sandstone. However, Avizo results for different samples show that filter cake around some rocks fluxed into the cement. Surrounded by fluid film the rock surface get limitations on direct interaction of cement with rock. Water treated samples absorbs the fluid better and have less film on a rock surface which gives maximum bonding degree.

Mineralogy

Although two shale types have similar porosity and permeability their behaviour towards bonding in the interfaces are different and cannot be explained just by permeability and porosity of the rock. The difference on shale behavior can be explained by mineral (calcite, clay, quartz, dolomite, pyrite, etc.) composition of shales. For instance: EagleFord shale has more calcite/dolomite (>50%) and less clay (20%), but Marcellus shale has less calcite/dolomite (3-48%) and more clay (10-45%) content. (see fig 4.1). Thus, mineralogy influences on cement bonding should be also considered.

Rock-mud bonding

Another reason of different shale behavior could be because of storage conditions of the shale types. Eagle Ford was kept in oil for a long term storage while Marcellus were dry initially. Though Eagle Ford samples wiped and were kept 10 minutes at normal conditions to run off excessive fluid the oil could remain on the shale surface which limits the interface between shale and mud/cement. However, from the table 5.2 we can see that Eagle Ford shale/mud bonding area is more than Marcellus shale has. The data on a tabel 5.2 denies the assumption of long term storage (in oil) effect on a shale bonding. The different behavior on bonding degree can be simply explained by amount of mud/cake coverage on shale types (Table 5.2).

Roughness

Tasong et al. (1998) mentioned effect of rock roughness on cement-formation bond. Carpenter et al. (1992) also found that casing with a high roughness gives better cement-casing bond. It is easy for a cement to bind on a rugged surface of sandstone than smooth surface of chalk or shale. When cement encounters only rock, roughness of a rock gives good



interface bonding. However, interfaces with existence of mud/cake do not obey to above mentioned theory and cement-rock bonding reduces. If we look at Table 5.2 we can also visualize that mud-rock bonding reduces with a reduced roughness of rock. Rock roughness not only provides easy bonding for a cement but also for the mud and filter cake. Roughness of rock affects first surrounded fluid type. If the first fluid layer is scratched or washed rock roughness can affect second fluid (cement) layer. Therefore, scrapers, preflushes, spacers and other chemical washers has to be used for effective mud removal procedure (Guillot et al., 2007, Raafat et al., 2002). It can be concluded that rock roughness can increase cement-formation bond of a sample without mud/cake, and reduce cement-formation bond mud/cake exists on interfaces. In this study roughness of the rock wasn't measured. The information about rock roughness attained from Opedal et al. (2014). In the future, roughness must be measured and its effect on bonding has to be researched.

Filter cake

The presence of filter cake reduces bonding percentage in all rock types. Results of samples covered with filter cake agree with studies of Randhol and Cerasi (2009) and Heathman and Vargo (2006). Bulk shrinkage occurs with cement drawing water from the filter cake. It reduces shear bond strengths and due to that debonding occurs. From the results it can be seen that bonding of samples covered with filter cake is lower than pristine samples, but is higher than the samples covered with drilling fluid for each cement type (except Marcellus shale). This can be explained by rock-mud bonding. Higher rock-fluid bonding (see table 5.2) means more contact area on a rock surface. Data show that mud get adsorbed by rock easier and get more contact area than filter cake (for each type of cement). Is it because of viscosity of the fluid or thickness of a fluid coverage? It is unknown and has to be researched.

Cement type

Salty and non-salty cement don't change the bonding degree on pristine samples. Table 5.1 shows different bonding results for OPC and SPC cement type with an interaction of different rock and fluid types. Salt in cement didn't reduce bonding degree of shales with drilling fluid coverage. Added salt even increased the percentage of bonding of Marcellus shale up to 81%. This is due to reduction of bulk shrinkage with added salt. The percentage of bonding also increases on Mons chalk. However, for Castlegate sandstone with drilling fluid coverage salty cement (SPC) reduced bonding critically to 2%. There is no mechanism



which could answer why salty cement increased bonding of chalk and reduced bonding of sandstone (both for mud and filter cake). Therefore, in the future, detailed analysis will be needed in micro scales to see the reaction between SPC and rock surface.

6.3. Discussion of results after experiments

6.3.1. CO₂ batch exposure

After sample preparation, samples were located into glass filled with brine and put into pressure chamber and heating oven. CO₂ was injected for 7 days at 15 bar and 66°C. After batch exposure cement-formation interface porosity or bonding didn't change. However, after experiments samples with a reaction of brine and CO₂ fluid mixture had chemical alteration (degradation) on rock and cement surfaces. The mechanism of degradation is described in sub-chapter 3.3. After batch exposure different colors appeared on the surface of samples. The appeared colors are same as what Duguid et al. (2005) mentioned in their report. In their experiment with cement and CO₂ brine mixture cement got white colored layer followed by grey and orange colors. White color is because of Ca²⁺ and orange color is due to oxidation of Fe (C₄AF or 4CaO • Al₂O₃ • Fe₂O₃).

After degradation cement gradually loses its ability to make isolation between well and carbonation zones and the well integrity becomes under danger.

Rapid degradation is typical for laboratory studies, while field case studies show quite slow degradation of a cement and rock. This is due to difference on conditions of CO₂ exposure and the availability of continuous CO₂ source. However, in real field cases it takes more time for carbon dioxide to reach cement after long migration distance in tiny leak paths. Also in laboratory small volume of cement and rock was exposed to acid attack which makes degradation faster than real field cases. If we consider that the integrity of CCS wells has to withstand for 1000 years the cement degradation in laboratory conditions can be the explanation for this case.

6.3.2. CO₂ core flooding

Three Eagle Ford shale samples with salty cement had been tested in CO₂ core flooding experiment. CO₂ core flooding demonstrates gas leakage through the cement-formation interfaces in laboratory conditions and can be equivalent of fluid leakage on annular well cement. During experiment injection and differential pressures, weight change, temperature and flow rate of Beckmann pump had been measured. Weight change represented flow rate in



grams and Beckmann pump was used only for qualitative purposes. Pressure difference and weight change relationship gives information about leakage through the interface. Pristine samples showed no pressure drop and had very low weight change (0.04-0.06 gram/min). It is because of impermeability of a shale and the very good (100%) bonding between the cement and rock. However, for Eagle Ford shale sample with mud there was highest pressure build-up than other samples. During the experiment it was easy for brine and CO₂ to flow through the weak cement-formation bonds which gave the maximum weight change (7.28 gr/min). According to micro-CT results Eagle Ford shale sample treated with mud had the lowest bonding degree (20%) before the experiment. The Eagle Ford with filter cake had less pressure drop which was due to better bonding (28%). Weight changings for this sample was 0.1-1.4 gr/min which is also lower than shale sample with mud.

Other affecting parameters for permeability can be the area of cross-section and the viscosity of the fluid which is shown in Darcy's law (equation 5).

Small gas leak model created in laboratory conditions showed that the amount of fluid flowing through the cement-formation interfaces are dependent on bonding degree, pressure difference and viscosity (brine or mixture) of the fluid flowing through the interfaces.

6.3.3. Rock-mud bonding

Table 5.4 shows reduction on mud-rock bonding after the experiments. From figure 5.4 it can be visualized mud/cake disappearance/reduction on the rock-mud interfaces of Eagle Ford shale samples with SPC. Continuous CO₂ and brine flow cleaned interfaces from mud and filter cake. For samples with batch exposure the volume of mud and cake didn't change. This is reasonable because no carbon dioxide and brine flow established through the cement-rock interface during exposure.

6.3.4. Cement-formation bonding changings

Batch exposure experiments had no alterations on the cement-rock interface porosity or bonding percentage. The degradation monitored on the cement and rock surfaces. Degradation was directed from surfaces to the center of sample; however, because of less time spent on a pressure chamber and heating oven, the degradation didn't reach cement-formation interface to make any alteration. Therefore, in the future long term batch exposure is needed to see CO₂ and brine effect on interface.



After flooding the cement formation bond slightly increased on a Eagle Ford shale with filter cake and decreased on Eagle Ford shale treated with mud (see table 5.3). Pristine sample due to no flow through the interface had the same bonding degree as before (100%). According to Agbasimalo (2005) the increase on cement-formation bonding percentage is due to precipitation of cement in the interfaces during flooding. It creates large pores in the interface which result with strengthening of bonding. He also mentioned that the pH of brine/CO₂ affects degradation of the cement which on its turn accelerate precipitation process. The decrease of bonding degree for Eagle Ford shale treated with mud can be due to erosion on leak pathways (microannuli). However, it is assumed to be not because of chemo-physical process on the interface but because of bad image quality has gotten from Micro-CT.

6.3.5. Image quality effect on bonding data accuracy

After sample preparation C3, C2, S3 and E5 showed full debond. Although cement surrounding the rock could easily be moved with mechanical force, the Micro-CT result gave higher numbers than that was expected. This can be due μ -CT apparatus, image reconstruction and sample size:

- 1) Quality of final cross-sectional images depends on many parameters such as voltage and scanning size. During scanning quite low voltage (75 kV) had been used (due to safety) which gave poor image resolutions.
- 2) Samples before and after experiments were scanned at different heights which is not reliable for comparative purposes.
- 3) Because of big size of samples intensity of images were low. It caused strong artefact effects such as beam hardening, smoothing, ringing, and alignment during reconstruction. Therefore reconstruction becomes inconclusive in Avizo. The software could determine mud and cake easily, but because of low intensity it is difficult for Avizo distinguish cement and rock voids. The inability to determine voids in the cement-rock interface gives higher bonding degrees than what was expected.



Chapter 7 Conclusion

- The degree of cement-formation bonding depends on the cement, rock and fluid types. Formation type has significant impact on bonding. The bonding degree changes with various formation types. Shale types had less debonding degree than chalk and sandstone.
- Porosity, permeability and mineralogy of the rock samples determine how well mud attaches to the rock and how much adsorbed fluid coverage can restrict cement from direct communication with a rock.
- Results showed that different fluids give different bonding percentages. Drilling fluid and filter cake reduce bonding between cement and formation while pristine samples treated with water shows full bonding degree. Filter cake showed better bonding results than the mud. The larger contact area between the rock and mud causes higher debonding degree.
- Salty cement had good effect on the shale and chalk but not to a sandstone. The effect of salt on the sandstone has to be researched.
- Higher pressure and temperature give higher debonded area during curing time.
- Samples reacted with CO₂ and brine in batch exposure got degradation on a cement and rock surfaces.
- The weight change of a fluid flowing through debondings is dependent on interface permeability, differential pressure, the cross-sectional area and the viscosity of a flooding fluid. Pristine Eagle Ford shale samples showed no leakage while debonded Eagle Ford shale samples treated with mud/cake had high leakage rate (flow rates through the interfaces).
- During core flooding mud and filter cake were washed from the interfaces. The bonding degree increased for Eagle Ford shale sample with filter cake and decreased for Eagle Ford shale sample treated with mud after experiments; however, the bonding data processed after Micro-CT scan is not 100% accurate because of low intensity and poor image resolution.



Chapter 8 Recommendations for Future Work

- More sample preparation with other rock and cement types has to be done. The prepared sample interfaces have to be tested and researched.
- Experiments can be done in HPHT conditions to see pressure and temperature effect on bonds.
- The same sample preparation procedure and CO₂ experiments have to be done with OBM changings on cement-rock-mud bondings.
- The smaller sample sizes have to be prepared. Scanning of the sample in Micro-CT has to be done from the same height before and after experiments in order to compare samples easily. Moreover, Micro-CT parameters have to be configured in way that it gives images with higher intensity.
- SEM images should be used for visualization of mineralogical changes on cement and rock interface and surface. Moreover the knowledge about thickness of filter cake will be beneficial on interface research.
- A shear bond strength has to be measured for cemented rock samples with presence of filter cake on the interface.
- Wettability and capillary pressure of samples also have to be measured to see the effect on bonding degree.



Chapter 9 Limitations

1. Scale of the samples were very tiny compared to realistic well cement/formation interface
2. Mud and filter cake film created in laboratory conditions are different from real well mud circulation and formation of fluid films on the wall.
3. Time factor: a) Samples in batch and core flooding get reaction earlier than in realistic wells due to continuous CO₂ and brine flow. b) The reaction from CO₂, brine, cement, rock and fluid film may give different results for different time period.
4. Low image resolution, low voltage and various scan height were main obstacles on getting good segmentation and accurate bonding percentages.



References

Agbasimalo NC, MSc thesis. Experimental study of the effect of drilling fluid contamination on the integrity of cement-formation interface. Craft & Hawkins Department of Petroleum Engineering, Louisiana State University, 2012. Link:

<http://etd.lsu.edu/docs/available/etd-07102012123331/unrestricted/agbasimalothesis.pdf>

Alqahtani AA, Mokhtari M, Tutuncu AN, Sonnenberg S, Colorado School of Mines). Effect of mineralogy and petrophysical characteristics on acoustic and mechanical properties of organic rich shale. SPE-168899-MS, Unconventional Resources Technology Conference, 12-14 August, Denver, Colorado, USA. Link:

<https://www.onepetro.org/download/conference-paper/SPE-168899-MS?id=conference-paper%2FSPE-168899-MS>

ANSI/API. Specification for cements and materials for well cementing: 2009.

API specification 10A, American Petroleum Institute. Standard. Published in 04/01/2002.

API RP 10B-2, Recommended Practice for Testing Well Cements, First Edition, July 2005

Aspdin, J. An Improvement in the Modes of Producing Artificial Stone, British Patent No. 5022 (1824. Britain), 1824.

ASTM C150/C150M - 12, Standard Specification for Portland cement, 2014)

Bachu S. and Bennion B. Experimental assessment of brine and/or CO₂ leakage through well cements at reservoir conditions. International Journal of Greenhouse Gas Control. Volume 3, Issue 4, July 2009, p. 494–501.

Backe KR, Skalle P, Lile OB, Lyomov SK, Jusnes H, Sveen J. Shrinkage of oil well cement slurries. The Journal of Canadian Petroleum Technology: September, 1998.

Barlet-Gouédard V, Ayache B, Rimmelé G. Cementitious Material Behaviour under CO₂ environment. A laboratory comparison. 4th Meeting of the Well Bore Integrity Network; 18–19 March; Paris, France: 2008.

Barlet-Gouédard V, Rimmelé G, Goffe, B and Porcherie, O. Mitigation strategies for the risk



of CO₂ migration through wellbores. SPE paper 98924. IADC/SPE Drilling Conference; 21–23 February; Miami Florida: 2006.

Bellabarba M, Bulte-Loyer H, Froelich B, Le Roy-Delaga S, Kujik R, Zeroug S, Guillot D, Moroni N, Pastor S, Zanchi A. Ensuring Zonal Isolation Beyond the life of the well, 2008.

Birgit Vignes. Qualification of well barrier elements. Copyright Society of Petroleum Engineers, 2011.

Bois AP, Garnier A, Rodot F, Saint-Marc J, Aimard N. How to prevent loss of zonal isolation through a comprehensive analysis of micro-annulus formation. Copyright 2011, Society of Petroleum Engineers, Inc.

Bonett A. and Pafitis D. Getting to the root of gas migration, 1996.

Bosma M, Ravi K, Driel W, Gerd JS. Design approach to sealant selection for the life of the well. SPE Annual Technical Conference and Exhibition; 3-6 October; Houston, Texas: 1999.

Boukhelifa L, Moroni N, James SG, Le Roy-Delaga S, Thiercelin MJ, Lemaire G. Evaluation of cement systems for oil- and gas-well zonal isolation in a full-scale annular geometry. Copyright Society of Petroleum Engineers, 2005.

Bourgoyne AT, Jr. , Scott SL, and Regg JB, MMS. Sustained casing pressure in offshore producing wells. Offshore Technology Conference, 3 May-6 May; Houston, Texas: 1999.

Bourgoyne AT, Milheim KK, Chenevert ME, Young FS. Applied Drilling Engineering. SPE Textbook Series Vol 2. 1986.

Bruner KR, Smosna R, URS Corporation. A comparative study of Mississippian Barnett Shale, Fort Worth Basin, and Devonian Marcellus Shale, Appalachian Basin. U.S. Department of Energy, 2011. Link:

<http://www.netl.doe.gov/File%20Library/Research/Oil-Gas/publications/brochures/DOE-NETL-2011-1478-Marcellus-Barnett.pdf>

Carroll AS, McNab WW and Torres SC. Experimental study of cement- sandstone/shale-



- Brine-CO₂ interactions. Research article, 2011. Link:
<http://www.ncbi.nlm.nih.gov/pmc/articles/PMC3354340/pdf/1467-4866-12-9.pdf>
- Carter LG., and Evans GW. Bonding studies of cementing compositions to pipe and formation. API Drilling and Production Practice (1961), 72–79.
- Celia, M. A., S. Bachu, J. M. Nordbotten, S. Gasda, H. K. Dahle, 2004. Quantitative estimation of CO₂ leakage from geological storage: Analytical models, numerical models, and data needs.
- CCS Browser. Extracted data on May 18th, 2014. Link: <http://www.ccsbrowser.com/#>
- Chief Council's Report, Macondo, 2011.
- Clark CR., and Carter LG. Mud Displacement with cement slurries. Journal of Petroleum Technology (July 1973) 25, No. 7, 775–783.
- Concure Products Inc. Capillary pressure and floor covering debonding Research Paper, 2010
Link:
http://www.concureproductsinc.com/concrete101/concrete_research_paper_debondingcauses.html
- Connell L, Heryanto D and Lupton N. Integrity of Wellbore cement in CO₂ storage wells.
State of art review, 28 May 2012.
- Dake LP, Shell international. Fundamentals of reservoir engineering. The Hague, Netherlands, 1977. Link:
[http://www.ing.unp.edu.ar/asignaturas/reservorios/Fundamentals%20of%20Reservoir%20Engineering%20\(L.P.%20Dake\).pdf](http://www.ing.unp.edu.ar/asignaturas/reservorios/Fundamentals%20of%20Reservoir%20Engineering%20(L.P.%20Dake).pdf)
- Deutsch CV, McLennan JA, University of Alberta. Guide to SAGD (Steam Assisted Gravity Drainage) reservoir characterization using geostatistics. 3rd Volume, 2005.
- DNV. Recommended practice, Geological storage of carbon dioxide. DNV-RP-J203, April 2012.
- Duguid A, Radonjic M., Scherer GW. Degradation of cement at the reservoir/cement interface from exposure to carbonated brine. Int. J. Greenhouse Gas Control 5, 1413-1428, 2011.



Duguid A, Radonjic M., Scherer GW. Degradation of Well cements exposed to carbonated brine. Fourth annual conference on Capture and Sequestration. May 2-5, 2005. Link:

<http://www.netl.doe.gov/publications/proceedings/05/carbon-seq/Tech%20Session%20Paper%20186.pdf>

Finnseth Ø, Talisman. Johnsen S, Total. Norwegian Oil and Gas Association recommended guidelines for Well Integrity, 2008. Link:

<http://www.norskoljeoggass.no/PageFiles/1166/117%20OLF%20recommended%20guidelines%20Well%20integrity%20rev4,%2006.06.%2011.pdf?epslanguage=no>

Fourmaintraux D, Bois AP, Franco C, Fraboulet B, Brossollet P. Efficient wellbore cement sheath design using the SRC (System Response Curve) method. SPE Europec/EAGE Annual Conference; 13-16 June; Madrid, Spain: 2005.

Garnier A, Le Roy-Delage S, Comet A, Presles JL, Bulte-Loyer H, Rodriguez IU. Self-healing cement system- A step forward in reducing long-term environmental impact. IADC/SPE Drilling Conference and Exhibition; 2-4 February; New Orleans, Louisiana, USA: 2010.

Gekengineering. Cementing Basics. Retrieved data on May, 2014

Link: http://gekengineering.com/Downloads/Free_Downloads/Cementing.pdf

Global CCS Institute. Extracted data on May 18th 2014.

Link: <http://www.globalccsinstitute.com/project/sn%C3%B8hvit-co2-injection>.

Guillot DJ., Desroches J., and Frigaard I. Are preflushes really contributing to mud displacement during primary cementing? SPE/IADC Drilling Conference; 20-22 February; Amsterdam, Netherlands: 2007.

Jafarzade G., NTNU. Leakage along annular cement. Specialization project, 2014.

Halliburton, cementing. Spacers and flushes. Extracted data on November 2014

Link: <http://www.halliburton.com/en-US/ps/cementing/materials-chemicals-additives/spacers-and-flushes/default.page?node-id=hfqelagh>

Heathman and Rogers H. Cementing Casing Equipment: Proper Selection Vital to Success. OTC 17083. 2005).



Heathman J and Vargo R, Halliburton. Salt vs non-salt cement slurries- A holistic review. Copyright AADE Drilling Fluids Technical Conference, 2006.

IEA, Overview. Extracted data on May 18th 2014

Link: <http://www.iea.org/Textbase/npsum/ccsSUM.pdf>

ISO 10426-1:2005. Petroleum and natural gas industries- Cements and materials for well cementing Part 1: Specification, 2005.

Jackson, P.B. and Murphey, C.E.: "Effect of casing pressure on gas flow through a sheath of set cement," SPE 25698. SPE/IADC Drilling Conference; Feb. 23-25; Amsterdam: 1993.

Jennings SS. Long-Term High-Temperature Laboratory Cement Data Aid in the selection of Optimized Cements. SPE paper 95816-MS presented in SPE Annual Technical Conference and Exhibition, 9-12 October; Dallas, Texas: 2005.

Kelessidis VC, Guillot DJ, Rafferty R, Borriello G, Merlo A. Field Data Demonstrate Improved Mud Removal Techniques Lead to Successful Cement Jobs. SPE Advanced Technology Series. 1996 05/01/1996;4(1):53-8. PubMed PMID: 00026982. English Schlumberger, NEXT P. Mud Removal. 2010.

Goodwin KJ, Crook RJ. Cement sheath stress failure. Copyright Society of Petroleum Engineers, 1992.

Krilov Z, Loncaric B and Miksa Z. Investigation of a Long-Term Cement Deterioration under a High-Temperature, Sour Gas Downhole Environment. SPE 58771, 2000.

Kutasov IM, Caruthers RM. Hole enlargement control during Arctic drilling. SPE California Regional Meeting; 23-25 March; Long Beach, California: 1988.

Kutchko BG, Strazisar BR, Dzombak DA Lowry GV, and Thaulow N. Degradation of wellbore cement by CO₂ under geologic sequestration conditions, Environ Sci. Technol. 41(13), 4787-4792, 2007.

Kutchko BG, Strazisar BR, Dzombak DA Lowry GV, and Thaulow N. Rate of CO₂ attack on Hydrated Class H Well Cement under geologic sequestration conditions, Environ Sci. Technol., 42(16), 6237-6242. DOI: 10.1021/es800049r, 2008.



Ladva HKJ, Craster B, Jines TGJ, Goldsmith G, Scott D. The cement-to-formation interface in zonal isolation. IADC/SPE Asia Pacific Drilling Technology Conference and Exhibition; 13-15 September; Kuala Lumpur, Malaysia: 2004.

McLean RH, Manry CW, Whitaker WW, Esso Production Research Co Displacement Mechanics in Primary Cementing. Copyright Society of Petroleum Engineers. Vol19 No 2. 1967.

Munz IA, Aagaard P, Skurtveit E, Regnault O, Brandvoll Ø. Risk assessment of CO₂ leakage through wells and cap rocks. Presented for IFE, 2009. Link:
<http://www.tekna.no/ikbViewer/Content/748417/Munz.pdf>

Napibour A, Joodi B. Finite Element simulation of downhole stresses in deep gas wells. SPE Deep Gas Conference and Exhibition; 24-26 January; Manama, Bahrain: 2010.

Natural gas organization. Well completion. Extracted data on May 2nd, 2014 Link:
http://www.naturalgas.org/naturalgas/well_completion.asp

Naus DJ. The effect of elevated temperature on concrete materials and structures—A Literature review. Prepared for the U.S. Nuclear Regulatory Commission Office of Nuclear Regulatory Research Under Interagency Agreement No. 1886-N674-1Y NRC FIN No. Y6741; November: 2005.

Nelson EB, Guillot D. Well Cementing, Second edition, 2006.

Opedal N, Torsæter M, Vrålstad T, Pierre C, Sintef. Leakage of CO₂ along cement-formation interfaces in wellbores. 7th Trondheim CCS Conference. Publication ID: CRISTin 1033649

Norsk olje&gass. Well integrity. Extracted data on May 18, 2014. Link:
<http://www.norskoljeoggass.no/>

NORSOK STANDARD. Well integrity in drilling and well operations. NORSOK STANDARD D-010; June: 2013. Link:
<http://www.standard.no/en/PDF/FileDownload/?redir=true&filetype=Pdf&item=644901&category=4>

OFITE. OFI Testing Equipment, Inc. Data extracted on May 26, 2014.

Link: <http://www.ofite.com/products/120-60.asp>



Oilandgasinfo. How hydraulic fracturing works. Extracted data on May 26, 2014.

Link: <http://www.oilandgasinfo.ca/fracopedia/hydraulic-fracturing-explained/>

Orban JA, Schlumberger, Parcevaux PA, Guillot DJ, Dowell Schlumberger. Specific mixing energy: A key factor for cement slurry quality. SPE paper (SPE 15578) was prepared for presentation at the 61st Annual Technical Conference and Exhibition of Society of Petroleum Engineers, New Orleans, LA October 5-8, 1986.

OTM consulting 2009. Extracted data on April 10, 2014.

Parcevaux PA, Sault PH. Cement shrinkage and elasticity: A new approach for a good zonal isolation. SPE Annual Technical Conference and Exhibition; 16-19 September; Houston, Texas: 1984.

Peterson, B.: "Bond of Cement Compositions for Cementing Wells", WPC-10123 presented at the 6th World Petroleum Congress, Frankfurt am Main, Germany, June 19 - 26, 1963.

Pilisi N, Maes M, Lewis DB. Deepwater Drilling for Arctic Oil and Gas Resources Development: A Conceptual Study in the Beaufort Sea. OTC paper 22092. Arctic Technology Conference held in Houston; Texas, USA: 2011.

Ptil. Petroleum Activity Summary Report NCS, Trends in risk level, 2008. Link: <http://www.ptil.no/getfile.php/PDF/RNNP%20sam%20eng%2008.%20til%20nettet.pdf>

Ptil. Petroleum Activity Summary Report NCS, Trends in risk level, 2009.

Link: <http://www.ptil.no/technical-reports-and-seminars/trends-in-risk-level-summary-report-2009-available-in-english-article6851-1049.html>

Raafat A, Cunningham E, Munk T, Bjelland B, Chukwueke V, Ferri A, Garrison G, Hollies D, Labat C, Moussa O. Solutions for long-term zonal isolation. Oilfield Review, 2002.

Randhol P and Cerasi P., SINTEF. CO₂ injection well integrity. 29 January, 2009.

Randhol P, Valencia K, Taghipour A, Akervoll I, Carlsen IM. Ensuring well integrity in connection with CO₂. 2007



- Reddy BR, Liang F, Fitzgerald R. Self-Healing Cements That Heal Without Dependence on Fluid Contact A Laboratory Study. SPE International Symposium on Oilfield Chemistry; 20-22 April; The Woodlands, Texas: 2009.
- Reddy BR, Ying Xu, Ravi K, and Gray D. Cement-shrinkage measurement in oilwell cementing- -A comparative study of laboratory methods and procedures. Journal paper 103610-PA presented in SPE Drilling & Completion Volume 24, number 1, March, 2009.
- Researchtopic.The difference between hydrophobic and hydrophilic Part 2. Extracted data on May, 2014. Link:
<http://researchthetopic.wikispaces.com/The+difference+between+hydrophobic+and+hydrophilic+Part+2>
- Richardson M. Well life cycle integrity guidelines-Oil and gas UK's approach. Well integrity forum; 6 June: 2012.
- Rocha JS, Calado V, Tavares F. Study of the influence of cement slurry composition in the gas migration. Copyright 2013, Offshore Technology Conference.
- Saint-Marc J, Garnier A, Bois AP. Initial State of stress: The key to achieving long-term cement-sheath integrity. SPE Annular Technical Conference and Exhibition; 21-24 September; Denver, Colorado: 2008.
- Sanchez, R.A. et al. The effect of drillpipe rotation on hole cleaning during directional well drilling. SPE Journal 4, No. 2, 101–108, 1999.
- Sangesland S, Torbergsen HB, Haga HB, Sæby J, Johnsen S, Rausand M, Lundeteigen MA. An Introduction to well integrity. Rev 0, December; Norway: 2012.
- Saucer, C.W. Mud Displacement during Cementing State of the Art. Journal of Petroleum Technology. SPE 14197, 1987.
- Schlumberger, NEXT P. Mud Removal. 2010.
- Schultz LG. Quantitative interpretation of mineralogical composition from X-ray and chemical data for the Pierre shale. Geological Survey Professional paper 391-C, 1964. Link:
<http://pubs.usgs.gov/pp/0391c/report.pdf>



Shen J. and Pye D. Effects of CO₂ attacks on Cement in High Temperature Applications, SPE/IADC 18618, SPE/IADC drilling conference; 28 February– 3 March; New Orleans, LA: 1989.

SINTEF. Well integrity, facts. Extracted data on May 18, 2014. Link: http://www.sintef.no/upload/Petroleumforskning/Brosjyrer/Well_Integrity.pdf

Skjervén T, Bp., Lunde Ø, Conoco Philips., Perander M, EniNorge., Williams B, ExxonMobil., Farquhar R, Marathon., Jinet JC, Nexen., Sæby J, Norske Shell., Haga HB, Statoil.,

Sohl NF. Upper Cretaceous Gastropods from the Pierre shale at Red Bird, Wyoming. Geological Survey Professional paper 393-B, 1967. Link: <http://pubs.usgs.gov/pp/0393b/report.pdf>

SPE forum. North Sea well integrity challenges, 2009.

Statoil web site. Carbon capture and storage, Snøvit. Extracted data on May 18th 2014. Link: <http://www.statoil.com/en/TechnologyInnovation/NewEnergy/Co2CaptureStorage/Pages/Snohvit.aspx>

Tahmourpour F, Exner M, Khallad I. Design and Operational Factors for the Life of the Well and Abandonment. CIPC/SPE Gas Technology Symposium Joint Conference; 16-19 June 2008; Calgary, Alberta, Canada: 2008.

Tahmourpour F. and Griffith JE. Use of Finite Element Analysis to Engineer the Cement Sheath for Production Operations. Canadian International Petroleum Conference; June 8 - 1; Calgary, Alberta: 2004.

Talabani S, Chukwu GA, Hatzignatiou DG. Gas channeling and micro-fractures in cemented annulus. Copyright 1993, Society of Petroleum Engineers, Inc.; 1993.

Tasong, W.A., Lynsdale, C.J., and Cripps, J.C.: "Aggregate-Cement Paste Interface. II: Influence of Aggregate Physical Properties", Cement and Concrete Research, Volume 28 Issue 10, pp. 1453-1465, 1998.

Thiercelin MJ, Bernard D, Baret JF, Rodriguez WJ. Cement design based on cement mechanical response. Copyright Society of Petroleum Engineers, 1998.



Vidick B, SPE, Dowell Schlumberger. Critical mixing parameters for good control of cement slurry quality. JPT, July 1990.

Wasan K, University of British Columbia. Flocculation and deflocculation. Retrieved data on June 4th, 2014. Link: <http://www.wasanlab.com/pharm/flocc.html>

Wikipedia. Homogenization (chemistry). Retrieved data on June 4th, 2014.
Link: [http://en.wikipedia.org/wiki/Homogenization_\(chemistry\)](http://en.wikipedia.org/wiki/Homogenization_(chemistry))

Wojtanowicz AK, Nishikawa S, Rong X, Louisiana State University. Final Report - Diagnosis and remediation of SCP in wells. Submitted to US Dept. of Interior, MMS, Virginia, July 31st, 2001.



Nomenclature

Abbreviations

ANSI	American National Standards Institute
API	American Petroleum Institute
ASTM	American Society for Testing and Materials
BOP	Blowout Preventer
CCS	Carbon Capture and Storage
CSH	Calcium Silicate Hydrate
FEA	Finite Element Analysis
GoM	Gulf of Mexico
HLB	Hydrophilic Lipophilic Balance
HPHT	High Pressure High Temperature
HPPB	High Pressure Piston Bottle
HSR	High Sulfate Resistant
ISO	International Organization for Standardization
LCM	Lost circulation material
LOT	Leak of Test
MW	Measured Weight
NCS	Norwegian Continental Shelf
OBM	Oil-base mud
OD	Outside Diameter
OPC	Ordinary Portland cement
PHPA	Partially Hydrolyzed Polyacrylamide
PSA	Petroleum Safety Authority Norway
PV	Plastic Viscosity



P&A	Plug and Abandonment
SAGD	Steam Assisted Gravity Drainage
SEM	Scanning Electron Microscope
SCP	Sustained Casing Pressure
SHC	Self-Healing Cement
SPC	Special Portland Cement
SRC	System Response Curve
UKCS	United Kingdom Continental Shelf
WBE	Well Barrier Element
WBM	Water-base mud
YP	Yield Point
ZI	Zonal Isolation

Symbols

<i>E</i>	Energy, kJ
<i>m</i>	Mass, Kg
<i>t</i>	Time, sec
<i>V</i>	Volume, m ³
<i>ω</i>	Rotational speed, rad/sec
<i>k</i>	Empirical constant ($6.1 \times 10^{-11} \text{ m}^2/\text{s}^3$)
<i>K</i>	Permeability of the medium, m ²
<i>Q</i>	Flow rate of the fluid, m ³ /s
<i>dP</i>	Pressure difference, Pascal
<i>dz</i>	The length over which the pressure drop is taking place, metr
<i>μ</i>	Viscosity of the fluid, Pa•sec
<i>A</i>	Cross-sectional area, m ²



Appendix A

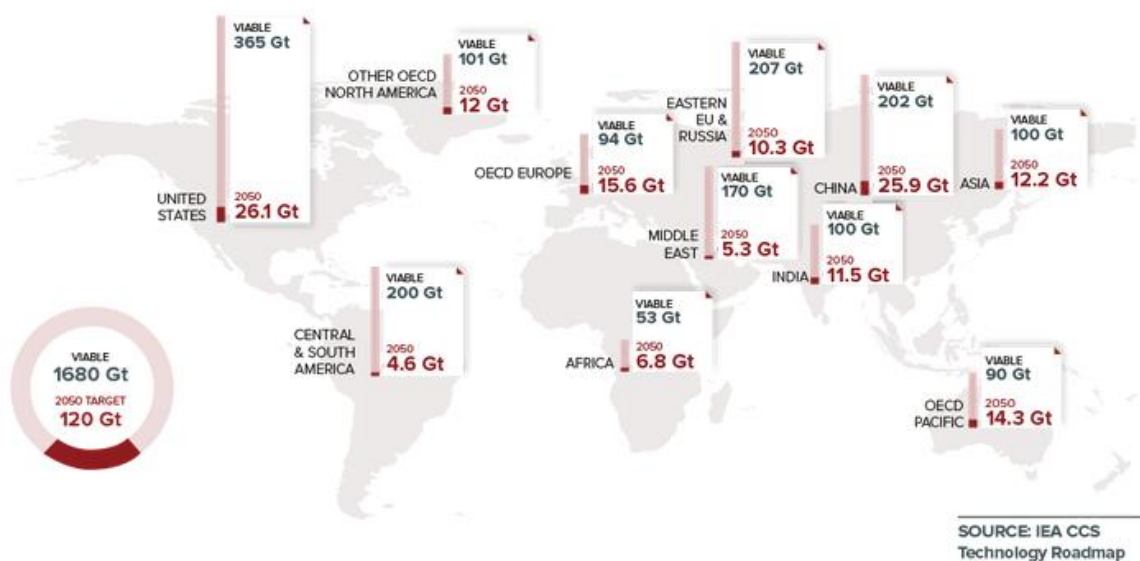


Figure A0. Viable and aimed (2050) CO₂ storage capacities in the world (IEA, 2014 and CCS Browser, 2014)

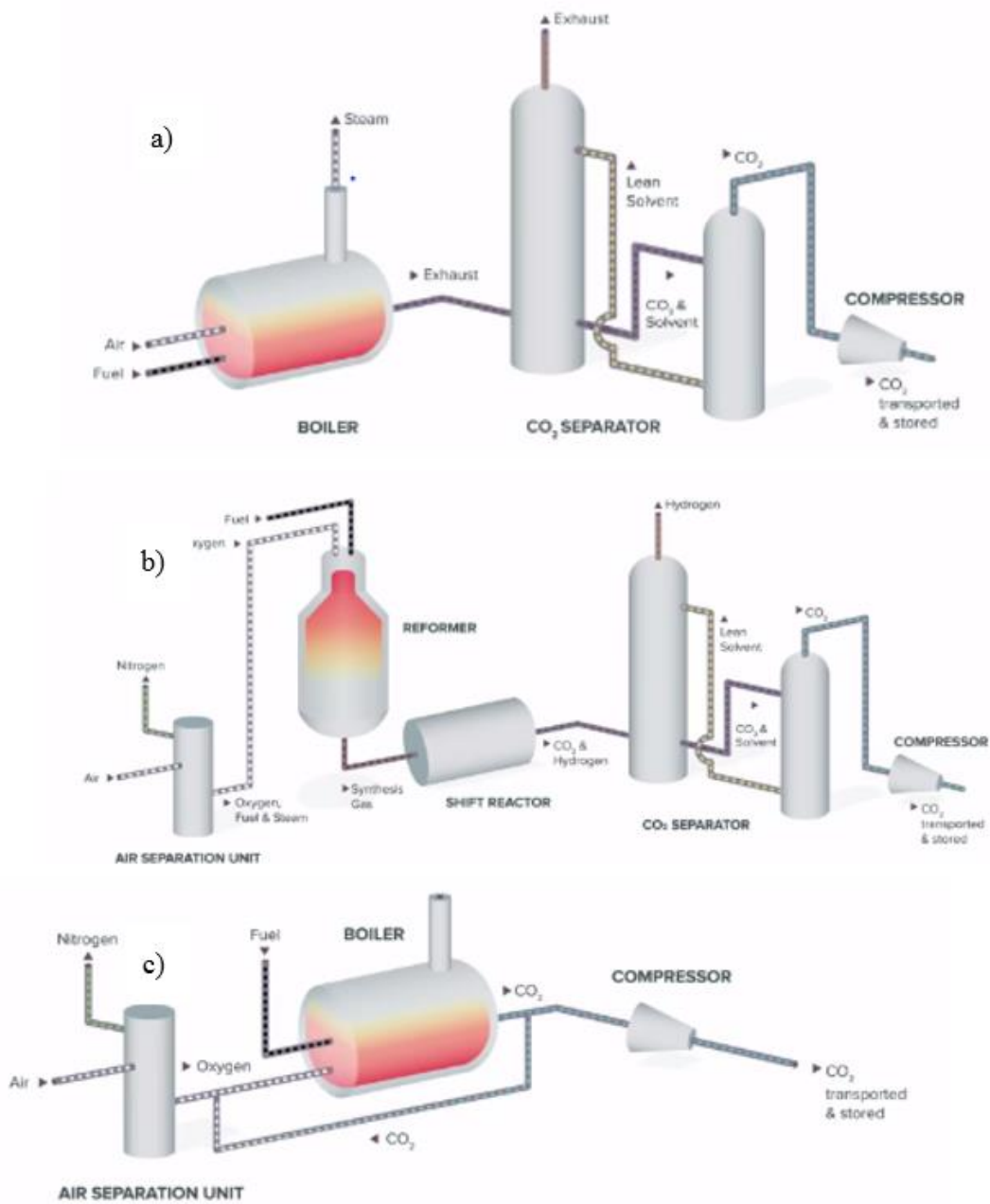


Figure A1. CO₂ capture mechanisms: a) post combustion, b) pre-combustion, c) oxyfiring (CCS, 2014).



Table A1. Costs for CCS project (IEA, 2014)

<i>Process name</i>		<i>Costs</i> <i>USD/ ton</i>
<i>Capture</i>		<i>25-50</i>
<i>Transportation</i>	<i>Pipeline</i> <i>km</i> <i>100</i>	<i>1-5</i>
	<i>Ship</i> <i>km</i> <i>5000</i>	<i>15-25</i>
<i>Storing</i>		<i>1-2</i>

API Class	Description
Class A	Intended for use from surface to depth of 6000 feet, when special properties are not required
Class B	Intended for use from surface to depth of 6000 feet, when conditions require use of moderate to high sulfate resistance. Has a lower C ₃ A content
Class C	Intended for use from surface to depth of 6000 feet, when conditions require high early strength. Available in all three degrees of sulfate resist
Class D	Intended for use at depth from 6000ft. to 10 000 ft. under conditions of moderately high temperatures and pressures.
Class E	Intended for use at depth from 10000ft. to 14,000 ft. under conditions of high temperatures and pressures.
Class F	Intended for use at depths from 10000ft. to 16,000 ft. under conditions of extremely high temperatures and pressures
Class G	Intended for use as a basic well cement
Class H	Intended for use from surface to depth of 8000 ft. as manufactured, but can be used with accelerators and retarders to cover a wide range of well depths and temperatures.

Figure A2. API classification based on depth, temperature and pressure.

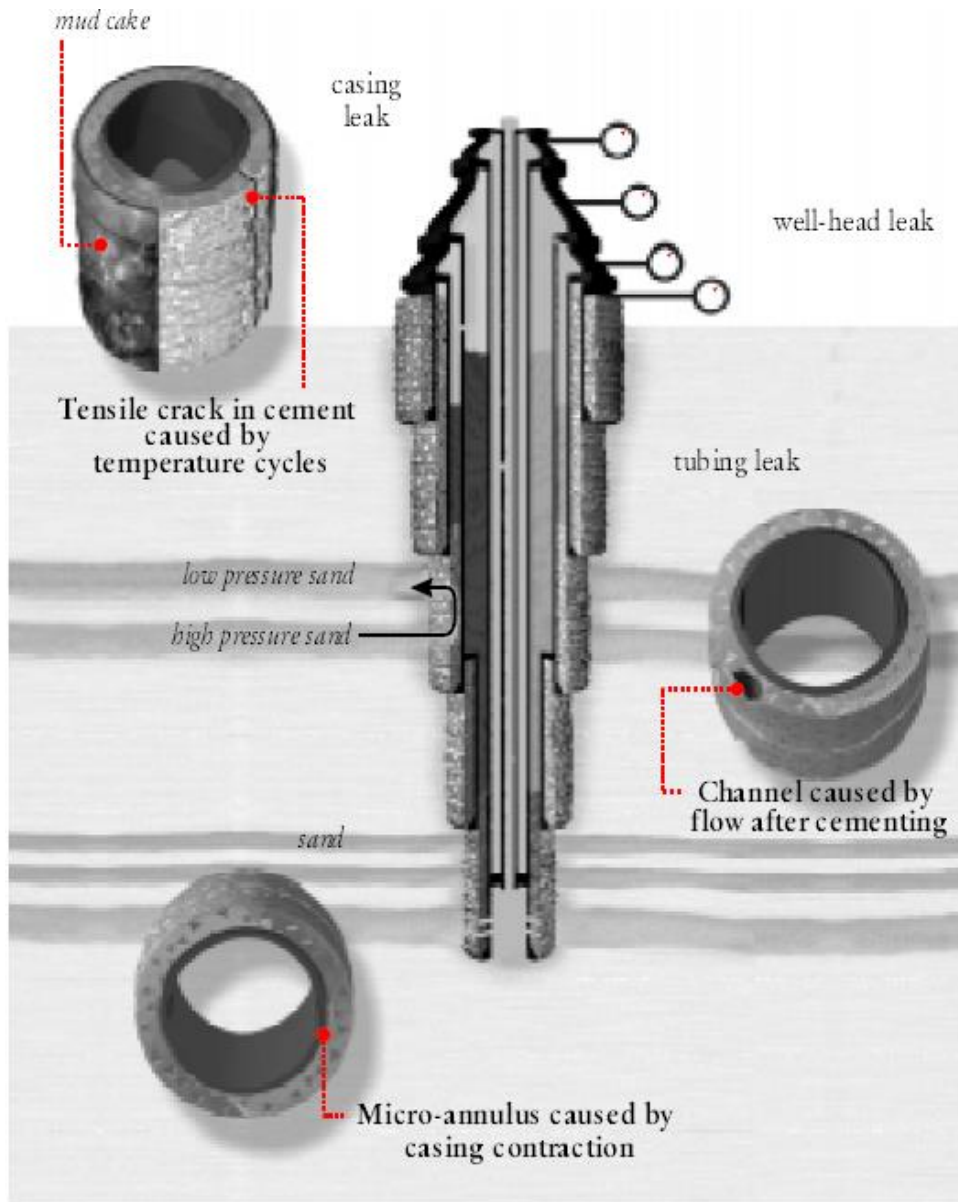


Figure A3. Origins of SCP (Bourgoyne et al., 1999).



Table A2 General recommendations on primary cementing.

	General recommendations on primary cementing (McLean et al., 1967, Tahmourpour et al., 2008)
1	Send a mud sample to the cementing company in order to run compatible tests with spacer/mud /cement
2	Use of centralizers, especially at critical points in the casing string (minimum 70% standoff is desired)
3	Clean the hole before pulling out
4	Lower yield point to 9-14 lb/ft ² and lower gel, thinning the mud, casing should be moved during the cement job. Reciprocate and rotate the casing to break gel-strength and to allow scratchers for optimum mud removal.
5	Isolating the cement by plugs while it is circulated down the casing
6	Establishing turbulence in the cement
7	Holding the cement slurry at least 2 lb/gal heavier than the mud and circulating the cement slurry at a very low rate of flow. Minimum 1 lb/gal is required.
8	Flow parameters of the mud (YP,PV,MW, gas-cut) should be monitored during circulation of casing volume
9	Ideally, the cement spacer should occupy 300 m of the annular volume or 10 minutes pumping time. Accurate volume calculation achievable by using of software

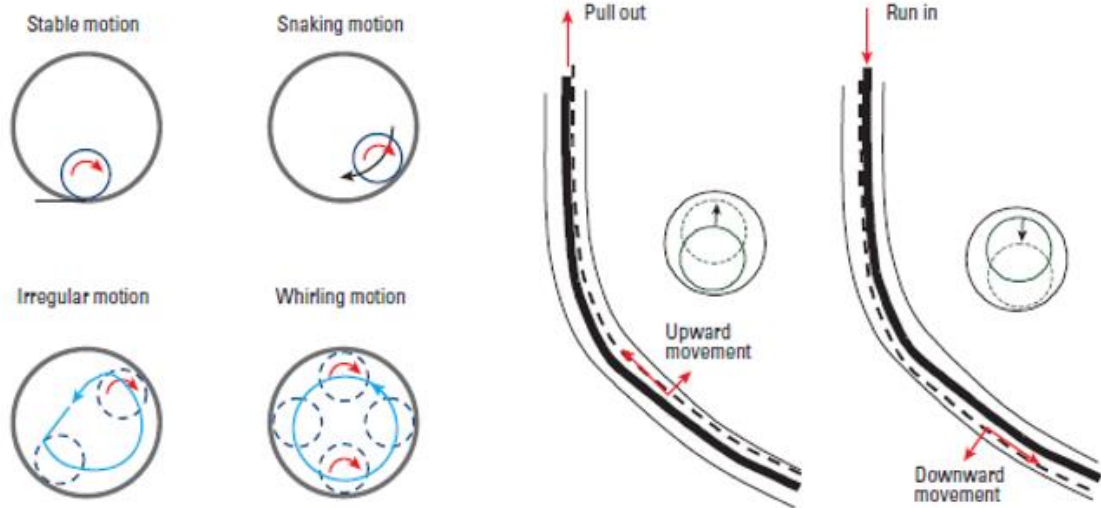
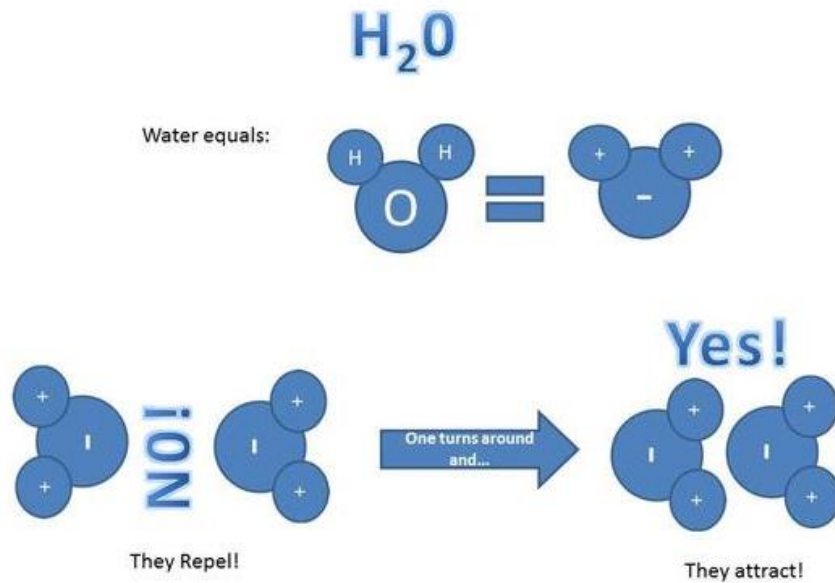


Figure A4. Schematic diagram showing orbital or whirling pipe motion during rotation and lateral pipe motion during reciprocation (Nelson and Guillot, 2006).



the hydrogen is positive and oxygen is negative

Figure A5. Hydrophilic when the molecules attract, Hydrophobic when they repel (Researchtopic, 2013).



Table A3. HLB values are significant for different applications (Nelson and Guillot, 2006).

HLB Value	Application
3 to 6	Water-in-oil emulsion stabilizer
7 to 9	Wetting agent
8 to 18	Oil-in-water emulsion stabilizer
13 to 15	Detergent
15 to 18	Solubilizer

Table A4. Effect of Mud type on bonding properties (Evans and Carter, 1961).

Mud Type	Time (days)	Hydraulic Bond (psi)	Shear Bond (psi)
New Pipe			
Water-base mud	2	175–225	46
Dry	2	375–425	284
Used (Slightly Rusty) Pipe			
Oil-base mud	2	–	75
Water-base mud	2	–	174
Dry	2	–	182



Table A5. Linear alpha olefin- (LAO) - based drilling fluid

Chemical	Concentration (g l ⁻¹)
LAO	500
Water	170
CaCl ₂	60
Lime	34.3
Organophilic clay	17.1
Emulsifier 1	14.3
Emulsifier 2	14.2
Fluid loss reducer	7.1
Drill solids	100
Barite	280

Table A6. Potassium chloride polymer mud formulation.

Chemical	Concentration (g l ⁻¹)
Potassium chloride	19.95
Xanthan	3.99
Starch	11.4
Fluid loss additive	5.13
Drill solids	28.5
Weighting agent	342

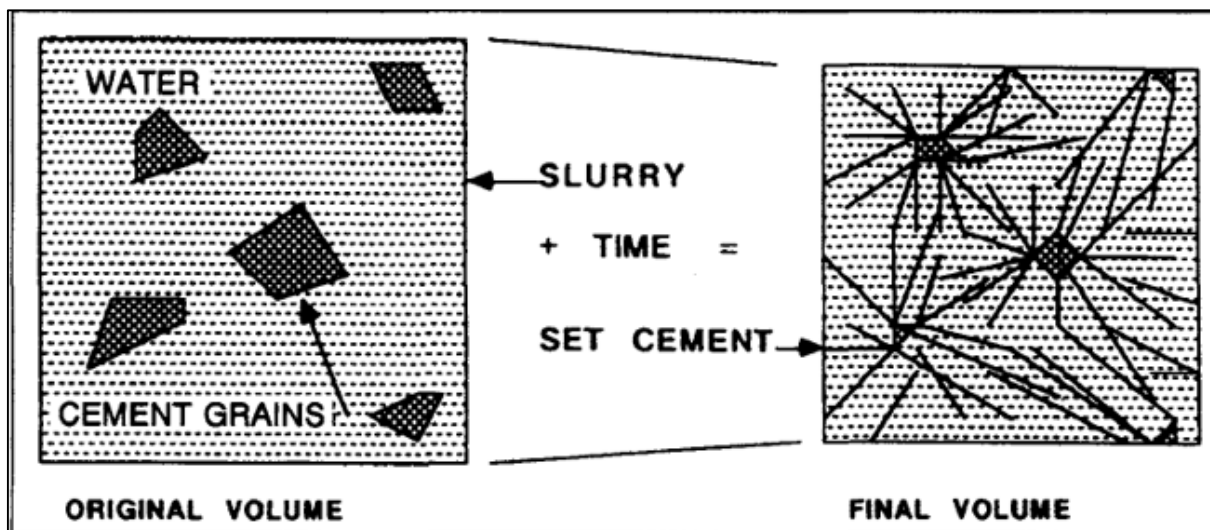


Figure A6. Chemical shrinkage produced during calcium silicate crystal formation.

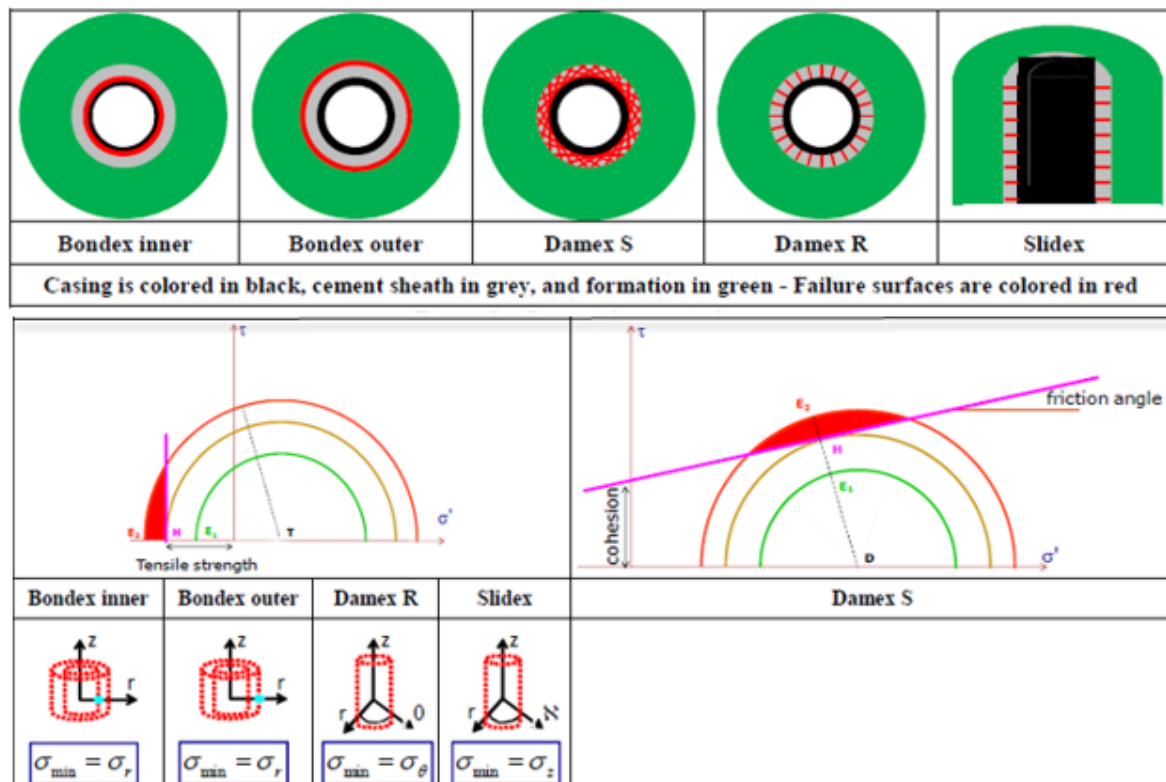


Figure A7. Bondex indicates the risk of de-bonding at the inner/outer cement sheath interfaces. Bondex inner/outer may help to understand inner/outer micro-annulus. Damex S indicates the risk of damage to the cement sheath by shear stress. Damex R indicates the risk of damage to the cement sheath by radial cracks. Slidex indicates the risk of damage to the cement sheath by axial sliding/disking.

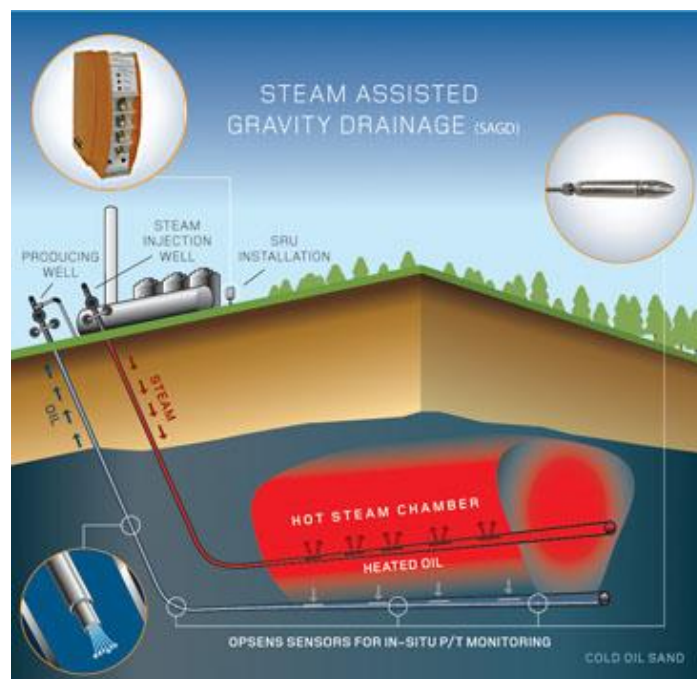


Figure A8. SAGD application. Based on Deutsch and McLennan (2005).



System	1 week	3 weeks	1months	3 months	6 months
Magnesium Potassium Phosphate	Not tested			Not tested	Not tested
Calcium Aluminate Phosphate	Not tested			Not tested	Not tested
Portland cement					
Portland/Fly ash type F	Not tested		Not tested		
Portland/Fly ash type C	Not Tested		Not Tested		
CO ₂ Resistant cement					

Figure A9. Validation of CO₂ durability of different cement systems (Barlet-Gouedard et al., 2008).

Table A7 . Bonding properties with new and used pipe (Evans and Carter, 1961)

Casing type	Time (days)	Hydraulic bond (psi)	Shear bond (psi)
New	8 hr	—	10
Use (rusted)	8 hr	—	53
New	1	300	79
New (sandblasted)	1	500	123
Used (slightly rusty)	2	500-700	182
Used (wire brushed)	2	500-700	335
New (sandblasted)	2	500-700	395
Used (rusted)	2	500-700	422



Appendix B

Table A8. Diameter, length and volume of each rock sample filled with water mud and filtercake.

	Name	Filled	Length, h (mm)		Diameter of rock sample, d (mm)	Volume, V (mm ³)
Sandstone	S-1	Water	27.36	(OPC)	13.66	373.7376
	S-2	Mud	27.39		13.64	373.5996
	S-3	Filter cake	27.45		13.63	374.1435
	S-4	Water	27.49	(SPC)	13.64	374.9636
	S-5	Mud	27.44		13.63	374.0072
	S-6	Filter cake	28.13		13.61	382.8493
Chalk	C-1	Water	31	(OPC)	13.5	418.5
	C-2	Mud	30.65		13.56	415.614
	C-3	Filter cake	31.2		13.3	414.96
	C-4	Water	31.4	(SPC)	13.55	425.47
	C-5	Mud	31.05		13.4	416.07
	C-6	Filter cake	30.47		13.53	412.2591
Shale Marcellus	M-1	Water	31.4	(OPC)	13.54	425.156
	M-2	Mud	31		13.2	409.2
	M-3	Filter cake	30.5		13.52	412.36
	M-4	Water	30.9		13.48	416,532



Shale Eagle Ford	M-5	Mud	31	(SPC)	13.5	418.5
	M-6	Filter cake	31.2		13.55	422.76
	P-1	Water	31	(OPC)	13.2	409.2
	P-2	Mud	31.5		13.1	412.65
	P-3	Filter cake	31.9		13.8	440.22
	P-4	Water	32	(SPC)	13.9	444.8
	P-5	Mud	31.2		13	405.6
	P-6	Filter cake	31.23		13.4	418.482

Table A9. Dimensions of cement-rock sample used in CO₂ flooding experiment

Dimensions (average)	P4	P5	P6
Diameter, mm	25.88	25.52	25.64
Length, mm	25.19	24.56	21

Table A10. CO₂ core flooding results for Eagle Ford shale (average numbers).

Parameters Sample	Flow rate of Beckman pump (ml/min)	Weight change (gr/min)	DP (mbar)	Pinj (mbar)
Pristine sample (SPC)	0.3	0.06	338.61	5.06
	0.6	0.04	338.61	5.60
	1	0.05	338.61	5.91
Shale with mud (SPC)	0.5	0	18.815	2.03
	1	0	19.145	2.02
	2	0	18.985	2.02
	5	2.98	53.221	2.1
	7	7.28	110.04	2.22
Shale with filter cake (SPC)	0.01	0.08	34.28	2.03
	0.5	0.39	31.59	2.04
	1	1.08	47.38	2.06
	2	1.5	26.02	2.04